# On the Lumbosacral Spine Geometry Variation and Spinal Load-Sharing: Personalized Finite Element Modelling

by

Sadegh Naserkhaki

A thesis submitted in partial fulfillment of the requirements for the degree of

Doctor of Philosophy

in

Structural Engineering

Department of Civil and Environmental Engineering
University of Alberta

**Abstract**

Computational modeling of the lumbar spine provides insights on kinematics and internal load development and distribution along the spine. Geometry (size and shape) of the spinal structures and more particularly sagittal curvature of the spine governs its response to mechanical loading. Thus, understanding how inter-individual sagittal curvature variation affects the spinal load-sharing between spinal components (discs, ligaments and facet joints) becomes of high importance. The load-sharing is an indicator of how spinal components interact together in a harmonic synergy to maintain its normal function.

This study aimed to investigate how the inter-individual sagittal curvature variation affects spinal load-sharing in flexed and extension postures using geometrically personalized Finite Element (FE) modeling.

This research used three lumbosacral spines with different curvatures: one hypo-lordotic (Hypo-L), one normal-lordotic (Norm-L) and one hyper-lordotic (Hyper-L) spines with low, normal and high lumbar lordosis (LL), respectively. A 3D nonlinear detailed FE model for the Norm-L spine with realistic geometry was developed and validated against a wide range of numerical and experimental (*in-vivo* and *in-vitro*) data.

The model was subjected to compressive Follower Load (FL) combined with moment to simulate flexed and extended postures. Load-sharing was expressed as percentage of total internal force/moment developed along the spine that each spinal component carried. These internal forces and moments were determined at the discs centers using static equilibrium approach and included the applied load and the resisting forces in the ligaments and facet joints.

Sensitivity of the model predictions to a wide range of FL (500-1100N) and moment (0-20Nm) magnitudes was performed. Optimal magnitudes that minimized the deviation of the model predictions from *in-vivo* data were determined by optimization.

Additional FE models were developed for the Hypo-L and Hyper-L spines. Their kinematics and load-sharing in flexed and extended postures were compared.

The kinematics, intradiscal pressure (IDP) and articular facet joint force (FJF) predicted by the FE model were in a good agreement with previous FE results and *in-vivo* and *in-vitro* data. The sensitivity analysis revealed that the intervertebral rotations (IVRs), disc moment, and the increase in disc force and moment from neutral to flexed posture were more sensitive to moment magnitude than FL magnitude in case of flexion. The disc force and IDP were more sensitive to the FL magnitude than moment magnitude. The optimal ranges of FL and flexion moment magnitudes were 900N-1100N and 9.9Nm-11.2Nm, respectively. To obtain reasonable compromise between the IDP and disc force, our findings recommend that FL of low magnitude must be combined with flexion moment of high intensity and vice versa.

The Hypo-L spine demonstrated stiffer behavior in flexion but more flexible response in extension compared to the Norm-L and Hyper-L spines. The excessive LL stiffened response of the Hyper-L spine to extension but did not affect its resistance to flexion compared to the Norm-L spine.

Result showed that contribution of the facet joints and ligaments in supporting bending moments produced additional forces and moments in the discs. Results demonstrated that internal forces produced by FL and flexion were mainly carried by the discs (75%) and posterior ligaments (25%) while contribution of ligaments in supporting internal moment was higher (~70%) compared to the discs (~20%). Role of the facet joints was negligible except at level L5-S1. This

force-sharing was almost similar in all the three spines. In the case of FL and extension, the discs, ligaments and facet joints shared spinal force with proportion of 55%, 20%, 25% respectively in the Hypo-L spine while facet joints contribution did not exceed 10% at levels L1-4 and reached up to 30% at levels L5-S1 in the Norm-L and Hyper-L spines. The facet joints carried up to 63% of the internal moment in the Hyper-L spine.

This study demonstrated that spinal load-sharing depends on applied load and varies along the spine. It also depends on spinal curvature. The three spines studied demonstrated that inter-individual curvature variation affects spinal load-sharing only in extended posture while no noticeable difference between the spines was found in flexed posture. Analyzing response of additional spines in each category under different loading conditions such as gravity load in future studies may reveal more significant effects of inter-individual curvature variations.

## Preface

This thesis is an original work by Sadegh Naserkhaki. The research project, of which this thesis is a part, received research ethics approval from the University of Alberta Health Research Ethics Board - Health Panel, Project Name "Effects of Variation in Individual Patient Anatomy on Load-Sharing in Lumbar Spine: Finite Element Analyses Using Personalized 3D Models.", No. Pro00037684, February 14, 2013.

The concluding analysis in chapters 3-6 are my original work, as well as the literature review in chapter 2.

Chapter 3 of this thesis has been published as S. Naserkhaki, J.L. Jaremko, S. Adeeb and M. El-Rich, "On the Load-Sharing Along the Ligamentous Lumbosacral Spine in Flexed and Extended Postures: Finite Element Study" Journal of Biomechanics, doi:10.1016/j.jbiomech.2015.09.050. I was responsible for the analysis as well as the manuscript composition. Dr. Jaremko provided the CT-scan data and the ethics approval and reviewed the manuscript. Dr. Adeeb provided the FE modelling support and reviewed the manuscript. Dr. El-Rich was the supervisory author and was involved with concept formation, FE analyses and manuscript composition.

Chapter 4 of this thesis has been submitted to the Journal of Biomechanical Engineering as S. Naserkhaki and M. El-Rich "Sensitivity of Lumbar Spine Response to Follower Load and Flexion Moment: Finite Element Study". I was responsible for the analysis as well as the manuscript composition. Dr. El-Rich was the supervisory author and was involved with concept formation, FE analyses and manuscript composition.

Chapter 5 of this thesis has been submitted to the Spine (Phila Pa.1976) as S. Naserkhaki, J.L. Jaremko, and M. El-Rich, "Effects of Inter-Individual Lumbar Spine Curvature Variation on Load-Sharing: Geometrically Personalized Finite Element Study". I was responsible for the analysis as well as the manuscript composition. Dr. Jaremko provided the CT-scan data and the ethics approval and reviewed the manuscript. Dr. El-Rich was the supervisory author and was involved with concept formation, FE analyses and manuscript composition.

This thesis is an original work by Sadegh Naserkhaki. No part of this thesis has been previously published.

**Acknowledgments**

I wish to take this opportunity to express my deep sincere gratitude to my parents whom I received their constant and unconditional support throughout my whole life and especially during my research program at the University of Alberta. They made the task of dealing with everyday life easier and more pleasant while I am not really able to give my appreciation just by words.

I would like to express my sincere gratitude to best supervisor of the world, Dr. Marwan El-Rich, for welcoming and bearing me in this PhD program. He patiently and kindly provided a peaceful and friendly environment. His knowledge, wisdom and attitude inspired and uplifted me. I wish to acknowledge all the support, advice, guidance, time, attention and effort he spared for me.

I also like to thank Dr. Samer Adeeb and Dr. Mustafa Gul for what I have learned from them during my PhD journey at the University of Alberta. I was lucky to take advantage of their valuable courses. Their precious comments and advices on my research are greatly appreciated.

I would like to thank Dr. Jacob L. Jaremko for his attention on my research from the initiation until the last stage. I appreciate his supports, encouragements and advices.

I also like to thank Dr. Greg Kawchuk for his valuable advices and comments.

Special thank is extended to Dr. Babak Bazrgari who kindly accepted the final review and examination of my research.

**Table of Contents**

**List of Tables**

**List of Figures**

# Chapter 1

# Introduction

### 1.1. Overview

The human spine serves as a column to support the body weight, facilitate the movement, and protect the spinal cord. It is constantly exposed to complex loads and movements during daily activities. The spine is sometimes the origin of human discomfort and disability because of pain. A harmonic synergy between the different components of the spine is necessary to maintain its normal function. Dysfunction of any spinal component results in system perturbation which may lead to immediate compensation from other components, long-term adaptation response and/or ultimately injury (Panjabi, 1992). For instance, it has been proved that a degenerated disc loses its load bearing efficiency which causes transfer of a major portion of the load toward the neural arc in the standing posture (Pollintine et al., 2004). Therefore, understanding the interaction of spinal components and their relative contribution in load-bearing (spinal load-sharing) during various physical activities is of prime importance for the determination of optimal postures and exercises, design of implants, and effective prevention, evaluation and treatment of spinal disorders. Moreover, most experts agree that the assessment of spinal curvature is a part of an evaluation in patients with lower back problems (Harrison et al, 2000). Thus, understanding the effects of inter-individual sagittal curvature variation on spinal load-sharing is also imperative.

Study the biomechanics of spine experimentally in *in-vivo* conditions although is ideal but faces many challenges and limitations due to its harmful and invasive nature. On the other hand, *in-vitro* experiments are costly and use limited number of specimens of elderly donors. Numerical tools such as Finite Element (FE) models represent a powerful tool that allows parametric study of the spine biomechanics in various loading conditions.

In the current research, a 3D nonlinear geometrically personalized FE model of the lumbosacral spine was created and validated. The model was employed first to determine the load-sharing along the spine in flexed and extended postures. FE models of three spines with varied geometries were then created. Their responses to mechanical load in terms of kinematics, internal loads and load-sharing were compared.

### 1.2. Hypothesis

Recognizing that the population inherently has large inter-subject variability it is hypothesized that the variation in geometry of the spine influences its mechanical behavior. Not only the size

and dimensions of each component of the spine affect the spine behavior but more importantly its overall shape defined by the sagittal curvature.

### 1.3. Objectives

The goal of this study is to understand how an individual's lumbosacral spine with its unique geometry responds to mechanical loads. The following objectives are defined to achieve the goal of this study:

**Objective 1**: To determine spinal load-sharing along the lumbosacral spine in flexed and extended postures using FE model.

*Specific Aim 1.1*: To develop and validate a 3D nonlinear FE model of ligamentous lumbosacral spine (Chapter 3).

*Specific Aim 1.2*: To predict internal loads (force and moment) developed in the load bearing components of the spine (i.e. disc, ligaments and facet joints) using FE model (Chapter 3).

*Specific Aim 1.3*: To calculate spinal force- and moment-sharing using equilibrium conditions at each segmental level (Chapter 3).

*Specific Aim 1.4*: To determine the loading mode that simulates realistically (physiologically) the flexed and extended postures (Chapter 4).

**Objective 2**: To investigate the effects of inter-individual lumbosacral spine curvature variation on load-sharing.

*Specific Aim 2.1*: To create 3D geometrically personalized FE models of three lumbosacral spines with different curvatures using their CT-scan data (Chapter 5).

*Specific aim 2.2*: To compare kinematics, internal loads and load-sharing of the three spines (Chapter 5).

### 1.4. Scope and limitations

The current research investigated effects of inter-individual sagittal curve variation on load-sharing of the lower back in flexed and extended postures. FE models of three lumbosacral (lumbar spine and sacrum) spines with distinct curvatures were created. The models considered 3D geometry of the spine and included only passive tissues such as intervertebral discs and ligaments. Follower load (FL) in combination with bending moments was used due to lack of muscles. Load-sharing of the discs, ligaments and articular facet joint was defined as portion of

total spinal force/moment that each structure carried. Only one set of material properties was assigned to all models. Time and loading rate dependent properties (e.g. viscosity) of the spinal components as well as the fluid-flow phenomenon in the disc and porous bone were not considered.

### 1.5. Research contribution

The FE model developed in this research stands out among the few existing detailed 3D FE models of the lumbar spine (Dreischarf et al., 2014). In addition to the kinematics, intradiscal pressure (IDP), force/strain in the ligaments, and contact force in the facet joints assessed by these models, the current model predicted the internal force and moment carried by the disc at all spinal levels using the equilibrium conditions. Despite some studies predicted total force and moment produced at each spinal level using FE models with simplified geometry (Bazrgari and Shirazi-Adl, 2007; Arjmand and Shirazi-Adl, 2005; El-Rich et al., 2004), to our best knowledge there is no data on force- and moment-sharing of the discs, ligaments and facet joints. This data is imperative for understanding how variation in sagittal curvature between individuals affects the response of their spines to mechanical load and distribution of spinal loads among discs, ligaments, and facet joints. The approach developed used individual's CT-Scan data to create personalized geometry and stress profile which can be correlated with subject-specific clinical history (e.g. with/without LBP). This research also revealed that prediction of FE model of the spine is sensitive to magnitude of FL and moment. Optimal intensities that minimized deviations of predicted results from *in-vivo* data were determined. Findings were presented in prestigious biomechanical engineering conferences such as the World Congress of Biomechanics (invited presentation) and Congress of The European Society of Biomechanics and published in high ranked scientific journals such as the Journal of Biomechanics. Two manuscripts are under review in Spine and in the journal of Biomechanical Engineering.

### 1.6. Outline of the thesis

This thesis comprises 6 chapters.

*Chapter 1*

A background on mechanical response of the lumbosacral spine as well as related numerical and experimental studies available in the literature is provided. The overall objectives and hypotheses

are defined and the scope and limitations of the study are explained. The thesis chapters are introduced and the links between chapters are justified since the thesis is written in a paper-based format.

*Chapter 2*

Anatomy and function of the lumbosacral spine are described. Details on sagittal curvature and the geometrical attributes used in this study to distinguish between the spines modeled are specified. A detailed description of the step-by-step procedure used to create the FE model is provided. The assumptions and limitations of the material properties and loading scenarios used are highlighted.

*Chapter 3*

Validation of the FE model predictions against experimental data as well as comparison with other models results are provided. Results of the spinal load-sharing in flexed and extended postures are detailed.

*Chapter 4*

Sensitivity of the model predictions to magnitude of FL and moment is discussed as there is no consensus on what magnitude simulates more realistically the flexed and extended postures. Optimal magnitudes that can simulate physiological conditions are determined by optimization .

*Chapter 5*

FE models of three spines with different curvatures were created. The models were subjected to FL and moment with the optimal magnitudes found in chapter 4. Responses of the three spines in terms of kinematics and internal loads produced in each component as well as load-sharing were compared.

*Chapter 6*

Findings of the current research are summarized. Conclusions and recommendation are provided.

**References**

Arjmand N., Shirazi-Adl, A., 2005. Biomechanics of changes in lumbar posture in static lifting. Spine 30, 2637-48.

Bazrgari, B., Shirazi-Adl, A., 2007. Spinal stability and role of passive stiffness in dynamic squat and stoop lifts. Computer Methods in Biomechanics and Biomedical Engineering 10, 351-360.

Dreischarf, M., Zander, T., Shirazi-Adl, A., Puttlitz, C.M., Adam, C.J., Chen, C.S., Goel, V.K., Kiapour, A., Kim, Y.H., Labus, K.M., Little, J.P., Park, W.M., Wang, Y.H., Wilke, H.J., Rohlmann, A., Schmidt, H., 2014. Comparison of Eight Published Static Finite Element Models of the Intact Lumbar Spine: Predictive Power of Models Improves when Combined Together. Journal of Biomechanics 47, 1757-1766.

El-Rich, M., Shirazi-Adl., A, Arjmand, N., 2004. Muscle activity, internal loads, and stability of the human spine in standing postures: combined model and in vivo studies. Spine 29, 2633-42.

Harrison, D.E., Harrison, D.D., Troyanovich, S.J., Harmon, S., 2000. A normal spinal position: It's time to accept the evidence. Journal of Manipulative and Physiological Therapeutics 23, 623-644.

Panjabi, M.M., 1992. The Stabilizing System of the Spine. Part I. Function, Dysfunction, Adaptation, and Enhancement. Journal of Spinal Disorders 5, 383-389, discussion 397.

Pollintine, P., Dolan, P., Tobias, J.H., Adams, M.A., 2004. Intervertebral Disc Degeneration can Lead to "Stress-Shielding" of the Anterior Vertebral Body: A Cause of Osteoporotic Vertebral Fracture? Spine 29, 774-782.

# Chapter 2

# Background

## 2.1. Overview

Chance of experiencing low back pain (LBP) in adults is higher than 50% (even up to 80%) in the lifetime with about 18% prevalence at any time (Manchikanti et al., 2009; Rubin, 2007; Panjabi, 2003; Trainor and Wiesel 2002). Pain in the lower area of the back is more common than chest and in particular neck area (Manchikanti et al., 2009; Rubin, 2007). LBP, in fact, has a multifactorial etiology, but perhaps mechanical load is the most important single factor (Pope and Novotny, 1993). A broad differential diagnosis has been presented for LBP, with estimates of prevalence in office practice as 97% and 3% for mechanical and non-mechanical factors, respectively (Deyo and Weinstein, 2001). Anyhow, the mechanical factor itself covers a broad range of problems such as lumbar strain/sprain, degenerated disc and facet joint, herniated disc, spinal stenosis, osteoporotic/traumatic fracture, spondylolysis/spondylolisthesis, congenital disease (severe kyphosis, scoliosis or transitional vertebrae), internal disc disruption and presumed instability. The relationship between mechanical loads, LBP, and spinal shape/anatomy adaptation can be conceptualized as shown in Fig. 2.1.

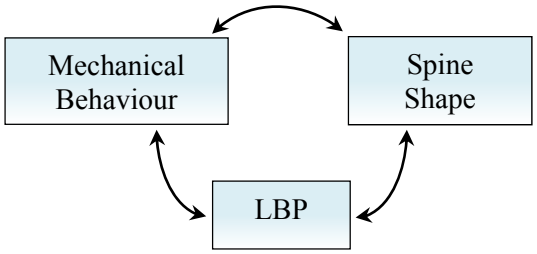


**Fig. 2.1.** Relationship between LBP, mechanical loads and anatomy of spine.

Influence of the spine shape and geometry (in particular the lumbar curvature) on the LBP has been subject of many clinical studies. Nonetheless, the outcome is controversial since some believe in correlation of flat spine to the LBP, while others conclude the correlation of LBP with excessive curvature (Chaleat-Valayer et al., 2011; Adams et al., 1999; Korovessis et al., 1999; Harrison et al., 1998; Christie et al., 1995; Jackson and McManus, 1994). On the other hand, a precipitation of pain in the spine may lead to postural adaptations (Christie et al. 1995). There is statistically significant association between loss of lumbar curvature and degeneration of the disc, vertebral body, and ligaments. Most experts agree that the assessment of spinal curvature is a part of an evaluation in patients with back problems (Harrison et al., 2000).

Shape and geometry of any structure such as the spine govern its response to mechanical load in terms of kinematics, internal loads and stability. Posture affects the spinal load-bearing as well. Minimal changes in posture (posterior pelvic tilt and lumbar flattening) substantially influenced muscle forces, internal loads and stability margin (Shirazi-Adl et al., 2005). Under gravity load alone, the lumbar spine needs to adopt optimal posture that minimizes the required muscle forces and the resulting spinal loads while maintaining the stability (El-Rich et al., 2004). Moreover, given similar external mechanical loads, such as lifting the same heavy objects at work, some people experience disabling LBP while others do not. Although many factors are involved in this variation, it is likely that the intensity of stresses on individual lumbar spine elements (such as intervertebral disc, endplate, ligaments, or facet joint) contributes. It is obvious that response to mechanical load varies based on each patient's spinal anatomy but effects of anatomy variation particularly the sagittal curvature on spinal load-sharing are unclear.

Studying biomechanics of the spine in *in-vivo* conditions although would deliver the most reliable and realistic behavior but is costly and limited by ethics. It may also involve invasive experiments with possible risks of degeneration process acceleration, injuries, and pain. *In-vitro* studies, as well, are costly and associated with many constraints such as sample size, age of donors, repeatability etc. Besides, there are many parameters that are hardly possible to be measured *in-vivo* or *in-vitro*. Therefore, complementary computational approaches such as the Finite Element (FE) method have been used to efficiently and effectively assist in understanding the spine biomechanics. FE model studies have proven themselves as reliable and robust tools when combined with *in-vivo* and *in-vitro* experiments. FE models are feasible, available, repeatable and adjustable to cover wide range of inter-subject variabilities in spine biomechanics and at the same time, advanced and sophisticated enough to include multiphysics formulations and complex material and structural properties.

We used FE modelling to seek the relationship between the spine shape and its mechanical behavior. The focus was on the lower back, so called lumbosacral spine, since the back pain complaints have been mostly reported in this area. The lumbosacral spine will be introduced and its geometrical attributes will be explained in the following section. In addition, the FE modelling will be elaborated and its essential parameters and assumptions will be clarified.

## 2.2. Lumbosacral spine

### 2.2.1. Lumbosacral spine anatomy

The human spine consists of 24 articulating vertebrae and 9 fused vertebrae in the sacrum and the coccyx (Fig. 2.2). It is divided into 4 regions, cervical spine (neck area), thoracic spine (chest area), lumbar spine (lower back) and sacrum. The lumbosacral spine includes the lumbar spine (5 lumbar vertebrae from L1 to L5 and the intervertebral discs) and the sacrum (5 fused vertebrae, S1-S5, and the coccyx). Each vertebra is divided into vertebral body, endplates, and posterior elements that include the lamina, pedicles, articular facets, spinous and transvers processes. Each disc provides the articulation between two adjacent vertebral bodies and is divided into annulus fibrosus as an outer ring which surrounds the nucleus pulposus. The vertebrae of the lumbosacral spine are attached to ligaments at different locations. The major ligaments are the anterior longitudinal ligament (ALL), posterior longitudinal ligament (PLL), capsular ligament (CL), intertransverse ligament (ITL), ligamentum flavum (LF), supraspinous ligament (ITL) and interspinous ligament (ISL). The spine also includes muscles assisting in its stability and locomotion (maintaining and changing posture) (Panjabi, 1992). Though, the muscular system is out of scope due to the complexity and redundancy it imposes to the analyses.

### 2.2.2. Lumbosacral spine curvature

The lumbar region of the spine is convex anteriorly and its curvature is defined by an angle called lumbar lordosis (LL) measured from the superior endplate of vertebra L1 to the inferior endplate of vertebra L5 (Fig. 2.3). The sacrum is curved as well, though its curve angle alone does not describe its structural behavior, its position with respect to the upper (spine) and lower (femur) structures affect the load transfer mechanism (Roussouly and Pinheiro-Franco, 2011). The sacral slope (SS) and pelvic incidence (PI) angles are two important geometry attributes used to describe the spinal sagittal alignment. The SS angle is measured between the line along the S1 endplate and the reference horizontal line. The PI angle is measured between the line joining the hip axis (line between two femoral heads) and the center of the vertebra S1 endplate and the perpendicular line to the S1 endplate. LL and SS are positional parameters changing with the posture while PI is an anatomic parameter and independent of posture. These angles vary between individuals and have a broad range even among normal (healthy) subjects (Table 2.1).

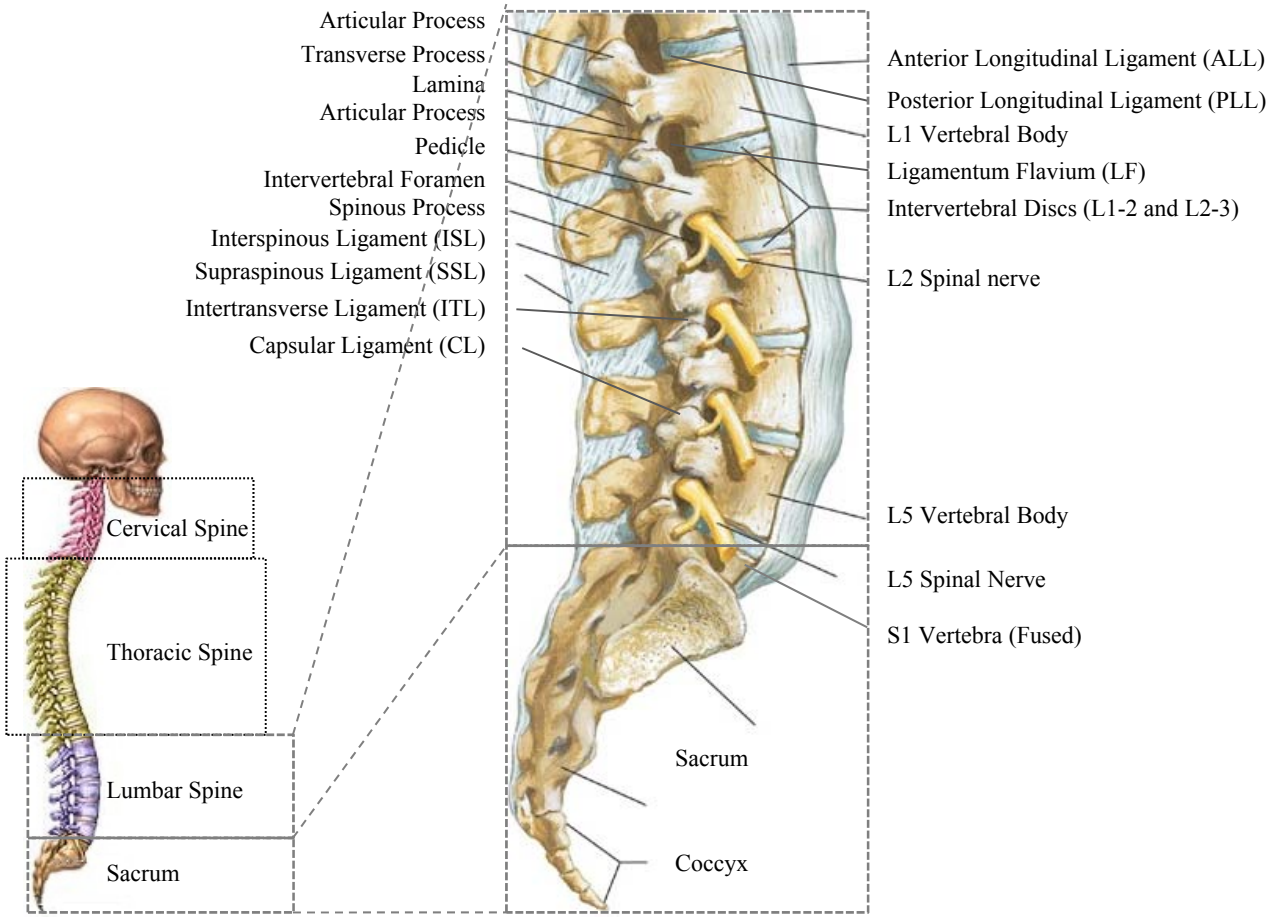


**Fig. 2.2.** Lumbosacral spine anatomy (Adopted from http://www.backpain-guide.com/Chapter_Fig_folders/Ch01_Spine_Folder/1LumbarAnat.html and http://pilates.about.com/od/technique/ss/human-spine-anatomy.htm).

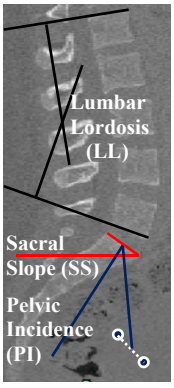


**Fig. 2.3.** Geometry attributes of the lumbosacral spine.

**Table 2.1.** Range of geometry attributes of the lumbosacral spine.

| | **PI** (°) (Vrtovec et al., 2012) | **SS** (°) (Roussouly et al., 2005; Roussouly et al., 2003) | **LL** (°) (De Smet, 1985; Propst-Proctor and Bleck, 1983); Stagnara et al., 1982) |
|---|---|---|---|
| Lower Limit | PI < 45 | SS < 35 | LL < 20 |
| Normal | 45 < PI < 62 | 35 < SS < 45 | 20 < LL < 61 |
| Upper Limit | 62 < PI | 45 < SS | 61 < LL |

The spine can be classified in four groups based on its geometry attributes (Roussouly, P., Pinheiro-Franco, J.L., 2011; Roussouly et al., 2005; Roussouly et al., 2003) (Fig. 2.4). The essential parameters in this classification are SS and PI as well as a qualitative description of the thoracic and lumbar curves. This classification considers the sagittal curvatures of both the lumbar and thoracic spines. Since Types 1 and 2 both have low SS and PI (they differ mostly by thoracic curvature), they are considered as one group called Hypo-Lordotic (straight or flat spine) in this study. Type 3 is considered as Normal-Lordotic and Type 4 as Hyper-Lordotic (highly curved) spine.

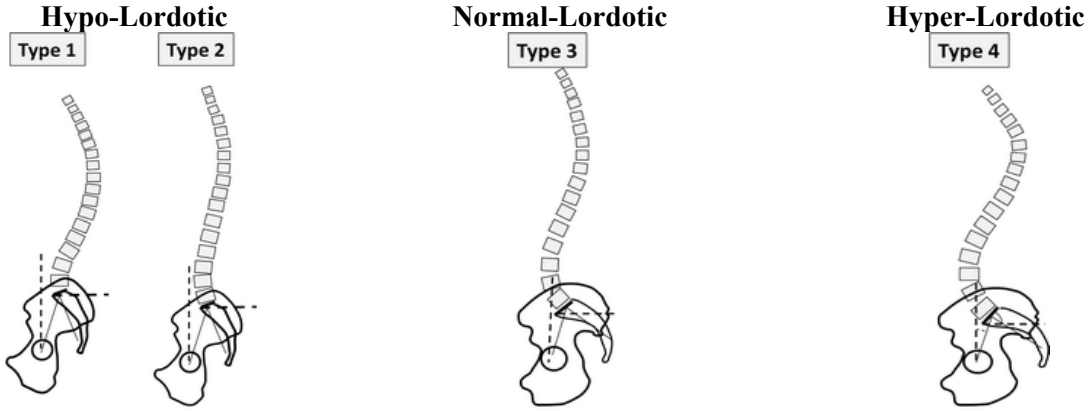


**Fig. 2.4.** Classification of spines based on geometry attributes (Adopted from Roussouly and Pinheiro-Franco, 2011).

**Geometry attributes relationship**

In this study, the LL, SS, and PI were measured on CT-scans of 24 subjects (age median and range: 28 and 20-48 years, respectively). The images were taken from the University of Alberta Hospital Database after receiving ethics approval. Measurements were taken at the median

sagittal plane. Figure 2.5 shows how these geometry attributes are related and where each spine stands with respect to the normal range defined in Table2.1. It was observed that, both LL and PI increased with SS while LL increased with PI which is consistent with the spine classification used in this study i.e. Hypo-Lordotic spine is straight whereas Hyper-Lordotic spine is highly curved. Three of these subjects with distinct SS, PI, and LL were selected to represent each category in spinal load-sharing investigation (Fig. 2.5).

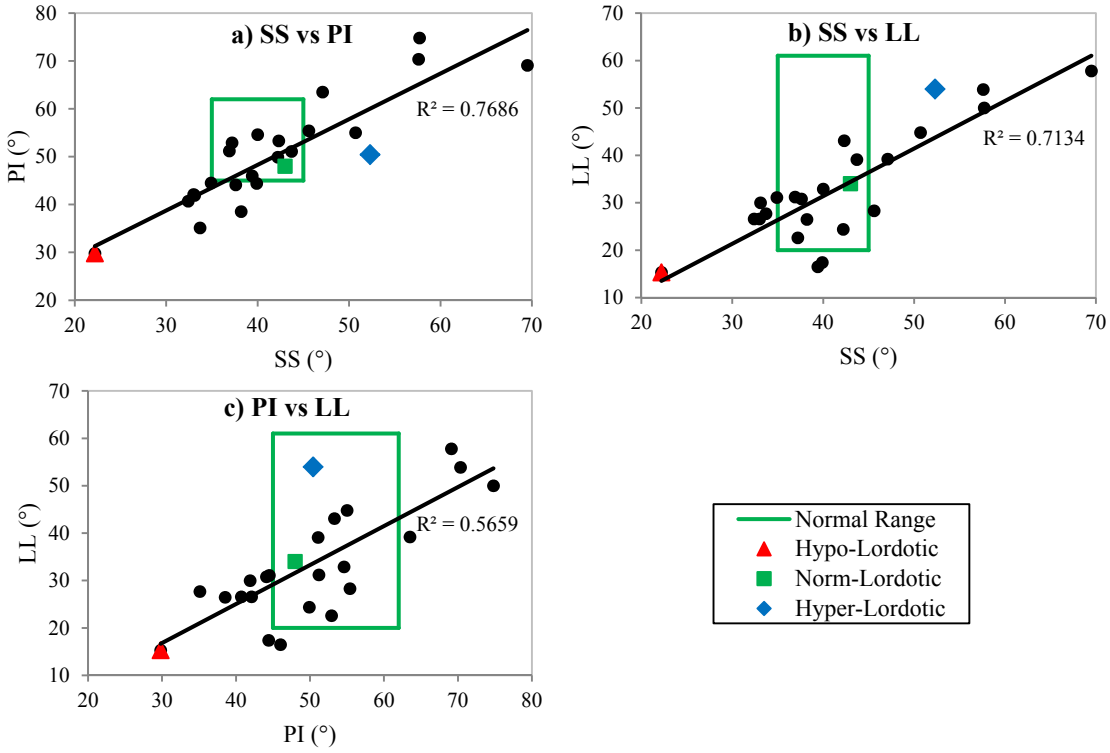


**Fig. 2.5.** Geometry attributes measures of sample group.

### 2.3. Finite Element (FE) modelling

This study used a geometrically personalized FE model which can be developed for any subject whose CT-scans are available. Meshing a complex 3D geometry such as the spine is very challenging if one wants to ensure a good quality and efficient mesh. A variety of elements was used to mesh the spinal structures. Nonlinearity of the material properties was also considered. The FE model development step-by-step procedure is explained in the following sections and details of the analysis and results are elaborated.

### 2.3.1. Geometry acquisition

CT-scans of 2mm thickness taken in horizontal, sagittal and coronal planes (Fig. 2.6a) were imported in the medical image processing software MIMICS (MIMICS Research 17.0, Materialize, Belgium). The segmentation was performed and 3D geometry of the bony components (vertebrae and sacrum) was reconstructed (Fig. 2.6b). Using the Geomagic (Geomagic Studio 2014, 3D Systems, USA), the 3D geometry was smoothened and cleaned from undesired irregularities and spikes without changing or affecting the individual geometry details. Particular attention was paid to the articular facets processes to ensure that the facets surfaces were clean with no interference. Some boundaries were introduced to separate the endplates from the vertebral body and to locate the regions of attachment to the disc which also helped divide the disc into nucleus pulposus and annulus fibrosus (Fig. 2.6c). Also, some boundaries were defined in the articular processes so the contact could be assigned.

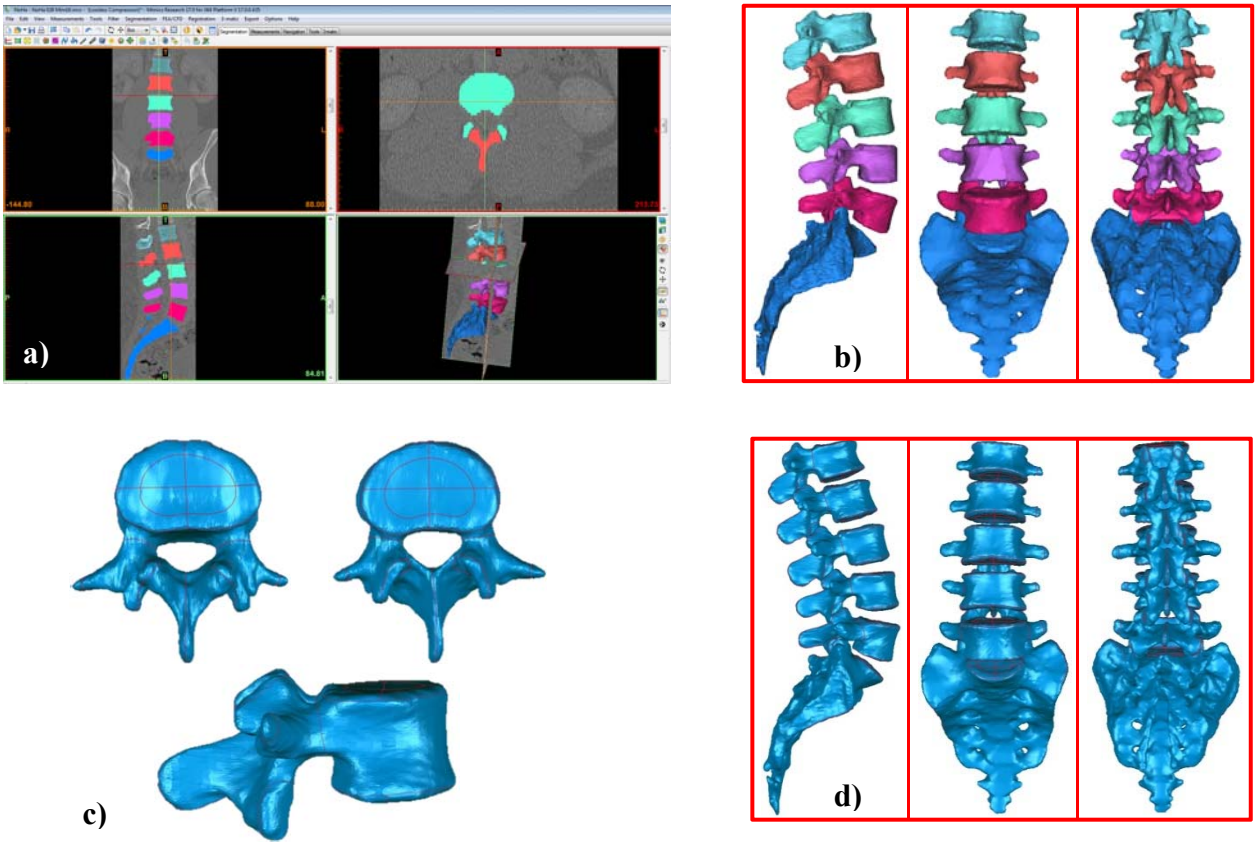


**Fig. 2.6.** 3D geometry acquisition steps of the bony components. a-b) segmentation using Mimics, c-d) smoothening and cleaning using Geomagic Studio.

### 2.3.2. Mesh

The software Hypermesh (Hyperworks 12.0, Altair, USA) was used to mesh the bone geometry and furthermore to create the intervertebral discs and ligaments. The cortical bone which is a dense tissue layer covering the outer surface of the vertebra was meshed by 3-node thin shell elements with a uniform thickness of 1mm. The endplates which are composed of a layer of thickened collagenous bone were also meshed with 3-node shell elements with a uniform thickness of 1mm. The Cancellous bone is spongy tissue (trabeculae) at the core of vertebrae. It was modelled by 4-node (tetra) solid elements that filled up the volume inside the vertebrae.

The disc mesh was generated by extrusion seven layers of 8-node (brick) solid elements between two adjacent endplates. The annulus ground comprised the 7 outer circumferential layers with 56% proportion of the whole disc and the nucleus pulposus comprised the remaining 44% inner layers (El-Rich et al., 2009; Schmidt et al., 2006). The annulus ground was reinforced by collagen fibers which were modeled by unidirectional nonlinear springs distributed in concentric lamellae with crosswise pattern close to ±35° (El-Rich et al., 2009; Schmidt et al., 2007).

The ligaments are bands of tough, fibrous dense regular connective tissue bundles, comprising collagenous fibers that are protected by dense irregular connective tissue sheaths. Depending to the amount and orientation of the fibers they resist tension but buckle under compression. Two-dimensional membrane elements can deliver a more realistic behaviour of the ligaments particularly if the ligament failure mode is desired (El-Rich et al., 2009). However, they can be simulated by sets of unidirectional nonlinear elements at each segmental level (Breau et al., 1991) in the physiological conditions. Three springs attached to the posterior tips of spinous processes represented the SSL and four springs positioned obliquely joining the superior spinous process with the adjacent inferior spinous process represented the ISL. The LF was simulated by three springs connecting the laminae. The CL at each side was simulated by eight springs joining the periphery of adjacent facet processes. The ALL was represented by five springs connecting the anterior edge of the endplates and attached to the disc. Similarly, the PLL was simulated by three springs connecting the posterior edge of the endplates and attached to the disc.

A reasonably refined mesh was used particularly for the articular facet joints to ensure accurate prediction (Ayturk and Puttlitz 2011) with low sensitivity to mesh size. Details of the FE mesh are shown in Fig. 2.7.

### 2.3.3. Material properties

*Vertebrae*

Bone is a nonhomogeneous material comprising of various cells, organic and inorganic substances. It is an anisotropic material and shows different mechanical properties in different directions. It is a visco-poro-elastic material and its properties are time and loading rate dependent. It is also a nonlinear material although in low strains it shows linearity. Despite all of the aforementioned complex properties of the bone it can be simplified as homogeneous isotropic linear elastic material in the current study because it analyzes the spinal response under static physiological loads. In these conditions, deformation of the vertebrae is ignorable. The material properties used to model the vertebrae are summarized in Table 2.2.

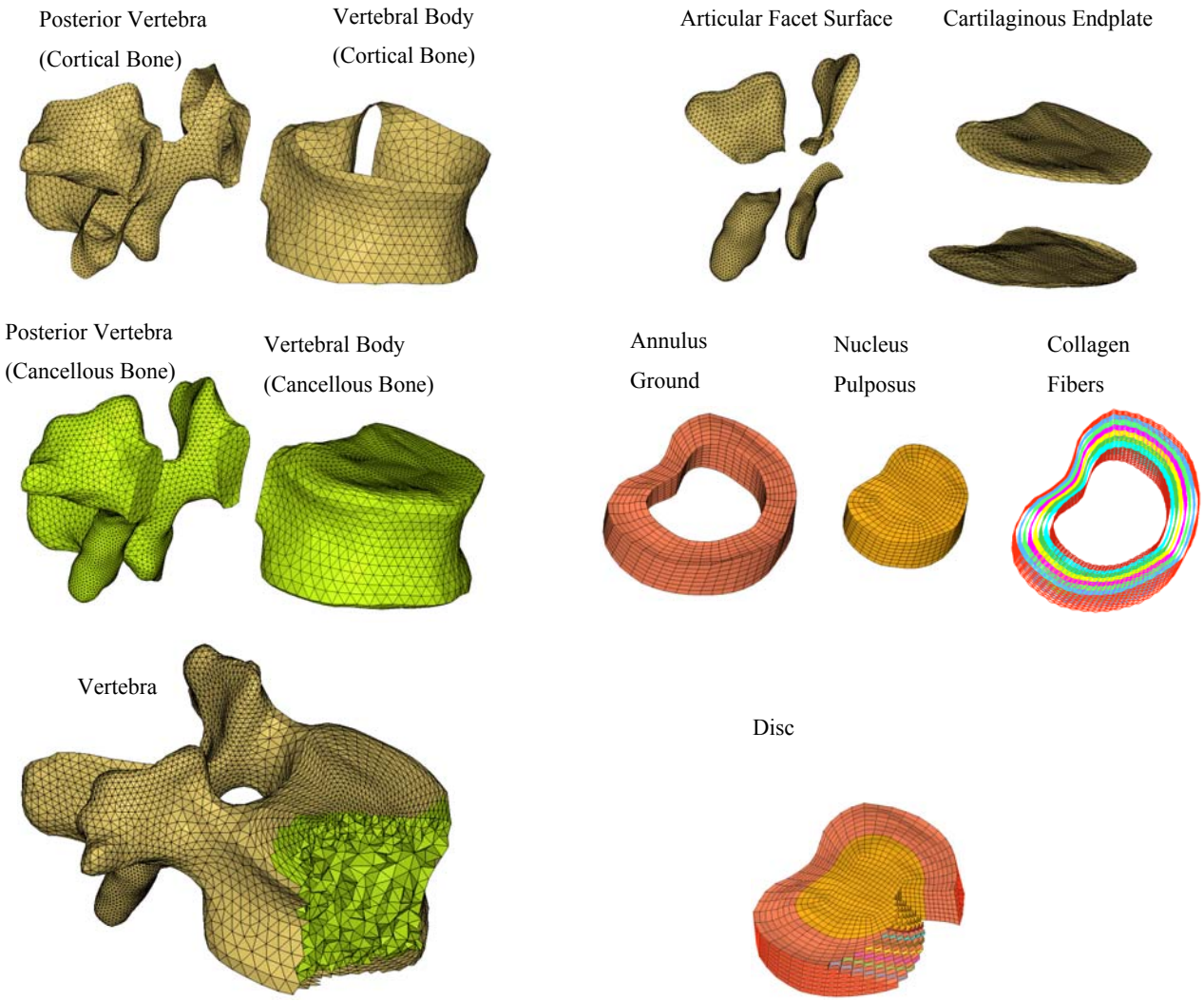


**Fig. 2.7.** Details of the mesh of the FE model.

**Table 2.2.** Material properties of the vertebrae (Schmidt et al., 2007; Goto et al., 2003).

| | E (MPa) | *v* |
|---|---|---|
| Cortical Bone | 12000 | 0.30 |
| Cancellous Bone | 200 | 0.25 |
| Cartilaginous Endplate | 23.8 | 0.40 |

*Discs*

The intervertebral disc is a complex structure that experiences large deformations because of its role in resisting and transmitting loads. The nucleus pulposus is a gelatinous material which withstands compression while the annulus fibrosus carries tensile forces. Many FE models have simulated the nucleus using incompressible fluid cavity and the annulus as solid (Mustafy et al., 2015; Park et al., 2013; Little et al., 2008). Nonetheless, there are also other FE models that simulate the nucleus with solid elements governed by elastic or hyper-elastic material laws low stiffness and extremely high poisson's ratio (*v*) (Ayturk and Puttlitz, 2011; El-Rich et al., 2009; Schmidt et al., 2007; Chen et al., 2001). Both options were tested in the current model and no significant difference in the disc behavior was found. Thus, solid elements with hyper-elastic behavior were used to simulate nucleus because of its reasonable accuracy and computational efficiency. First-order of the Mooney–Rivlin formulation was adopted for the annulus ground and nucleus. The coefficients were taken from the literature (El-Rich et al., 2009; Schmidt et al., 2007) (Table 2.3). Creep/relaxation and swelling/osmolarity (Schmidt et al., 2013) of the disc were ignored.

**Table 2.3.** Material properties of the intervertebral disc.

| | C10 | C01 |
|---|---|---|
| Annulus Ground Substance | 0.18 | 0.045 |
| Nucleus Pulposus | 0.12 | 0.030 |

The annulus ground is made of a multilayer fibrocartilage with highly aligned collagen fiber networks within discrete layers. These fibers resist tension only and their stiffness reduces from outer layer to inner layer. This change is due to both structural (reduction of the cross section area) and material (reduction of the cross elasticity constants) properties as presented in Table 2.4. The annular fibers make about 16% of the total volume of the annulus ground (Shirazi-Adl et al., 1986). The current model used force-displacement curves (Fig. 2.8) as the fibers were simulated by nonlinear springs. These curves were derived from the stress-strain relationship

proposed by Schmidt et al. (2006) and Shirazi-Adl et al. (1986) and by using the geometrical measures of the disc.

**Table 2.4.** Distribution of the annular fiber properties among layers (Shirazi-Adl et al., 1986).

| | Outer Layer | Mid-Layers | | Inner Layer |
|---|---|---|---|---|
| Ratio of Cross Section Area | 1.0 | 0.78 | 0.62 | 0.47 |
| Ratio of Elasticity Constants | 1.0 | 0.90 | 0.65 | 0.65 |

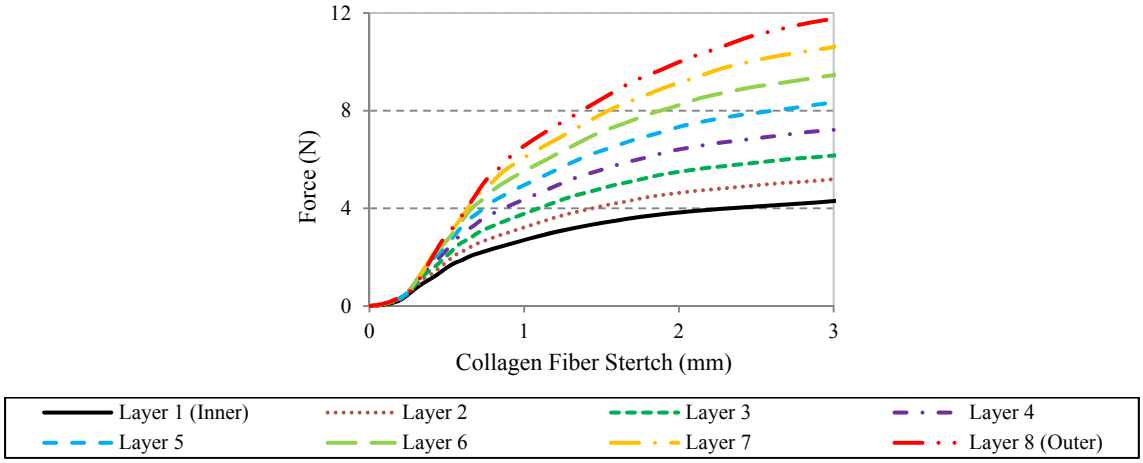


**Fig. 2.8.** Force displacement relationship of the annular fibers.

*Ligaments*

Each ligament can be simply represented by a set of unidirectional elements resisting tension only. Two types of elements are commonly used in FE models to simulate ligaments; elements that explicitly include geometrical (cross section area) and material (modulus of elasticity) property of the ligament like beam, truss/bar and cable elements (Park et al., 2013; Little et al., 2008; Chen et al., 2001) or elements that use ligament stiffness like spring elements (Rohlmann et al., 2006). However, the former elements will not predict accurately the ligament behavior in large deformation conditions if they use small deformation theory (Sharma et al., 1995). The advantage of spring elements is that they can have nonlinear stiffness that takes into account a wide range of strains. Ligaments of the current model used nonlinear stiffnesses adopted from Rohlmann et al. (2006) (Table 2.5). The resulting nonlinear force displacement curves (Fig. 2.9) were determined based on the average length of ligaments.

**Table 2.5.** Nonlinear stiffness of the ligaments.

| *Ligaments* | *ε (%)* | *k (N/mm)* | *ε (%)* | *k (N/mm)* | *ε (%)* | *k (N/mm)* | *ε (%)* | *k (N/mm)* |
|---|---|---|---|---|---|---|---|---|
| ALL | ε < 0 | 0 | 0 < ε < 12.2 | 347 | 12.2 < ε < 20.3 | 787 | 20.3 < ε | 1864 |
| PLL | | | 0 < ε < 11.1 | 29.5 | 11.1 < ε < 23 | 61.7 | 23 < ε | 236 |
| CL | | | 0 < ε < 25 | 36 | 25 < ε < 30 | 159 | 30 < ε | 384 |
| ITL | | | 0 < ε < 18.2 | 0.3 | 18.2 < ε < 23.3 | 1.8 | 23.3 < ε | 10.7 |
| LF | | | 0 < ε < 5.9 | 7.7 | 5.9 < ε < 49 | 9.6 | 49 < ε | 58.2 |
| SSL | | | 0 < ε < 20 | 2.5 | 20 < ε < 25 | 5.3 | 25 < ε | 34 |
| ISL | | | 0 < ε < 13.9 | 1.4 | 13.9 < ε < 20 | 1.5 | 20 < ε | 14.7 |

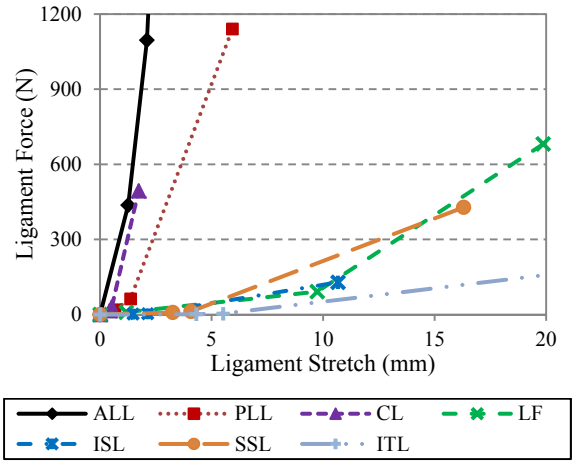


**Fig. 2.9.** Force-displacement curves of ligaments.

*Articular Facet Joints*

Two adjacent facet processes form the facet joint between two vertebrae. The capsular ligament connects the facet surfaces in the periphery boundary to create a closed volume which is filled by synovial fluid. The synovial fluid and cartilaginous surfaces of the facet joints provide the articulation in the facet joint. This complex structure is difficult to model numerically. It was tried in this study to use 2D capsular ligament to cover the joint and assign incompressible fluid cavity instead of synovial fluid. Nonetheless, the model would not converge due to distortion of the capsular ligament elements and the contact problem between ligaments and facet processes. In FE models, generally, the facet joint articulation is simply defined by contact between two adjacent articular facets (Dreischarf et al., 2014). Therefore, a frictionless surface to surface contact with minimum gap distance equal to 2 mm was used to simulate the facet joint articulation.

### 2.3.4. Loading and boundary conditions

Real loading conditions of the human spine are very complicated and not fully charactrized. The loading conditions used in this study were limited to the sagittal movement. Applying the trunk weight and taking into account the muscle forces is apprantly the most realistic loading mode (Rohlmann et al., 2006; Arjmand and Shirazi-Adl, 2005; El-Rich et al., 2004; Goel et al., 1993), though it is very complex due to redundacy of the system. Ignoring the muscle forces and applying only trunk weight irrespective of the loading mode (gravity load applied either at one level or distributed along the spine) can cause spinal instabilities and result in large deformations which is not consistent with physiological conditions (Kiefer et al., 1997).

In a search for loading configurations that stabilize the spine, the computed passive ligamentous lumbosacral and thoracolumbar spinal compression load-bearing capacities were found to substantially increase when the compression loads were applied through wrapping cables (i.e. cables that pass through the spine to follow the curvature) (Shirazi and Parnianpour, 2000) . This was performed by applying follower load (FL) (Renner et al., 2007) or wrapping element (Shirazi-Adl, 2006). The FL concept was used in this study because of its simplicity. It is a compressive force that passes though the vertebral bodies and follows the spine curvature (Fig. 2.10).

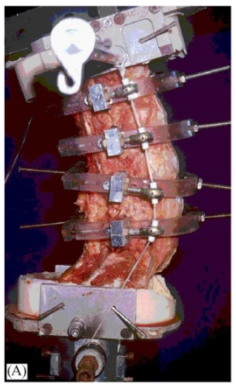


**Fig. 2.10.** Lateral view of the *in-vitro* follower load technique (Adopted from Renner et al., 2007).

In addition to the FL, a bending moment was applied to simulate flexed/extended posture. A moment was applied to ensure that the magnitude remains equal and constant at all spinal levels and to avoid any artifact deformations (Panjabi, 2007).

The FL combined with moment is a simplified loading mode which can simulate the flexed/extended posture of the spine when it lacks muscles. It is a reasonable approximation of the real loading condition and has been used commonly in the FE studies (Rohlmann et al., 2009). Nonetheless, there are some concerns regarding the capability of this simplified load to deliver realistic physiological conditions. Particularly, the magnitudes of the FL and moment for which predictions of the FE models approach better the *in-vivo* data are still controversial. This loading mode will be extensively discussed and elaborated in chapter 4.

## 2.4. Spinal response

Spinal response to mechanical loading is usually characterized by spine kinematics (range of motion, intervertebral rotation IVRs) and internal loads (stress/strain, forces, moment) developed in the spinal structures.

### 2.4.1. Kinematics

The total rotation of the vertebra L1 with respect to the vertebral L5 or sacrum, depending if the model considers the lumbar spine only or includes the sacrum, describes the total range of motion. By plotting the applied moment versus the total rotation, the flexural stiffness of the spine can be determined. The relative rotation of a vertebra with respect to its adjacent vertebra is called intervertebral rotation (IVR). Measuring these rotations *in-vivo* and *in-vitro* is common in experimental studies of the spine (Rohlmann et al., 2001; Lin et al., 1994; Panjabi et al., 1994; Yamamoto et al., 1989; Pearcy et al., 1984). This data served to validate most of the lumbar spine FE models (Ibarz et al., 2013; Park et al., 2013; Goto et al., 2003; Chen et al., 2001).

Translational movements due to axial deformation and intervertebral shearing also occur during spinal movements. However, their measurement is challenging and involves a lot of uncertainties.

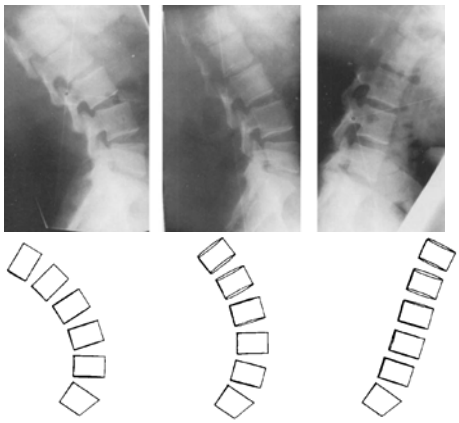

**Fig. 2.11.** Lumbar spine after flexion extension movement (Adopted from Pearcy et al., 1984).

### 2.4.2. Internal loads

*Stress/Pressure*

Spinal loads refer to loads developed in each load-bearing component of the spine. Intradiscal pressure (IDP) which refers to the pressure inside the nucleus pulposus (Fig. 2.12), is one of the most important parameters assessed in experimental (Wilke et al., 2001; Sato et al., 1999; Brinckmann and Grootenboer, 1991) and numerical studies (Dreischarf et al., 2014). IDP is one of the determinant parameters which many FE models use for validation purposes. For instance, it was the only parameter studied to determine the magnitude of the FL in the work of Rohlmann et al. (2009a,b). Although a relation between disc compression and IDP was reported in an *in-vitro* study (Brinckmann and Grootenboer, 1991), it is hardly possible to determine this relation in *in-vivo* conditions (Dreischarf et al., 2013).

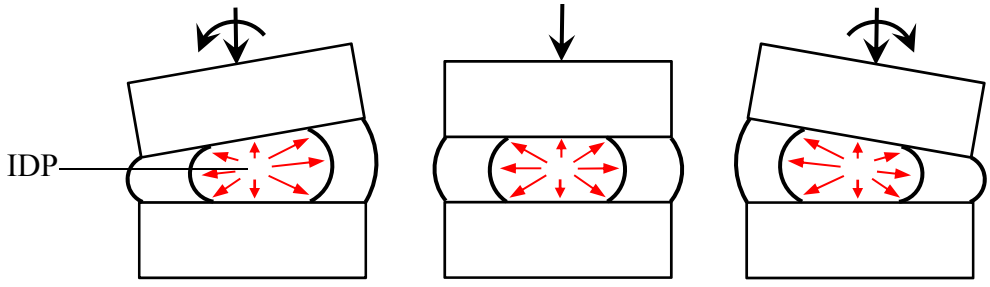


**Fig. 2.12.** Schematic intradiscal pressure (IDP) in the nucleus pulposus under various loading modes.

Assessing strain of the annular fibers gives an idea about states of stress in the annulus ground when the disc is loaded. The pressure developed in the nucleus creates tension in the annulus fibrosus (Fig. 2.12) which is mainly resisted by the fibers especially those located in the inner layers. The posterior and anterior fibers experience higher strain under flexion and extension moments, respectively (Fig. 2.13, Schmidt et al., 2007).

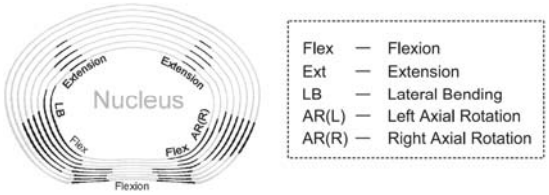


**Fig. 2.13.** Location of the predicted tensile strains in the annular fibers under pure moments (Adopted from Schmidt et al., 2007).

Stress also develops in the vertebrae under different loading modes. These stresses are high in high rate of impact conditions (Terai et al., 2010; El-Rich et al., 2009; El-Rich et al., 2006) and should be considered if failure of bone is of interest which is out of the scope of this research.

*Force/Moment*

The load bearing components of the ligamentous spine are the disc, facet joints and ligaments. The ligaments are tension only resisting components while the facet joints are responsible for articulation between two adjacent vertebrae in the posterior area. In this articulation a contact between two adjacent facet surfaces occurs which creates contact force called facet join force (FJF). This articulation plays important role in resisting extension movement and reducing the ROM. In flexion movement, the facet surfaces of the same articular joint separate usually which create zero contact forces unless the flexion movement is associated with high axial compressive forces. The disc is the most important load bearing component which withstands force and moment. Finding internal force and moment in discs of a 3D FE model is not straight forward due to complex structure which includes nucleus pulposus, annulus ground substance and collagen fibers. However, the disc loads can be predicted directly in simplified models that simulate the disc with 3D beam element (Arjmand and Shirazi-Adl, 2005; El-Rich et al., 2004).

Measuring the disc loads in *in-vivo* conditions is very challenging. To our best knowledge, there is no data available on disc loads measured in healthy person. Nevertheless, there are some

reported forces measured from implant acting on a vertebral body replacement (Dreischarf et al., 2015) but these forces may not represent normal persons. Also, there is no *in-vivo* data on the FJF, all the reported values were measured on cadaveric spines (Wilson et al., 2006). Tensile strain in ligament is usually measured instead of ligament force. Panjabi et al. (1982) reported physiologic strains in the lumbar spinal ligaments measured *in-vitro*.

### 2.4.3. Spinal load-sharing

The discs, ligaments, and facet joints (passive structures) are responsible of bearing spinal loads while muscles (active structures) facilitate the movement and are mostly responsible for stabilization of the spine. A harmonic synergy between the passive and active components of the spine is necessary to maintain its normal function. Dysfunction of any spinal component results in system perturbation which may lead to immediate compensation from other components, long-term adaptation response and/or ultimately injury (Panjabi, 1992). Therefore, understanding the interaction of spinal components and their relative contribution in load bearing is crucial to the spine function.

For instance *in-vitro* experiments by Pollintine et al. (2004) showed that in a healthy spinal segment about 92% of the axial load is carried by the disc and the rest by the neural arch in the standing posture (Fig. 2.14). A degenerated disc loses its load bearing efficiency and a major portion of the load transfers toward the neural arch. If a healthy segment undergoes forward flexion load-sharing of the disc becomes higher and almost no load goes to neural arch which reveals that disc load-sharing in forward bending is not effected by the disc status (healthy or degenerated) (Fig. 2.14). This finding was found by employing the superposition concept i.e. subsequent dissection of the spinal components. Otherwise, measuring experimentally the load-sharing in an intact spinal segment is difficult due to the indeterminacy of the system. The experimental data available are useful for model validation. Spinal load-sharing can be determined by optimization with reasonable accuracy if appropriate objective function with adequate constraints is defined (Goel et al., 1987). Nonetheless, FE models can predict load-sharing of not only spinal segment but the entire spine. Load-sharing in three spines with different geometry was compared in Chapter 5.

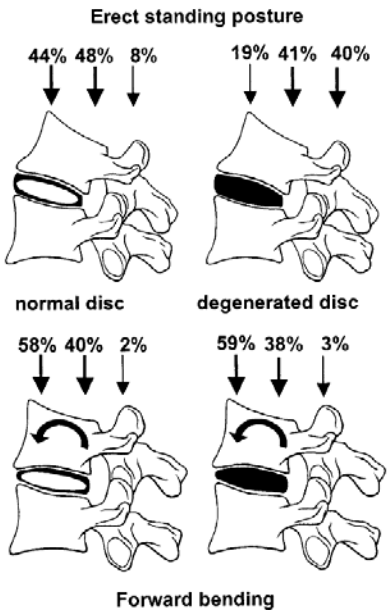


**Fig. 2.14.** The effects of posture and disc degeneration on spinal load-sharing (Adopted from Pollintine et al., 2004).

**References**

Adams, M.A., Mannion, A.F., Dolan, P., 1999. Personal risk factors for first-time low back pain. Spine 24, 2497-2505.

Arjmand N., Shirazi-Adl, A., 2005. Biomechanics of changes in lumbar posture in static lifting. Spine 30, 2637-48.

Ayturk, U.M., Puttlitz, C.M., 2011. Parametric Convergence Sensitivity and Validation of a Finite Element Model of the Human Lumbar Spine. Computer Methods in Biomechanics and Biomedical Engineering 14, 695-705.

Ayturk, U.M., Puttlitz, C.M., 2011. Parametric Convergence Sensitivity and Validation of a Finite Element Model of the Human Lumbar Spine. Computer Methods in Biomechanics and Biomedical Engineering 14, 695-705.

Breau, C., Shirazi-Adl, A., de Guise, J., 1991. Reconstruction of a Human Ligamentous Lumbar Spine using CT Images--a Three-Dimensional Finite Element Mesh Generation. Annals of Biomedical Engineering 19, 291-302.

Brinckmann, P., Grootenboer, H., 1991. Change of disc height, radial disc bulge, and intradiscal pressure from discectomy. An in vitro investigation on human lumbar discs. Spine 16, 641-646.

Chaleat-Valayer, E., Mac-Thiong, J.M., Paquet, J., Berthonnaud, E., Siani, F., Roussouly, P., 2011. Sagittal spino-pelvic alignment in chronic low back pain. European Spine Journal : Official Publication of the European Spine Society, the European Spinal Deformity Society, and the European Section of the Cervical Spine Research Society 20, 634-640.

Chen, C. S., Cheng, C. K., Liu, C. L., Lo, W.H., 2001. Stress Analysis of the Disc Adjacent to Interbody Fusion in Lumbar Spine. Medical Engineering & Physics 23, 483-491.

Chen, C.S., Cheng, C.K., Liu, C.L., Lo, W.H., 2001. Stress Analysis of the Disc Adjacent to Interbody Fusion in Lumbar Spine. Medical Engineering & Physics 23, 483-491.

Christie, H.J., Kumar, S., Warren, S.A., 1995. Postural aberrations in low back pain. Archives of Physical Medicine and Rehabilitation 76, 218-224.

De Smet, A.A., 1985. Radiographic Evaluation, Chapter 2. Radiology of Spinal Curvature, Edited by A. A. De Smet. St. Louis, CV Mosby Company, 23-58.

Deyo, R.A., Weinstein, J.N., 2001. Low Back Pain. The New England Journal of Medicine 344, 363-370.

Dreischarf, M., Albiol, L., Zander, T., Arshad, R., Graichen, F., Bergmann, G., Schmidt, H., Rohlmann, A., 2015. In Vivo Implant Forces Acting on a Vertebral Body Replacement during Upper Body Flexion. Journal of Biomechanics 48, 560-565.

Dreischarf, M., Rohlmann, A., Zhu, R., Schmidt, H., Zander,T., 2013. Is it Possible to Estimate the Compressive Force in the Lumbar Spine from Intradiscal Pressure Measurements? A Finite Element Evaluation. Medical Engineering & Physics, 35, 1385-1390.

Dreischarf, M., Zander, T., Shirazi-Adl, A., Puttlitz, C.M., Adam, C.J., Chen, C.S., Goel, V.K., Kiapour, A., Kim, Y.H., Labus, K.M., Little, J.P., Park, W.M., Wang, Y.H., Wilke, H.J., Rohlmann, A., Schmidt, H., 2014. Comparison of Eight Published Static Finite Element Models of the Intact Lumbar Spine: Predictive Power of Models Improves when Combined Together. Journal of Biomechanics 47, 1757-1766.

El-Rich, M., Arnoux, P., Wagnac, E., Brunet, C., Aubin, C.E., 2009. Finite Element Investigation of the Loading Rate Effect on the Spinal Load-Sharing Changes Under Impact Conditions. Journal of Biomechanics 42, 1252-1262.

El-Rich, M., Aubin, C.E., Villemure, I., Labelle, H., 2006. A Biomechanical Study of L5-S1 Low-Grade Isthmic Spondylolisthesis using a Personalized Finite Element Model. Studies in Health Technology and Informatics 123, 431-434.

El-Rich, M., Shirazi-Adl., A, Arjmand, N., 2004. Muscle activity, internal loads, and stability of the human spine in standing postures: combined model and in vivo studies. Spine 29, 2633-42.

Goel, V.K., Kong, W., Han, J.S., Weinstein, J.N., Gilbertson, L.G., 1993. A Combined Finite Element and Optimization Investigation of Lumbar Spine Mechanics with and without Muscles. Spine 18, 1531-1541.

Goel, V.K., Winterbottom, J.M., Weinstein, J.N., Kim, Y.E., 1987. Load Sharing among Spinal Elements of a Motion Segment in Extension and Lateral Bending. Journal of Biomechanical Engineering 109, 291-297.

Goto, K., Tajima, N., Chosa, E., Totoribe, K., Kubo, S., Kuroki, H., Arai, T., 2003. Effects of Lumbar Spinal Fusion on the Other Lumbar Intervertebral Levels (Three-Dimensional Finite Element Analysis). Journal of Orthopaedic Science : Official Journal of the Japanese Orthopaedic Association 8, 577-584.

Harrison, D.D., Cailliet, R., Janik, T.J., Troyanovich, S.J., Harrison, D.E., Holland, B., 1998. Elliptical modeling of the sagittal lumbar lordosis and segmental rotation angles as a method to discriminate between normal and low back pain subjects. Journal of Spinal Disorders, 11, 430-439.

Harrison, D.E., Harrison, D.D., Troyanovich, S.J., Harmon, S., 2000. A normal spinal position: It's time to accept the evidence. Journal of Manipulative and Physiological Therapeutics 23, 623-644.

Ibarz, E., Herrera, A., Mas, Y., Rodriguez-Vela, J., Cegonino, J., Puertolas, S., Gracia, L., 2013. Development and Kinematic Verification of a Finite Element Model for the Lumbar Spine: Application to Disc Degeneration. BioMed Research International 2013, 705185.

Jackson, R.P., McManus, A.C., 1994. Radiographic analysis of sagittal plane alignment and balance in standing volunteers and patients with low back pain matched for age, sex, and size. A prospective controlled clinical study. Spine 19, 1611-1618.

Kiefer, A., Shirazi-Adl, A., Parnianpour, M., 1997. Stability of the Human Spine in Neutral Postures. European Spine Journal : Official Publication of the European Spine Society, the European Spinal Deformity Society, and the European Section of the Cervical Spine Research Society 6, 45-53.

Korovessis, P., Stamatakis, M., Baikousis, A., 1999. Segmental roentgenographic analysis of vertebral inclination on sagittal plane in asymptomatic versus chronic low back pain patients. Journal of Spinal Disorders 12, 131-137.

Lin, R.M., Yu, C.Y., Chang, Z.J., Lee, C.C., Su, F.C., 1994. Flexion-Extension Rhythm in the Lumbosacral Spine. Spine 19, 2204-2209.

Little, J.P., de Visser, H., Pearcy, M.J., Adam, C.J., 2008. Are Coupled Rotations in the Lumbar Spine Largely due to the Osseo-Ligamentous Anatomy?-a Modeling Study. Computer Methods in Biomechanics and Biomedical Engineering 11, 95-103.

Manchikanti, L., Singh, V., Datta, S., Cohen, S.P., Hirsch, J.A., 2009. Comprehensive Review of Epidemiology, Scope, and Impact of Spinal Pain. Pain Physician, 12, E35-70.

Mustafy, T., Moglo, K., Adeeb, S., El-Rich, M., 2015. Injury mechanisms of the ligamentous cervical C2-C3 Functional Spinal Unit to complex loading modes: Finite Element study. Journal of the Mechanical Behavior of Biomedical Materials, 53, 384-396.

Panjabi, M.M., 1992. The Stabilizing System of the Spine. Part I. Function, Dysfunction, Adaptation, and Enhancement. Journal of Spinal Disorders 5, 383-389, discussion 397.

Panjabi, M.M., 2003. Clinical spinal instability and low back pain. Journal of Electromyography and Kinesiology 13, 371-379.

Panjabi, M.M., 2007. Hybrid Multidirectional Test Method to Evaluate Spinal Adjacent-Level Effects. Clinical Biomechanics (Bristol, Avon) 22, 257-265.

Panjabi, M.M., Goel, V.K., Takata, K., 1982. Physiologic Strains in the Lumbar Spinal Ligaments. an in Vitro Biomechanical Study 1981 Volvo Award in Biomechanics. Spine 7, 192-203.

Panjabi, M.M., Oxland, T.R., Yamamoto, I., Crisco, J.J., 1994. Mechanical Behavior of the Human Lumbar and Lumbosacral Spine as shown by Three-Dimensional Load-Displacement Curves. The Journal of Bone and Joint Surgery. American Volume 76, 413-424.

Park, W. M., Kim, K., Kim, Y. H., 2013. Effects of Degenerated Intervertebral Discs on Intersegmental Rotations, Intradiscal Pressures, and Facet Joint Forces of the Whole Lumbar Spine. Computers in Biology and Medicine 43, 1234-1240.

Park, W.M., Kim, K., Kim, Y.H., 2013. Effects of Degenerated Intervertebral Discs on Intersegmental Rotations, Intradiscal Pressures, and Facet Joint Forces of the Whole Lumbar Spine. Computers in Biology and Medicine 43, 1234-124.

Pearcy, M., Portek, I., Shepherd, J., 1984. Three-Dimensional x-Ray Analysis of Normal Movement in the Lumbar Spine. Spine 9, 294-297.

Pollintine, P., Dolan, P., Tobias, J.H., Adams, M.A., 2004. Intervertebral Disc Degeneration can Lead to "Stress-Shielding" of the Anterior Vertebral Body: A Cause of Osteoporotic Vertebral Fracture? Spine 29, 774-782.

Pope, M.H., Novotny, J.E., 1993. Spinal Biomechanics. Journal of Biomechanical Engineering 115, 569-574.

Propst-Proctor, S.L., Bleck, E.E., 1983. Radiographic determination of lordosis and kyphosis in normal and scoliotic children. Journal of Pediatric Orthopedics 3, 344-346.

Renner, S.M., Natarajan, R.N., Patwardhan, A.G., Havey, R.M., Voronov, L.I., Guo, B.Y., Andersson, G.B., An, H.S., 2007. Novel Model to Analyze the Effect of a Large Compressive Follower Pre-Load on Range of Motions in a Lumbar Spine. Journal of Biomechanics 40, 1326-1332.

Rohlmann, A., Bauer, L., Zander, T., Bergmann, G., Wilke, H.J., 2006. Determination of Trunk Muscle Forces for Flexion and Extension by using a Validated Finite Element Model of the Lumbar Spine and Measured in Vivo Data. Journal of Biomechanics 39, 981-989.

Rohlmann, A., Neller, S., Claes, L., Bergmann, G., Wilke, H.J., 2001. Influence of a follower load on intradiscal pressure and intersegmental rotation of the lumbar spine. Spine 26, E557-E561.

Rohlmann, A., Zander, T., Rao, M., Bergmann, G., 2009. Realistic Loading Conditions for Upper Body Bending. Journal of Biomechanics 42, 884-890.

Rohlmann, A., Zander, T., Rao, M., Bergmann, G., 2009a. Applying a Follower Load Delivers Realistic Results for Simulating Standing. Journal of Biomechanics 42, 1520-1526.

Rohlmann, A., Zander, T., Rao, M., Bergmann, G., 2009b. Realistic Loading Conditions for Upper Body Bending. Journal of Biomechanics 42, 884-890.

Roussouly, P., Berthonnaud, E., Dimnet, J., 2003. Geometrical and Mechanical Analysis of Lumbar Lordosis in an Asymptomatic Population: Proposed Classification," Revue Du Chirurgie Orthopedique Et Traumatologique 89, 632-639.

Roussouly, P., Gollogly, S., Berthonnaud, E., Dimnet,J., 2005. Classification of the Normal Variation in the Sagittal Alignment of the Human Lumbar Spine and Pelvis in the Standing Position. Spine 30, 346-353.

Roussouly, P., Pinheiro-Franco, J.L., 2011. Biomechanical Analysis of the Spino-Pelvic Organization and Adaptation in Pathology. European Spine Journal 20, S609-S618.

Rubin, D.I., 2007. Epidemiology and Risk Factors for Spine Pain. Neurologic Clinics, 25, 353-371.

Sato, K., Kikuchi, S., Yonezawa, T., 1999. In Vivo Intradiscal Pressure Measurement in Healthy Individuals and in Patients with Ongoing Back Problems. Spine 24, 2468-2474.

Schmidt, H., Galbusera, F., Rohlmann, A., Shirazi-Adl,A., 2013. What have we Learned from Finite Element Model Studies of Lumbar Intervertebral Discs in the Past Four Decades? Journal of Biomechanics 46, 2342-2355.

Schmidt, H., Heuer, F., Simon, U., Kettler, A., Rohlmann, A., Claes, L., Wilke, H.J., 2006. Application of a New Calibration Method for a Three-Dimensional Finite Element Model of a Human Lumbar Annulus Fibrosus. Clinical Biomechanics 21, 337-344.

Schmidt, H., Kettler, A., Heuer, F., Simon, U., Claes, L., Wilke, H.J., 2007. Intradiscal Pressure, Shear Strain, and Fiber Strain in the Intervertebral Disc Under Combined Loading. Spine 32, 748-755.

Sharma, M., Langrana, N. A., Rodriguez, J., 1995. Role of Ligaments and Facets in Lumbar Spinal Stability. Spine, 20, 887-900.

Shirazi-Adl, A., 2006. Analysis of Large Compression Loads on Lumbar Spine in Flexion and in Torsion using a Novel Wrapping Element. Journal of Biomechanics 39, 267-275.

Shirazi-Adl, A., Ahmed, A.M., Shrivastava, S.C., 1986. Mechanical Response of a Lumbar Motion Segment in Axial Torque Alone and Combined with Compression. Spine 11, 914-927.

Shirazi-Adl, A., Parnianpour, M., 2000. Load-bearing and stress analysis of the human spine under a novel wrapping compression loading. Clinical Biomechanics 15, 718–725

Stagnara, P., De Mauroy, J. C., Dran, G., Gonon, G. P., Costanzo, G., Dimnet, J., & Pasquet, A. (1982). Reciprocal angulation of vertebral bodies in a sagittal plane: Approach to references for the evaluation of kyphosis and lordosis. Spine, 7(4), 335-342.

Terai, T., Sairyo, K., Goel, V.K., Ebraheim, N., Biyani, A., Faizan, A., Sakai, T., Yasui, N., 2010. Spondylolysis Originates in the Ventral Aspect of the Pars Interarticularis: A Clinical and Biomechanical Study. Journal of Bone and Joint Surger (Br) 98, 1123-1127.

Trainor, T.J., Wiesel, S.W., 2002. Epidemiology of back pain in the athlete. Clinics in Sports Medicine 21, 93-103.

Wilke, H., Neef, P., Hinz, B., Seidel, H., Claes, L., 2001. Intradiscal Pressure Together with Anthropometric Data--a Data Set for the Validation of Models. Clinical Biomechanics (Bristol, Avon) 16, S111-26.

Wilson, D.C., Niosi, C.A., Zhu, Q.A., Oxland, T.R., Wilson, D.R., 2006. Accuracy and repeatability of a new method for measuring facet loads in the lumbar spine. Journal of Biomechanics 39, 348-353.

Yamamoto, I., Panjabi, M.M., Crisco, T., Oxland, T., 1989. Three-Dimensional Movements of the Whole Lumbar Spine and Lumbosacral Joint. Spine 14, 1256-1260.

# Chapter 3

# On the Load-Sharing Along the Ligamentous Lumbosacral Spine in Flexed and Extended Postures: Finite Element Study

This chapter has been published as Naserkhaki, S., Jaremko, J.L., Adeeb, S., El-Rich, M., 2015. Journal of Biomechanics, DOI: ttp://dx.doi.org/10.1016/j.jbiomech.2015.09.050.

**Abstract**

A harmonic synergy between the load-bearing and stabilizing components of the spine is necessary to maintain its normal function. This study aimed to investigate the load-sharing along the ligamentous lumbosacral spine under sagittal loading. A 3D nonlinear detailed Finite Element (FE) model of lumbosacral spine with realistic geometry was developed and validated using wide range of numerical and experimental (*in-vivo* and *in-vitro*) data. The model was subjected to 500 N compressive Follower Load (FL) combined with 7.5 Nm flexion (FLX) or extension (EXT) moments. Load-sharing was expressed as percentage of total internal force/moment developed along the spine that each spinal component carried. These internal forces and moments were determined at the discs centers and included the applied load and the resisting forces in the ligaments and facet joints. The contribution of the facet joints and ligaments in supporting bending moments produced additional forces and moments in the discs.

The intervertebral discs carried up to 81% and 68% of the total internal force in case of FL combined with FLX and EXT, respectively. The ligaments withstood up to 67% and 81% of the total internal moment in cases of FL combined with EXT and FLX, respectively. Contribution of the facet joints in resisting internal force and moment was noticeable at levels L4-S1 only particularly in case of FL combined with EXT and reached up 29% and 52% of the internal moment and force, respectively. This study demonstrated that spinal load-sharing depended on applied load and varied along the spine.

**Keywords:** lumbosacral spine; internal loads; load-sharing; spinal synergy; finite element analysis; static equilibrium; follower load; extension; flexion.

### 3.1. Introduction

A harmonic synergy between the load-bearing and stabilizing components of the spine is necessary to maintain its normal function. The ligamentous spine (devoid of muscles) which includes: vertebrae, endplates, discs, facet joints and ligaments is responsible for carrying and transferring loads to the hip and lower joints whereas the spine muscles provide both passive and active actions to maintain the spine stability. The biomechanical response of the ligamentous lumbar spine to mechanical load in terms of range of motion (ROM), intervertebral rotations (IVR), facet joints forces (FJF), intradiscal pressure (IDP) in the nucleus pulposus, and stress in the annulus fibrosus has been comprehensively studied (Park et al., 2013; Schmidt et al., 2010; Little et al., 2008; Goto et al., 2003). Forces in the spinal ligaments (Alapan et al., 2014; Wang et al., 1999) as well as forces and moments in the discs (Arjmand and Shirazi-Adl, 2006; El-Rich et al., 2004) were also predicted. Dysfunction of any spinal component results in system perturbation which may lead to immediate compensation from other components, long-term adaptation response and/or ultimately injury (Panjabi, 1992). Therefore, understanding the interaction of spinal components and their relative contribution in load-bearing (spinal load-sharing) is crucial to the spine function.

The load-sharing in cadaveric lumbar Functional Spinal Units (FSUs) subjected to extension (Adams et al., 1988) as well as flexion (Adams et al., 1980) has been investigated by removing the FSU's components one by one and then comparing the responses of the altered and intact FSUs. Similar approach was used in a numerical study conducted by Sharma et al. (1995) in which the effect of ligaments and facet joints partial/total removal on rotational instabilities of lumbar FSU was investigated. This approach provided important insights onto the role of each spinal component in the functional mechanism of an altered FSU after ligaments removal, facetectomy, or nucleotomy (Ivicsics et al., 2014; Noailly et al., 2007; Najarian et al., 2005; Sharma et al., 1995). However, using this superposition approach is not appropriate to explain the load-sharing in an intact FSU or a whole spine as it neglects the nonlinear interaction between spinal components while carrying load.

On the other hand, static equilibrium equations were used to estimate the forces in lumbar FSUs subjected to extension/lateral bending coupled or not with compressive preload (Goel et al., 1987). The multibody approach was also employed to study the load-sharing of the lumbar L4-5 FSU under extension/flexion moment (Abouhossein et al., 2011). The load-sharing in cervical

FSUs was also studied by comparing the strain energy (Mustafy et al., 2014) and load carrying proportion (Panzer and Cronin, 2009; Goel and Clausen, 1998) among the spinal components using the Finite Element (FE) method.

The aforementioned studies have definitely provided valuable insight onto the spinal load-sharing, however, to our best knowledge there is no information on how spinal load-sharing varies with loading mode along the lumbosacral spine. This study aimed to investigate the load-sharing in the ligamentous lumbosacral spine under flexion (FLX) and extension (EXT) moment coupled with compressive follower load (FL) using nonlinear FE modeling. A 3D nonlinear detailed FE model with realistic geometry developed at tissue level was used. The responses of this model to various loading scenarios were compared to available numerical and experimental results (Dreischarf et al., 2014). The equilibrium conditions in all directions were satisfied at each spinal level to estimate the internal forces and moments in the spinal components. These internal loads were used to calculate the spinal load-sharing. In addition, the ROM, IVR, IDP, and strain in the annular fibers, were also determined.

## 3.2. Materials and methods

### 3.2.1. 3D geometry acquisition

3D geometry of the bony structures which consist of the vertebrae L1 through L5 (L1-5) and the sacrum was reconstructed from a 20 years old male CT-Scans of 1 mm thickness taken from the University of Alberta Hospital data base. Segmentation was performed using the medical image processing software Mimics (MIMICS Research 17.0, Materialise, Belgium). Then, the geometry was cleaned from spikes and sharp edges using the software Geomagic Studio (Geomagic Studio 2014, 3D Systems, USA) (Fig. 3.1a).

### 3.2.2. Mesh generation

The obtained geometry was meshed using the software Hypermesh (Hyperworks 12.0, Altair, USA) (Fig. 3.1b). The cortical bone and endplates were meshed using 3-node shell elements with a uniform thickness of 1 mm. The cortical bone was then filled with 4-node (tetrahedral) solid elements to represent the cancellous core. The mesh of two intervening endplates was used to create the disc by extruding 7 circumferential layers of solid elements for the annulus fibrosus ground enclosing the nucleus mesh (Fig. 3.1b). These layers were reinforced by unidirectional

springs distributed in concentric lamellae with crosswise pattern close to ±35° (El-Rich et al., 2009; Schmidt et al., 2007) to represent the annular fibers (Fig. 3.1b). The disc volume was divided with a proportion according to the histological findings (44%_nucleus and 56%_annulus) (El-Rich et al., 2009; Schmidt et al., 2006). The ligaments included the Anterior Longitudinal Ligament (ALL), Posterior Longitudinal Ligament (PLL), Capsular Ligament (CL), Intertransverse Ligament (ITL), Ligamentum Flavium (LF), Supraspinous Ligament (SSL), and Interspinous Ligament (ISL) and were modeled by unidirectional springs (Breau et al., 1991). A frictionless surface to surface contact with minimum gap distance equal to 2 mm was used to simulate the facet joint articulation. A fine mesh particularly in the facet joints areas was used to ensure the accuracy of the predicted response (Ayturk and Puttlitz, 2011).

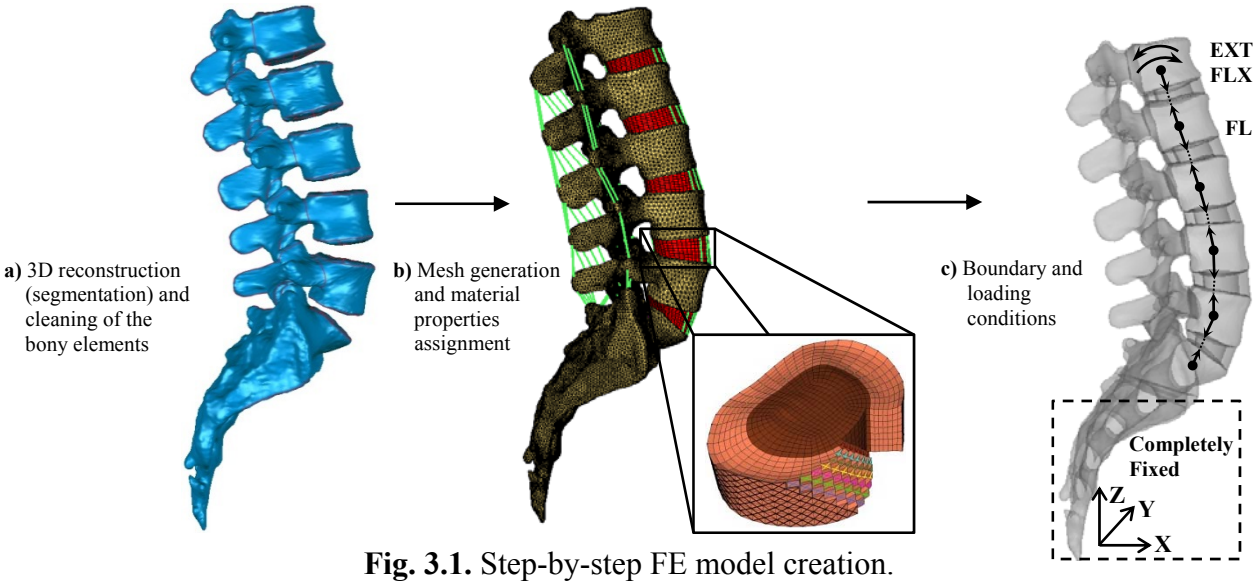


**Fig. 3.1.** Step-by-step FE model creation.

### 3.2.3. Material properties

The behavior of the bony structures and cartilaginous endplates was assumed linear elastic while the annulus and nucleus were governed by hyper-elastic material law using the first-order of Mooney–Rivlin formulation. The properties are summarized in Table 3.1. Nonlinear force displacement curves adopted from Rohlmann et al. (2006) (Table 3.1) were assigned to the ligament springs to resist tension only. The annular fibers had nonlinear force displacement relationship with stiffness increasing from inner to outer lamella (Schmidt et al., 2006; Shirazi et al., 1986).

**Table 3.1.** Material properties of the spinal components.

| *Spinal Components* | | *Material Behaviour* | *Mechanical Properties* | | *Reference* |
|---|---|---|---|---|---|
| **Bone** | Cortical Bone | Linear Elastic | E=12000 (MPa) | $\nu$=0.30 | *Park et al., 2013; Goto et al., 2003* |
| | Cartilaginous Endplate | | E=23.8 (MPa) | $\nu$=0.40 | *Schmidt et al., 2007; Goto et al., 2003* |
| | Cancellous Bone | | E=200 (MPa) | $\nu$=0.25 | *Shih et al., 2013; Schmidt et al., 2007* |
| **Disc** | Annulus Ground Substance | Hyper-Elastic (Mooney-Rivlin) | C10=0.18 | C01=0.045 | *El-Rich et al., 2009; Schmidt et al., 2007* |
| | Nucleus Pulposus | | C10=0.12 | C01=0.030 | |

| | | *Strain (%)* | *Stiffness (N/mm)* | *Strain (%)* | *Stiffness (N/mm)* | *Strain (%)* | *Stiffness (N/mm)* | *Strain (%)* | *Stiffness (N/mm)* | *Refe-rence* |
|---|---|---|---|---|---|---|---|---|---|---|
| **Ligaments** | ALL | $\varepsilon < 0$ | 0 | $0 < \varepsilon < 12.2$ | 347 | $12.2 < \varepsilon < 20.3$ | 787 | $20.3 < \varepsilon$ | 1864 | *Rohlmann et al. (2006)* |
| | PLL | | | $0 < \varepsilon < 11.1$ | 29.5 | $11.1 < \varepsilon < 23$ | 61.7 | $23 < \varepsilon$ | 236 | |
| | CL | | | $0 < \varepsilon < 25$ | 36 | $25 < \varepsilon < 30$ | 159 | $30 < \varepsilon$ | 384 | |
| | ITL | | | $0 < \varepsilon < 18.2$ | 0.3 | $18.2 < \varepsilon < 23.3$ | 1.8 | $23.3 < \varepsilon$ | 10.7 | |
| | LF | | | $0 < \varepsilon < 5.9$ | 7.7 | $5.9 < \varepsilon < 49$ | 9.6 | $49 < \varepsilon$ | 58.2 | |
| | SSL | | | $0 < \varepsilon < 20$ | 2.5 | $20 < \varepsilon < 25$ | 5.3 | $25 < \varepsilon$ | 34 | |
| | ISL | | | $0 < \varepsilon < 13.9$ | 1.4 | $13.9 < \varepsilon < 20$ | 1.5 | $20 < \varepsilon$ | 14.7 | |

### 3.2.4. Loading and boundary conditions

The FE analyses were conducted using the implicit solver of Abaqus (Abaqus 6.13-4, Dassault Systems Simulia Corp., USA). To minimize the intervertebral rotations and improve the spine stability under compression while it lacks muscles, the model was subjected to compressive FL whose line of action followed the spine curvature and passed through the vertebral bodies centroids (Fry et al., 2014; Kim et al., 2011, Renner et al., 2007; Shirazi-Adl, 2006). This FL was applied using pre-compressed unidirectional springs inserted between the centroids of two adjacent vertebral bodies (Fig. 3.1c) (Naserkhaki et al., 2014).

#### *Validation tests*

As the available numerical and experimental data used for validation correspond to the lumbar spine, only the segment L1-5 of the current model was used in the comparison (validation) tests. It was subjected to a FL of similar magnitude along the spine combined or not with EXT/FLX moments (Table 3.2) applied at the centroid of L1's vertebral body. The model response was compared to *in-vivo* and *in-vitro* data as well as the median response of eight published FE models (Dreischarf et al., 2014).

**Table 3.2.** Loading scenarios.

| | *Loading Combinations* | *FL (N)* | *Moment (Nm)* | *References* |
|---|---|---|---|---|
| Validation Tests | FL+EXT | 100 | 10 | *Panjabi et al., 1997* |
| | FL+FLX | 100 | 10 | |
| | EXT | - | 7.5 | *Heuer et al. 2007; Rohlmann et al., 2001* |
| | FLX | - | 7.5 | |
| | FL | 1000 | - | *Brinckmann and Grootenboer, 1991* |
| | FL+EXT | 500 | 7.5 | *Rohlmann et al., 2009* |
| | FL+FLX | 1175 | 7.5 | |
| Load-Sharing Study | FL+EXT | 500 | 7.5 | - |
| | FL+FLX | | 7.5 | |

***Load-sharing study***

The lumbosacral spine model was fixed at the lower sacrum level and free to move elsewhere (Fig. 3.1c). A FL of 500 N was initially applied to the model and then coupled with 7.5 Nm EXT/FLX moments.

### 3.2.5. Load-sharing calculation

At the deformed configuration, an imaginary section was created at each segmental level and Free Body Diagrams (FBDs) of the upper vertebrae were drawn. The internal forces and moments in the discs were calculated using the equilibrium equations which included the applied loads and the forces in the ligaments and facet joints predicted by the FE model. These forces were represented as vectors with known coordinates and directions; the FJF was normal to the articular surface at each contact node while the ligament force was aligned with the ligament direction at the deformed shape (Fig. 3.2). For instance, the FBD of the vertebra L1 used to calculate the forces and moments in the disc L1-2 is shown in Fig. 3.2. These loads were calculated as follows:

$$\sum \vec{F} = \vec{0} \quad \rightarrow \quad \overrightarrow{Disc_{force}} = \overrightarrow{FL} + \overrightarrow{FJF} + \sum \overrightarrow{Ligament_{\iota_{force}}}$$

$$\sum \vec{M} = \vec{0} \rightarrow \overrightarrow{Disc_{moment}} = \overrightarrow{Applied\ Moment} + \overrightarrow{r_{FJF}} \times \overrightarrow{FJF} + \overrightarrow{r_{Ligament_{\iota}}} \times \overrightarrow{Ligament_{\iota_{force}}}$$

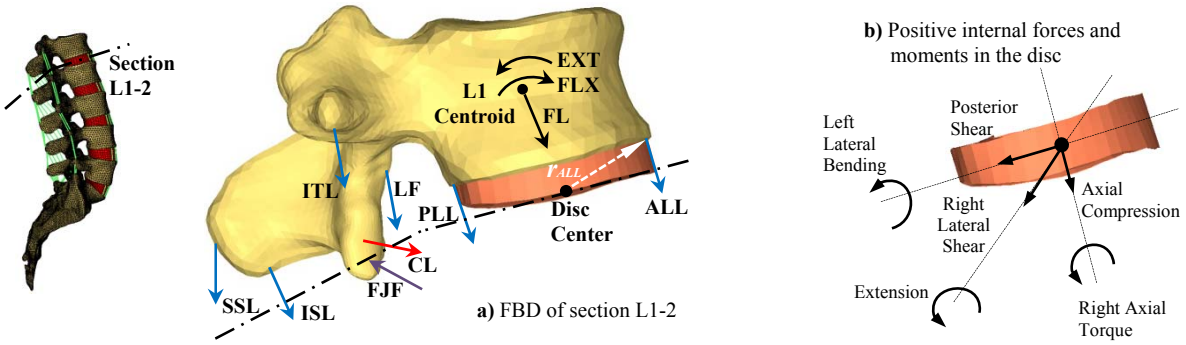


**Fig. 3.2.** FBD of the isolated disc, L1 vertebra and ligaments at level L1-2. The FJF vectors are normal to the articular surface at each contact node. The FJ resultant force is schematically represented in the FBD.

Where $\rightarrow$ indicates force vector expressed in the global coordinate system X,Y,Z (Fig. 3.1c) and $i$ corresponds to the seven ligaments. $\overrightarrow{r_{FJF}}$ is direction vector for the FJF and $\overrightarrow{r_{Ligament_i}}$ is direction vector for each ligament force. The moments were calculated about the disc center.

In addition, these force and moment vectors were defined in the local (disc) coordinates system (Fig. 3.2b) to determine the compression, anterior-posterior, and lateral shear experienced by the disc.

The compression, shear and moments in the discs were produced by both the applied loads and the resisting action of the ligaments and facet joints.

The spinal load-sharing was estimated by calculating the percentage of the total internal force/moment at each level that the disc, facet joints and ligaments carried. The total internal force-sharing was calculated as:

$$Disc\ Force - Share = 100\left(\frac{\left|\overrightarrow{Disc_{force}}\right|}{Total\ Internal\ Force}\right)$$

$$Ligament\ Force - Share = 100\left(\frac{\sum\left|\overrightarrow{Ligament_{i,force}}\right|}{Total\ Internal\ Force}\right)$$

$$FJ\ Force -\ Share = 100\left(\frac{\left|\overrightarrow{FJF}\right|}{Total\ Internal\ Force}\right)$$

$$Total\ Internal\ Force = \left|\overrightarrow{Disc_{force}}\right| + \left|\overrightarrow{FJF}\right| + \sum\left|\overrightarrow{Ligament_{i,force}}\right|$$

The total internal moment-sharing was estimated using similar equations with the moments of the spinal components evaluated at the disc centre.

### 3.3. Results

#### 3.3.1. Validation test

The L1-5 total rotation predicted by the model was close to the upper limit and 2.5º less than the lower limit of the *in-vitro* data reported by Rohlmann et al. (2001) under EXT and FLX respectively (Fig. 3.3a).

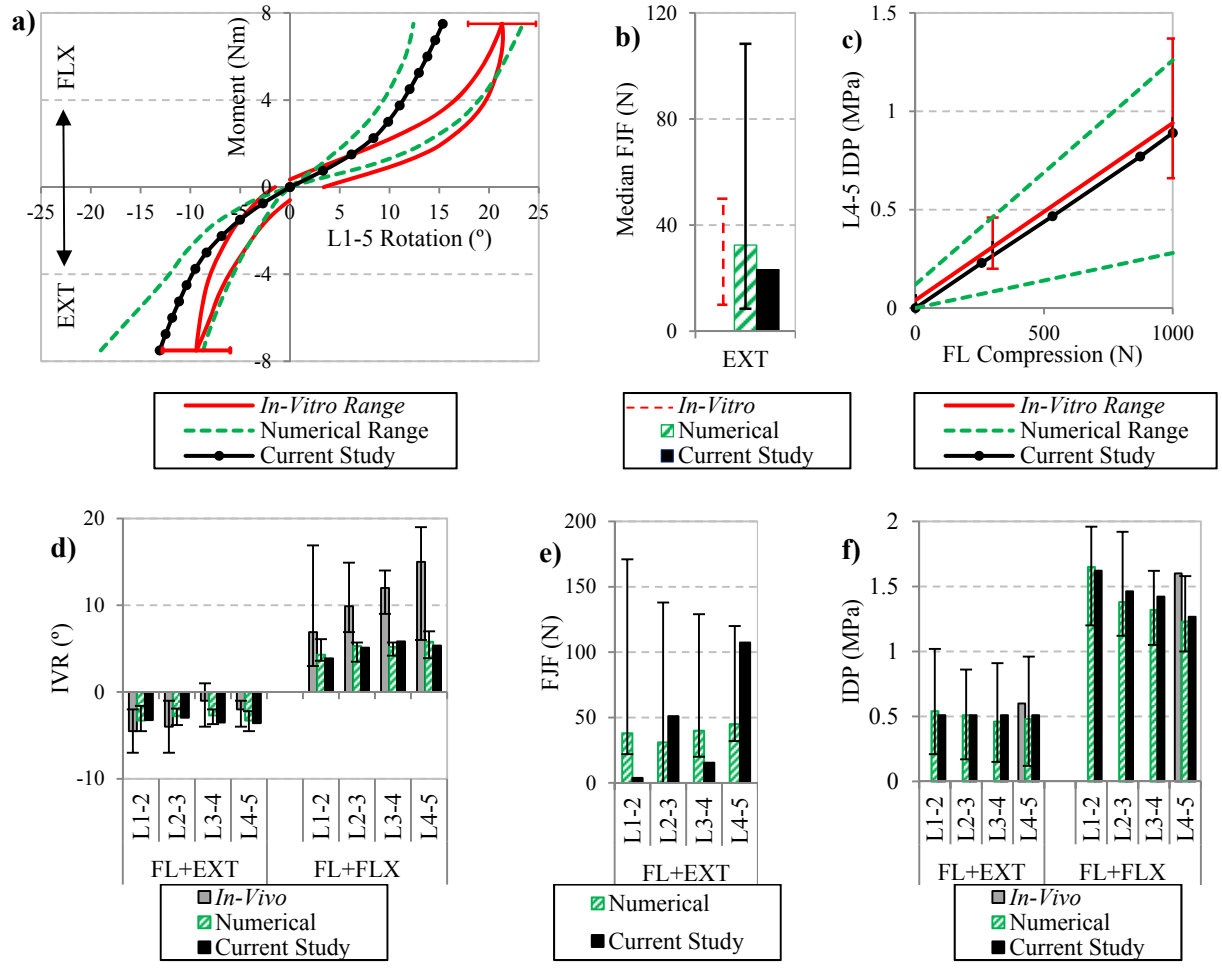


**Fig. 3.3.** Model response vs. numerical and experimental data: the numerical data are based on the FE studies by Dreischarf et al. (2014), **a)** ROM (*in-vitro* data from Rohlmann et al. (2001)), **b-e)** FJFs (*in-vitro* data from Wilson et al. (2006)), **c-f)** IDPs (*in-vitro* data from Brinckmann and Grootenboer (1991) and *in-vivo* data from Wilke et al. (2001), **d)** IVRs (*in-vivo* data from Pearcy and Tibrewal (1984), Pearcy et al. (1984) and Pearcy (1985)).

Variations of IVR at different levels with moment were in acceptable agreement with the *in-vitro* data reported by Heuer et al. (2007) and Guan et al. (2007) but smaller than those reported by Panjabi et al. (1994) particularly under FLX (Fig. 3.4). The median of the FJFs predicted at levels L1-5 in pure EXT was inside the *in-vitro* range as well (Fig. 3.3b). The IDP in the disc L4-5 increased with the FL and followed the *in-vitro* median value (Fig. 3.3c). Additionally, results of the current model fell within the ranges predicted by other FE models (Fig. 3.3a,b,c).

In case of FL+EXT, the model predicted IVRs in good agreement with the *in-vivo* values (Fig. 3.3d). Nonetheless the current model like the other FE models predicted smaller IVRs under FL+FLX compared to *in-vivo* values. At levels L2-3 and L4-5, the predicted FJFs were inside the numerical range and 20 N and 63 N higher than their median (Fig. 3.3e). However, the model predicted smaller FJFs at levels L1-2 and L3-4. The IDP at all levels agreed very well with the median of the numerical results (Fig. 3.3f). The IDP at level L4-5 was 0.09 MPa and 0.33 MPa smaller than the *in-vivo* value in FL+EXT and FL+FLX cases, respectively.

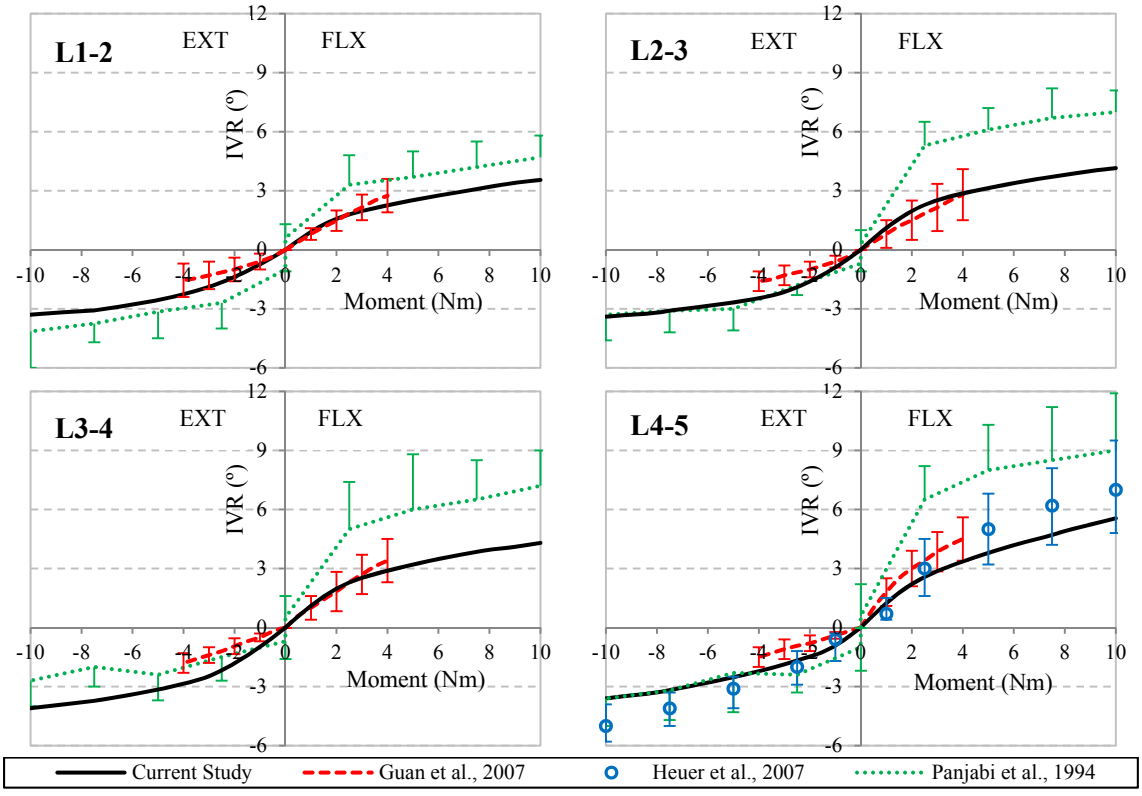


**Fig. 3.4.** Comparison of the IVRs from current FE model and *in-vitro* data.

### 3.3.2. Response of the lumbosacral spine

***Kinematics***

Applying the FL caused slight flexion. The L1-S1 total rotation was equal to 1.3º, 16.8º, and 23.5º under the FL, FL+EXT, and FL+FLX, respectively (Fig. 3.5a). The smallest IVRs occurred at levels L2-3 (3º) and L1-2 (3.4º) under FL+EXT and FL+FLX, respectively. The largest IVR was found at level L4-5 in both load combinations (3.6º for FL+EXT, 5.3º for FL+FLX) (Fig. 3.5b).

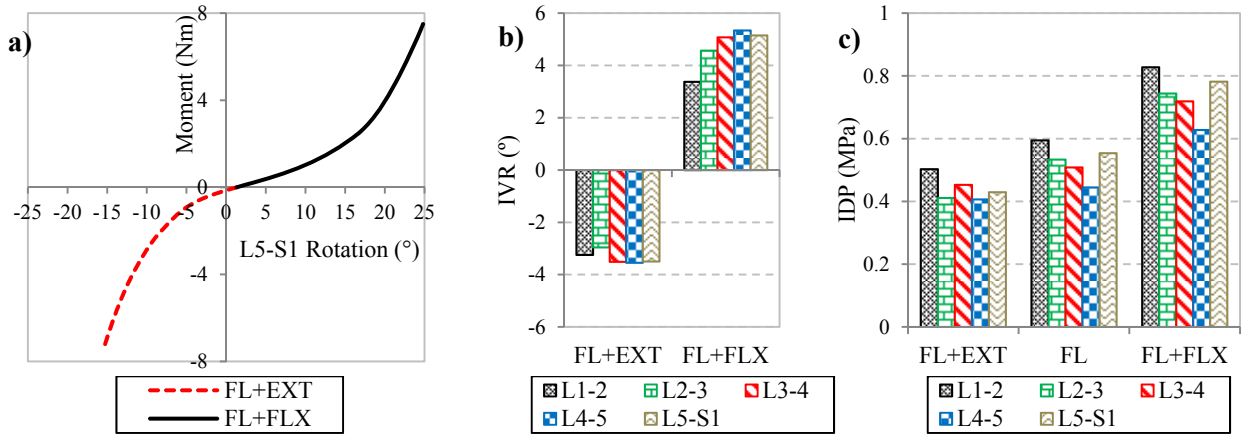


**Fig. 3.5.** Response of the lumbosacral spine to combined loads: **a)** Moment-rotation curve, **b)** IVRs, **c)** IDP.

***Internal loads in the discs***

FL produced IDP which decreased from level L1 to level L4. Adding EXT decreased the IDP whereas an increase in IDP was found in the FLX case (Fig. 3.5c). The disc L1-2 experienced the highest IDP while the lowest magnitude was found in the disc L4-5 in all loading cases.

FL+EXT produced high tensile strain in the collagen fibers particularly in the posterolateral area of the outermost lamella and in the anterior area of the innermost lamella. In case of FL+FLX, higher strains were developed in the anterolateral area of the innermost lamella and were extended to outer lamellae in the discs L4-5 and L5-S1 (Fig. 3.6).

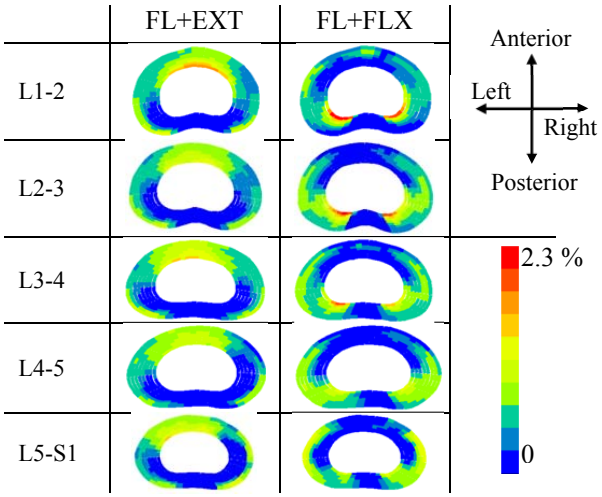


**Fig. 3.6.** Tensile strain distribution in the annular fibers at levels L1-S1.

When combined with FL, FLX increased compression by ~30% in all discs while EXT decreased it by up to 40% at level L5-S1. Sagittal shear occurred in both loading modes and its magnitude was higher in case of FL and EXT at levels L4-S1 (it reached up to 110N at level L4-5). Small lateral shear (up to 28N at level L4-5) was produced at all levels in both loading cases (Fig. 3.7a). In general, when coupled with FL, EXT produced higher internal moment in the sagittal (up to 3Nm at level L1-2) and axial (up to 1Nm at level L4-5) compared to FLX. Magnitude and direction of internal moment in the lateral direction varied with loading mode along the spine. The maximum magnitude reached 1.1Nm at levels L4-5 and L5-S1 under FL with FLX and FL with EXT, respectively (Fig. 3.7b). Moments in the sagittal direction were generally more significant than in the axial and lateral directions.

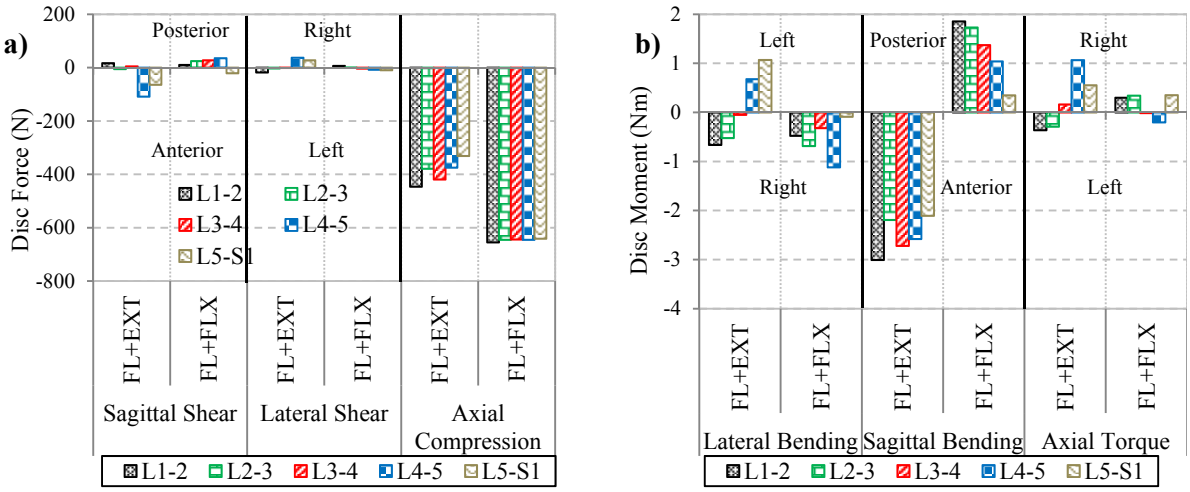


**Fig. 3.7.** Internal forces (a) and moments (b) in L1-S1 discs.

***Spinal load-sharing***

In addition to the FL, the discs, ligaments and facet joints resisted additional forces up to 220 N and 483 N resulting from coupling FL with EXT and FLX, respectively (Figs. 3.8a-b). Also, the resisting forces in these components added extra moments to the applied FLX and EXT moments. These extra moments were calculated at the discs centers (Figs. 3.8c-d). The magnitudes of the additional forces were greater in case of FL+FLX with highest magnitude in the level L5-S1, whereas, the additional moments had counter effect and reduced the applied moment by up to 0.5 Nm except at level L5-S1. Unlike FLX, coupling FL with EXT produced larger additional moments up to 2.7 Nm and their magnitudes increased from the cranial to caudal levels.

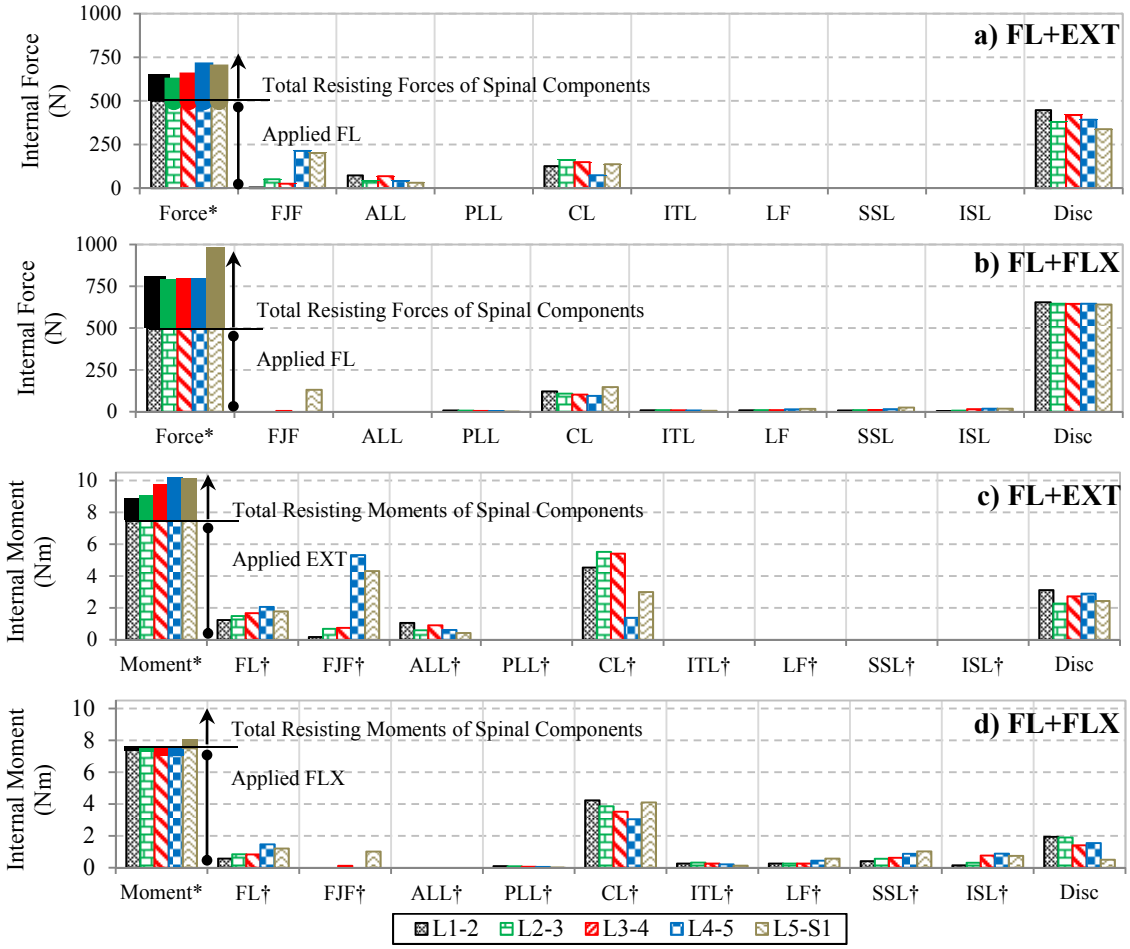


* The total internal force/moment including applied FL+EXT/FLX and spinal components resisting action.
† Moments evaluated at discs centers.

**Fig. 3.8.** Internal loads distribution in spinal segments L1-S1 calculated from equilibrium considerations.

The FL+FLX was mainly resisted by the disc and the CL ligament at all levels. Silent contribution of the ligaments LF, SSL, and ISL was found at all levels as well as the facet joints except at the level L5-S1. In the EXT case, the load was carried by the disc and CL and ALL ligaments at all levels as well as the facet joints particularly at levels L4-S1 (Fig. 3.8).

The discs resisted almost 80% of the total force produced by the FL+FLX and the ligaments carried the remaining 20% at levels L1-5. At level L5-S1, the disc, ligaments, and facet joints resisted 66%, 21%, and 13% of the total force respectively (Fig. 3.9). The ligaments resisted 77% of the total moment (i.e. applied and resulting from the spinal components resistance) produced by FL+FLX while the remaining 23% was carried by the discs at levels L1-5. At level L5-S1, the ligaments, disc and facet joints carried 81%, 6%, and 13% of the total moment, respectively.

In the case of FL+EXT, the total force was shared by the disc and ligaments in proportion of 64% and 36% respectively at L1-2 level (Fig. 3.9). At levels L2-S1, the disc, ligaments, and facet joints contribution in carrying load varied between 51% and 63%, 15% and 35%, and 4% and 29%, respectively. The disc resisted 34% of the total moment while the remaining 65% was carried by the ligament at level L1-2. At levels L2-S1, the proportions carried by the discs, ligaments, and facet joints varied between 24% and 28%, 20% and 68%, 8% and 52%, respectively.

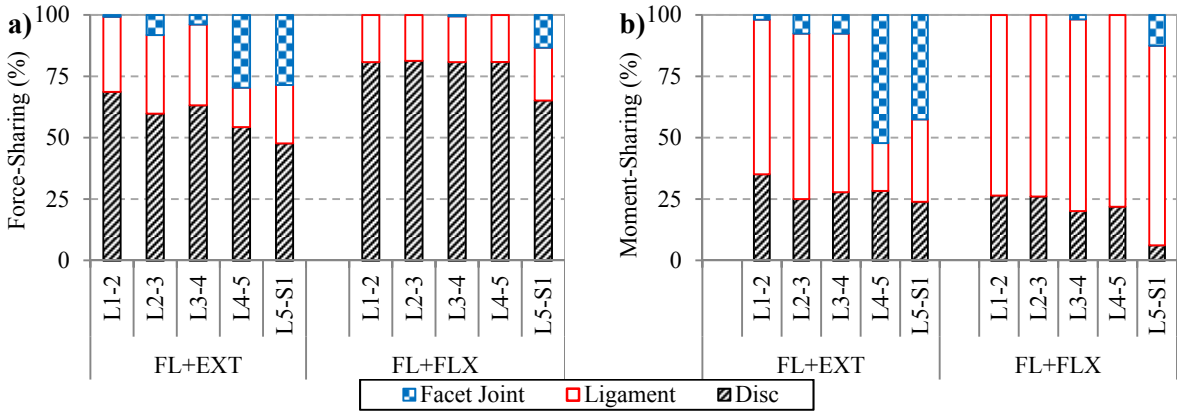


**Fig. 3.9.** Load-sharing along the spine under all loading cases: **a)** force-sharing, **b)** moment-sharing.

### 3.4. Discussions

The current study used a 3D nonlinear FE model with real and detailed geometry. To investigate the spinal load-sharing in ligamentous lumbosacral spine in flexed and extended posture, FL coupled with FLX/EXT moments was applied (Rohlmann et al., 2009). Although the FL concept is widely used in experimental and numerical studies of lumbar spine with no muscles, we are however aware of its limitations in simulating physiological flexion-extension movement. In general, the FL has constant magnitude and is combined with flexion/extension moment whereas previous studies have demonstrated that under flexed or extended posture, spinal compression substantially increased compared to neutral condition with no external moments (El-Rich et al, 2004; Arjmand and Shirazi-Adl, 2006). In addition, the FL magnitude of 1175N used by Rohlmann et al. (2009) to mimic the IDP in physiological flexion is significantly greater than disc force (640N) measured *in-vivo* recently by Dreischarf et al. (2015) which confirms the necessity of thorough investigation of the spinal response sensitivity to FL and moment magnitude. The model was kept free to move out of the sagittal plane to assess the coupling lateral and axial responses and it used material properties taken from literature. The time-dependent properties of the spinal components as well as the fluid-flow phenomenon in the disc and porous bone were not considered as the current model studied only the spine response to static loads. The disc bulge resulted from the pre-stressed ligaments (Little et al., 2008.) was not considered in this study.

#### 3.4.1. Model validation

The model was validated against various reported *in-vitro* data by applying similar loading conditions. However, the *in-vivo* measurements available in the literature were rather used to verify the model prediction as they resulted from different loading and environment (*in-vivo*) conditions. Also predictions of the current model were compared with the median of eight published FE models.

The ROM produced by pure EXT/FLX moments or FL combined with EXT/FLX fell well within the range predicted by previous numerical, *in-vitro*, and *in-vivo* studies. However, like the majority of the previous numerical models mentioned here, the current model demonstrated relatively stiffer response to FLX while its response to EXT compared satisfactory well with experimental data reported by Rohlmann et al. (2001) and Panjabi et al. (1994). Nevertheless, the

FLX response was in a better agreement with other recent *in-vitro* data (Guan et al., 2007; Heuer et al., 2007). The IVRs produced by the FL+EXT/FLX were also in good agreement with numerical results but smaller than the *in-vivo* data in the FL+FLX case which confirms the limitations of applying FL combined with bending moments to mimic the *in-vivo* conditions. The segmental FJFs produced by EXT or FL+EXT compared very well with experimental and numerical ranges. However, the model predicted smaller FJFs at levels L1-2 and L3-4 which is most likely due to the facet joints geometry. The segmental IDP also matched well the numerical and experimental results in all loading scenarios. In general, the response of the current model to all loading scenarios was in good agreement with most of the published FE models and its predictions were close to *in-vivo* and *in-vitro* available data.

### 3.4.2. Response of the lumbosacral spine

The model predicted nonlinear response to FL+EXT/FLX with stiffer behavior in EXT due to the facet joints role in supporting EXT moment. The IVRs were unequal which might be caused by the variation in geometry of the discs and facet joints along the spine (Meijer et al., 2011; Dupont et al., 2002; Robin et al., 1994). The FL+FLX increased significantly the IDP (up to 40%) at all levels which augmented the discs loads (Dolan and Adams, 2001). Whereas, a decrease in IDP (up to 23%) was found under FL+EXT particularly at levels L2-3 and L5-S1 due to the facet joints support. The IDP produced high tensile hoop stress in the annulus particularly in the innermost lamella leading to high tensile strains in the annular fibers. In the FL+FLX case, the location of higher tensile strains was found in the posterolateral area of the innermost lamella while the FL+EXT load produced high tensile strains in the anterior and anterolateral regions of the disc which agreed with previous findings (Schmidt et al., 2007). High tensile strains were also found in the posterolateral region of the outermost lamella under FL+EXT indicating the potential location of disc bulge (Adams et al., 1988). Adding FLX/EXT to the FL affected the compression and produced sagittal shears and internal moments with variable magnitude and direction at all disc levels. It also produced lateral shears and moments as well as axial moments due to the spine asymmetry and the boundary conditions applied.

***Internal loads and load-sharing***

Understanding the spinal load-sharing is very relevant in clinical applications (Adams, 2004). In the current study, it was determined as the percentage of the total internal forces or moments

produced along the spine that each spinal component carried. These internal loads were calculated at each level using the equilibrium considerations to account for the applied load as well as the resisting actions of the spinal components. Results demonstrated that spinal load-sharing varied along the spine and depended on the applied load. The contribution of the facet joints and ligaments in supporting bending moments produced additional force in the disc which explains the significant increase of IDP under FL+FLX loading. There were also additional moments which their magnitudes depended on the ligaments and facet joints locations with respect to the discs centers. These findings revealed a trade-off between the contribution of ligaments and facet joints in load support and the amount of forces and moments that they produced in the discs in addition to the applied load. Moreover, due to its posterior location with respect to the discs centers (Kim et al., 2011); the FL produced small moments at the discs centers. These moments increased under FL+EXT as the distance between the FL and the discs centers increased but they decreased in the FL+FLX case.

In the FL+EXT case, small contribution of the facet joints was found at cranial levels (L1-L4) as the internal forces and moments were mainly resisted by the discs and ligaments, respectively. This study demonstrated the resistance of the ligament CL and facet joints to extension movement which agreed with in-vitro findings (Dolan and Adams, 2001; Adams et al., 1988). At the caudal levels (L4-S1), the role of the facet joints was more evident particularly in carrying internal moments. While the discs moment-sharing was almost similar at all levels, contribution of the facet joints in resisting moment was more significant at levels L4-S1 which reduced the ligament moment-sharing at that levels. . Similarly, the internal forces and moments produced by FL+FLX were mainly supported by the discs and ligaments, respectively. Only at level L5-S1 the facet joints and the discs shared small portion of the internal forces and moments while the ligaments contribution remained similar at all levels. Results of the current study not only confirmed the resistance of posterior ligaments to flexion moment (Dolan and Adams, 2001; Adams et al., 1980) but also revealed their beneficial role in reducing the discs moments.

In conclusion, load-sharing in ligamentous lumbosacral spine subjected to FL combined with FLX/EXT varied along the spine and depended on applied load.

**Conflict of interest statement**

The Authors have no conflict of interest to declare.

**Acknowledgements**

This study was supported by NSERC Discovery Grant, Canada.

**References**

Abouhossein, A., Weisse, B., Ferguson, S.J., 2011. A Multibody Modelling Approach to Determine Load Sharing between Passive Elements of the Lumbar Spine. Computer Methods in Biomechanics and Biomedical Engineering 14, 527-537.

Adams, M.A., 2004. Biomechanics of Back Pain. Acupuncture in Medicine 22, 178-188.

Adams, M.A., Dolan, P., Hutton, W.C., 1988. The Lumbar Spine in Backward Bending. Spine 13, 1019-1026.

Adams, M.A., Hutton, W.C., Stott, J.R., 1980. The Resistance to Flexion of the Lumbar Intervertebral Joint. Spine 5, 245-253.

Alapan, Y., Sezer, S., Demir, C., Kaner,T., Inceoglu, S., 2014. Load Sharing in Lumbar Spinal Segment as a Function of Location of Center of Rotation. Journal of Neurosurgery Spine 20, 542-549.

Arjmand, N., Shirazi-Adl, A., 2006. Model and in Vivo Studies on Human Trunk Load Partitioning and Stability in Isometric Forward Flexions. Journal of Biomechanics 39, 510-521.

Ayturk, U.M., Puttlitz, C.M., 2011. Parametric Convergence Sensitivity and Validation of a Finite Element Model of the Human Lumbar Spine. Computer Methods in Biomechanics and Biomedical Engineering 14, 695-705.

Breau, C., Shirazi-Adl, A., de Guise, J., 1991. Reconstruction of a Human Ligamentous Lumbar Spine using CT Images--a Three-Dimensional Finite Element Mesh Generation. Annals of Biomedical Engineering 19, 291-302.

Brinckmann, P., Grootenboer, H., 1991. Change of disc height, radial disc bulge, and intradiscal pressure from discectomy. An *in vitro* investigation on human lumbar discs. Spine 16, 641-646.

Dolan, P., Adams, M A., 2001. Recent Advances in Lumbar Spinal Mechanics and their Significance for Modelling. Clinical Biomechanics 16, S8-S16.

Dreischarf, M., Zander, T., Shirazi-Adl, A., Puttlitz, C.M., Adam, C.J., Chen, C.S., Goel, V.K., Kiapour, A., Kim, Y.H., Labus, K.M., Little, J.P., Park, W.M., Wang, Y.H., Wilke, H.J.,

Rohlmann, A., Schmidt, H., 2014. Comparison of Eight Published Static Finite Element Models of the Intact Lumbar Spine: Predictive Power of Models Improves when Combined Together. Journal of Biomechanics 47, 1757-1766.

Dreischarf, M., Albiol, L., Zander, T., Arshad, R., Graichen, F., Bergmann, G., Schmidt, H., Rohlmann, A., 2015. In Vivo Implant Forces Acting on a Vertebral Body Replacement during Upper Body Flexion. Journal of Biomechanics 48, 560-565.

Dupont, P., Lavaste, F., Skalli, W., 2002. The Role of Disc, Facets and Fibres in Degenerative Process: A Sensitivity Study. Studies in Health Technology and Informatics 88, 356-359.

El-Rich, M., Arnoux, P., Wagnac, E., Brunet, C., Aubin, C., 2009. Finite Element Investigation of the Loading Rate Effect on the Spinal Load-Sharing Changes Under Impact Conditions. Journal of Biomechanics 42, 1252-1262.

El-Rich, M., Shirazi-Adl, A., Arjmand, N., 2004. Muscle Activity, Internal Loads, and Stability of the Human Spine in Standing Postures: Combined Model and in Vivo Studies. Spine 29, 2633-2642.

Fry, R.W., Alamin, T.F., Voronov, L.I., Fielding, L.C., Ghanayem, A.J., Parikh, A., Carandang, G., Mcintosh, B.W., Havey, R.M., Patwardhan, A.G., 2014. Compressive Preload Reduces Segmental Flexion Instability After Progressive Destabilization of the Lumbar Spine. Spine 39, E74-E81.

Goel, V.K., Clausen, J.D., 1998. Prediction of Load Sharing among Spinal Components of a C5-C6 Motion Segment using the Finite Element Approach. Spine 23, 684-691.

Goel, V.K., Winterbottom, J.M., Weinstein, J.N., Kim, Y.E., 1987. Load Sharing among Spinal Elements of a Motion Segment in Extension and Lateral Bending. Journal of Biomechanical Engineering 109, 291-297.

Goto, K., Tajima, N., Chosa, E., Totoribe, K., Kubo, S., Kuroki, H., Arai, T., 2003. Effects of Lumbar Spinal Fusion on the Other Lumbar Intervertebral Levels (Three-Dimensional Finite Element Analysis). Journal of Orthopaedic Science: Official Journal of the Japanese Orthopaedic Association 8, 577-584.

Guan, Y., Yoganandan, N., Moore, J., Pintar, F.A., Zhang, J., Maiman, D.J., Laud, P., 2007. Moment-Rotation Responses of the Human Lumbosacral Spinal Column. Journal of Biomechanics 40, 1975-1980.

Heuer, F., Schmidt, H., Klezl, Z., Claes, L., Wilke, H.J., 2007. Stepwise Reduction of Functional Spinal Structures Increase Range of Motion and Change Lordosis Angle. Journal of Biomechanics 40, 271-280.

Ivicsics, M.F., Bishop, N.E., Püschel, K., Morlock, M.M., Huber, G., 2014. Increase in Facet Joint Loading after Nucleotomy in the Human Lumbar Spine. Journal of Biomechanics 47, 1712-1717.

Ibarz, E., Herrera, A., Mas, Y., Rodriguez-Vela, J., Cegonino, J., Puertolas, S., Gracia, L., 2013. Development and Kinematic Verification of a Finite Element Model for the Lumbar Spine: Application to Disc Degeneration. BioMed Research International 2013, 705185.

Kim, K., Kim, Y.H., Lee, S., 2011. Investigation of Optimal Follower Load Path Generated by Trunk Muscle Coordination. Journal of Biomechanics 44, 1614-1617.

Little, J.P., de Visser, H., Pearcy, M.J., Adam, C.J., 2008. Are Coupled Rotations in the Lumbar Spine Largely due to the Osseo-Ligamentous Anatomy?-a Modeling Study. Computer Methods in Biomechanics and Biomedical Engineering 11, 95-103.

Meijer, G. J., Homminga, J., Veldhuizen, A.G., Verkerke, G.J., 2011. Influence of Interpersonal Geometrical Variation on Spinal Motion Segment Stiffness: Implications for Patient-Specific Modeling. Spine 36, E929-E935.

Mustafy, T., El-Rich, M., Mesfar, W., Moglo, K., 2014. Investigation of Impact Loading Rate Effects on the Ligamentous Cervical Spinal Load-Partitioning using Finite Element Model of Functional Spinal Unit C2-C3. Journal of Biomechanics 47, 2891-2903.

Najarian, S., Dargahi, J., Heidari, B., 2005. Biomechanical Effect of Posterior Elements and Ligamentous Tissues of Lumbar Spine on Load Sharing. Bio-Medical Materials and Engineering 15, 145-158.

Naserkhaki, S., Jaremko, J.L., Kawchuk, G., Adeeb, S., El-Rich, M., 2014. Investigation of Lumbosacral Spine Anatomical Variation Effect on Load-Partitioning Under Follower Load Using Geometrically Personalized Finite Element Model. ASME International Mechanical Engineering Congress and Exposition, Proceedings (IMECE), IMECE2014-40231, 3-V003T03A050.

Noailly, J., Wilke, H., Planell, J.A., Lacroix, D., 2007. How does the Geometry Affect the Internal Biomechanics of a Lumbar Spine Bi-Segment Finite Element Model? Consequences on the Validation Process. Journal of Biomechanics 40, 2414-2425.

Panjabi, M.M., 1992. The Stabilizing System of the Spine. Part I. Function, Dysfunction, Adaptation, and Enhancement. Journal of Spinal Disorders 5, 383-389, discussion 397.

Panjabi, M.M., Oxland, T.R., Yamamoto, I., Crisco, J.J., 1994. Mechanical Behavior of the Human Lumbar and Lumbosacral Spine as shown by Three-Dimensional Load-Displacement Curves. The Journal of Bone and Joint Surgery. American Volume 76, 413-424.

Panzer, M.B., Cronin, D.S., 2009. C4-C5 Segment Finite Element Model Development, Validation, and Load-Sharing Investigation. Journal of Biomechanics 42, 480-490.

Park, W.M., Kim, K., Kim, Y.H., 2013. Effects of Degenerated Intervertebral Discs on Intersegmental Rotations, Intradiscal Pressures, and Facet Joint Forces of the Whole Lumbar Spine. Computers in Biology and Medicine 43, 1234-124.

Pearcy, M., Portek, I., Shepherd, J., 1984. Three-dimensional x-ray analysis of normal movement in the lumbar spine. Spine 9, 294-297.

Pearcy, M.J., 1985. Stereo radiography of lumbar spine motion. Acta orthopaedica Scandinavica, S212, 1-45.

Pearcy, M.J., Tibrewal, S.B., 1984. Axial rotation and lateral bending in the normal lumbar spine measured by three-dimensional radiography. Spine 9, 582-587.

Renner, S.M., Natarajan, R.N., Patwardhan, A.G., Havey, R.M., Voronov, L.I., Guo, B.Y., Andersson, G.B., An, H.S., 2007. Novel Model to Analyze the Effect of a Large Compressive Follower Pre-Load on Range of Motions in a Lumbar Spine. Journal of Biomechanics 40, 1326-1332.

Robin, S., Skalli, W., Lavaste, F., 1994. Influence of Geometrical Factors on the Behavior of Lumbar Spine Segments: A Finite Element Analysis. European Spine Journal: Official Publication of the European Spine Society, the European Spinal Deformity Society, and the European Section of the Cervical Spine Research Society 3, 84-90.

Rohlmann, A., Bauer, L., Zander, T., Bergmann, G., Wilke, H.J., 2006. Determination of Trunk Muscle Forces for Flexion and Extension by using a Validated Finite Element Model of the Lumbar Spine and Measured in Vivo Data. Journal of Biomechanics 39, 981-989.

Rohlmann, A., Zander, T., Rao, M., Bergmann, G., 2009. Realistic Loading Conditions for Upper Body Bending. Journal of Biomechanics 42, 884-890.

Rohlmann, A., Neller, S., Claes, L., Bergmann, G., Wilke, H.J., 2001. Influence of a follower load on intradiscal pressure and intersegmental rotation of the lumbar spine. Spine 26, E557-E561.

Schmidt, H., Heuer, F., Simon, U., Kettler, A., Rohlmann, A., Claes, L., Wilke, H.J., 2006. Application of a New Calibration Method for a Three-Dimensional Finite Element Model of a Human Lumbar Annulus Fibrosus. Clinical Biomechanics 21, 337-344.

Schmidt, H., Kettler, A., Heuer, F., Simon, U., Claes, L., Wilke, H.J., 2007. Intradiscal Pressure, Shear Strain, and Fiber Strain in the Intervertebral Disc Under Combined Loading. Spine 32, 748-755.

Schmidt, H., Shirazi-Adl, A., Galbusera, F., Wilke, H., 2010. Response Analysis of the Lumbar Spine during Regular Daily activities-A Finite Element Analysis. Journal of Biomechanics 43, 1849-1856.

Sharma, M., Langrana, N.A., Rodriguez, J., 1995. Role of Ligaments and Facets in Lumbar Spinal Stability. Spine 20, 887-900.

Shih, S.L., Liu, C.L., Huang, L.Y., Huang, C.H., Chen, C.S., 2013. Effects of Cord Pretension and Stiffness of the Dynesys System Spacer on the Biomechanics of Spinal Decompression- a Finite Element Study. BMC Musculoskeletal Disorders 14, 191.

Shirazi-Adl, A., 2006. Analysis of Large Compression Loads on Lumbar Spine in Flexion and in Torsion using a Novel Wrapping Element. Journal of Biomechanics 39, 267-275.

Shirazi-Adl, A., Ahmed, A.M., Shrivastava, S.C., 1986. Mechanical Response of a Lumbar Motion Segment in Axial Torque Alone and Combined with Compression. Spine 11, 914-927.

Wang, J.L., Parnianpour, M., Shirazi-Adl, A., Engin, A.E., 1999. Rate Effect on Sharing of Passive Lumbar Motion Segment Under Load-Controlled Sagittal Flexion: Viscoelastic Finite Element Analysis. Theoretical and Applied Fracture Mechanics 32, 119-128.

Wilke, H., Neef, P., Hinz, B., Seidel, H., Claes, L., 2001. Intradiscal pressure together with anthropometric data - a data set for the validation of models. Clinical Biomechanics (Bristol, Avon) 16, S111-S126.

Wilson, D.C., Niosi, C.A., Zhu, Q.A., Oxland, T.R., Wilson, D.R., 2006. Accuracy and repeatability of a new method for measuring facet loads in the lumbar spine. Journal of Biomechanics 39, 348-353.

# Chapter 4

# Sensitivity of Lumbar Spine Response to Follower Load and Flexion Moment: Finite Element Study

This chapter has been submitted as Naserkhaki, S., El-Rich, M., 2015, to Journal of Biomechanical Engineering.

**Abstract**

The Follower Load (FL) combined with moments is commonly used to approximate physiological flexed/extended posture of the lumbar spine in absence of muscles in Finite Element (FE) and *in-vitro* studies. A wide range of magnitudes was used to simulate the flexed posture but there is a lack of consensus as to what magnitudes simulate better the physiological conditions. These magnitudes were selected such that the intradiscal pressure (IDP) and/or intervertebral rotations (IVRs) predicted or measured mimic the *in-vivo* values while the disc loads were ignored due to lack of *in-vivo* data. In this study, sensitivity of the spinal response to different FL and flexion moment magnitudes was investigated using a 3D nonlinear FE model of ligamentous lumbosacral spine. Optimal magnitudes of FL and moment that minimize deviation of the model predictions from *in-vivo* data were determined. Results revealed that the spinal parameters i.e. the IVRs, disc moment, and the increase in disc force and moment from neutral to flexed posture were more sensitive to moment magnitude than FL magnitude in case of flexion. The disc force and IDP were more sensitive to the FL magnitude than moment magnitude. The optimal ranges of FL and flexion moment magnitudes were 900N-1100N and 9.9Nm-11.2Nm, respectively. The FL magnitude had reverse effect on the IDP and disc force. Thus, we could not find single magnitude for FL or flexion that minimizes the deviation of all the spinal parameters together from the *in-vivo* data. To obtain reasonable compromise between the IDP and disc force, our findings recommend that FL of low magnitude must be combined with flexion moment of high intensity and vice versa. In addition, it is speculated that applying FL with increasing magnitude from level L1-2 to level L5-S1 will improve the FE model predictions and simulate better the neutral and flexed postures of the lumbosacral spine.

**Keywords:** Lumbosacral spine; sensitivity; optimal load; follower load; finite element study.

## 4.1. Introduction

Although muscle forces were predicted in some studies of spinal response (Rohlmann et al., 2006; Arjmand and Shirazi-Adl, 2005; El-Rich et al., 2004; Goel et al., 1993), most of *in-vitro* (Fry et al., 2014; Rohlmann et al., 2001) and Finite Element (FE) studies (Naserkhaki et al., 2015; Dreischarf et al., 2014; Schmidt et al., 2010; Rohlmann et al., 2009b; Goto et al., 2003) have omitted the muscular system due to its complexity and redundancy and have used the concept of Follower Load (FL) (Patwardhan et al., 1999) as an approximation to physiological conditions. It is well known that FL minimizes the intervertebral rotations (IVRs) and improves the spine resistance to high compressive force when it lacks muscles. Among the various simplified loading modes applied to simulate the complex behavior of the lumbar spine, a FL with magnitude of 500N was found to be the best loading mode to simulate standing posture for which the intradiscal pressure (IDP) predicted by FE model agreed well with *in-vivo* data (Rohlmann et al., 2009a). It was also demonstrated that applying upper body weight, FL, and muscle forces together or FL combined with a bending moment to simulate flexion and extension delivers results in good agreement with *in-vivo* data (Rohlmann et al., 2009b). Bending moment was applied to ensure that its magnitude remains equal and constant at all spinal levels (Panjabi, 2007; Rohlmann et al., 2001; Oxland et al., 1992). Moreover, in previous *in-vitro* studies a wide range of bending moment magnitudes was applied to simulate the physiological movement of the lumbar spine accurately. These magnitudes varied between 4.0Nm (Guan et al., 2007), 7.5Nm (Niosi et al., 2008; Sawa and Crawford, 2008; Rohlmann et al., 2001) and 10Nm (Kiapour et al., 2012; Yamamoto et al., 1989). In FE studies, moments with magnitudes of 7.5Nm (Dreischarf et al., 2014; Woldtvedt et al. 2011; Rohlmann et al., 2009b) and 10Nm (Chen et al., 2013; Park et al., 2013; Goto et al., 2003; Robin et al., 1994) were applied on the most superior vertebra of the lumbar spine to simulate flexion/extension movement. A higher magnitude of moment equal to 15-20Nm was applied to investigate the response of the lumbar spine to sagittal/lateral moments (Wang et al., 1999; Shirazi-Adl, 1994). In most of these studies, moments with similar magnitude but opposite directions were applied to simulate flexion/extension.

In a recent study that compared the IVRs predicted by eight published FE models of intact lumbar spine with *in-vivo* data, it was found that applying 7.5Nm moment is inadequate to simulate flexion (Dreischarf et al., 2014). Optimal load combinations of 700N FL and 7.8Nm lateral bending (Dreischarf et al., 2012) as well as 720N FL and 5.5Nm axial moment

(Dreischarf et al., 2011) were found to have the best agreement with averaged *in-vivo* IVRs and IDP data. Furthermore, Rohlmann et al. (2009b) suggested that a 500N FL produces reasonable IDP in extension while higher magnitude (1175N) is needed to predict realistic IDP in flexion. Other magnitudes of FL ranging from 265N to 500N were also considered in FE models (Naserkhaki et al., 2015; Chen et al., 2013; Park et al., 2013; Goto et al., 2003) which approximately represent the compression in the discs in neutral standing posture (Kim and Kim, 2008; El-Rich et al., 2004).

The FL was found to increase the IDP in lumbar discs, slightly reduces the IVRs for axial rotation, and hardly affects IVRs for lateral bending and flexion/extension loading modes (Rohlmann et al., 2001). Nevertheless, force and moment produced in the intervertebral discs were not assessed in previous studies of loading modes that simulate physiological conditions which is probably due to lack of *in-vivo* data. Moreover, our recent study has revealed that resistance of ligaments to flexion creates additional compressive force and moment in the lumbar discs, while a reduction of compressive force was found in the extension case due to the articular facet joints contribution (Naserkhaki et al. 2015). Thus, magnitude of the FL and combined moment should consider not only the IDP and IVRs, but also the internal force and moment developed in the discs.

This study aimed to investigate sensitivity of the mechanical response of ligamentous lumbosacral spine to magnitudes of FL and combined flexion moment using FE modeling. It also sought to define optimal ranges of FL and flexion moment magnitudes that produce spinal response in terms of IVRs, IDP, and disc force and moment in agreement with *in-vivo* data.

## 4.2. Materials and methods

### 4.2.1. FE model

A validated FE model of ligamentous lumbosacral spine (Naserkhaki et al., 2015; Naserkhaki et al., 2014) was employed in this study. Briefly, it consisted of five lumbar vertebrae L1 to L5 (L1-5), sacrum, intervening discs, and surrounding ligaments (Fig. 4.1a). The behavior of the cortical and cancellous bones was assumed linear elastic while the nucleus and annulus were modeled using hyper-elastic material law. The annular fibers and ligaments were simulated using nonlinear springs which resist tension only. The material properties are summarized in Table 4.1. The facet joint articulation was simulated by frictionless surface to surface contact.

**Table 4.1.** Material properties of the spinal components.

| *Spinal Components* | | *Material Behaviour* | *Mechanical Properties* | | *References* |
|---|---|---|---|---|---|
| **Bone** | Cortical Bone | Linear Elastic | E=12000 (MPa) | *v*=0.30 | *Park et al., 2013; Schmidt et al., 2007; Goto et al., 2003* |
| | Cartilaginous Endplate | | E=23.8 (MPa) | *v*=0.40 | |
| | Cancellous Bone | | E=200 (MPa) | *v*=0.25 | |
| **Disc** | Annulus Ground Substance | Hyper-Elastic (Mooney-Rivlin) | C10=0.18 | C01=0.045 | *El-Rich et al., 2009; Schmidt et al., 2007* |
| | Nucleus Pulposus | | C10=0.12 | C01=0.030 | |
| **Annular Fibers** | | Nonlinear Force Displacement Curve | | | *Schmidt et al., 2006; Shirazi-Adl et al., 1986* |
| **Ligaments** | | Nonlinear Force Displacement Curve | | | *Rohlmann et al. (2006)* |

Only the lower sacrum was constrained in all degrees of freedom while all other components were free to move (Fig. 4.1b). A FL with constant magnitude along the spine was applied using preloaded unidirectional springs inserted between two adjacent vertebral bodies (Fig. 4.1b). The flexion moment was applied at the centroid of the vertebra L1. In separate cases, four magnitudes (500N, 700N, 900N or 1100N) of FL combined with flexion moment which increased from 0 to 20Nm were applied to the model. The moment increased with automatic increments not exceeding 0.05Nm. The IVRs and IDPs were predicted by the FE model while the forces and moments produced in the discs were calculated at the discs centers by satisfying the equilibrium conditions (Naserkhaki et al., 2015).

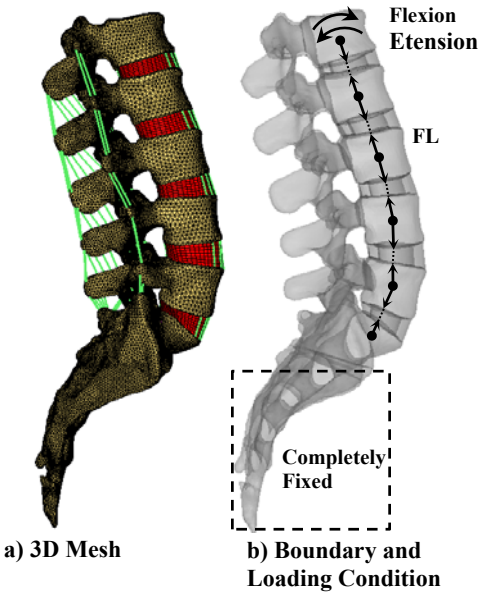


**Fig. 4.1.** 3D FE Model of the lumbosacral spine.

### 4.2.2. Optimization

Optimal magnitudes of FL and combined flexion moment were determined by minimizing the deviation (error) of the predicted disc force, disc moment, increase in disc force, and increase in disc moment at level L1-2 as well as IDP in the disc L4-5 and IVRs at levels L1-S1 considered together from their corresponding mean *in-vivo* values as follows:

$$F_{Obj} = a\left[\left(\frac{IDP_{L4-5_{FE}} - IDP_{L4-5_{In}-vivo}}{IDP_{L4-5_{in}-vivo}}\right)^2\right] + b\left[\sum_{i=L1-2}^{L5-S1}\left(\frac{IVR_{i_{FE}} - IVR_{i_{in}-vivo}}{IVR_{i_{in}-vivo}}\right)^2\right]$$
$$+ c\left[\left(\frac{F_{L1-2\_FE} - F_{L1-2\_in-vivo}}{F_{L1-2\_in-vivo}}\right)^2 + \left(\frac{F_{L1-2-Inc\_FE} - F_{L1-2-Inc\_in-vivo}}{F_{L1-2-Inc\_in-vivo}}\right)^2\right.$$
$$\left. + \left(\frac{M_{L1-2\_FE} - M_{L1-2\_in-vivo}}{M_{L1-2\_In-vivo}}\right)^2 + \left(\frac{M_{L1-2-Inc\_FE} - M_{L1-2-Inc\_in-vivo}}{M_{L1-2-Inc\_in-vivo}}\right)^2\right]$$

Where:

- $F_{L1-2\_FE}$ and $M_{L1-2\_FE}$ are the predicted magnitudes of internal force and moment in the disc L1-2 in flexed posture, respectively.
- $F_{L1-2\_in-vivo}$ and $M_{L1-2\_in-vivo}$ are the *in-vivo* magnitudes of internal force and moment in the disc L1-2 in flexed posture, respectively. They were measured on vertebral body implants in patients with fractured vertebra (Dreischarf et al., 2015) (Table 4.2).
- $F_{L1-2-Inc\_FE}$ and $M_{L1-2-Inc\_FE}$ are the predicted increase in magnitudes of internal force and moment in the disc L1-2 due to change from upright to flexed posture, respectively.
- $F_{L1-2-Inc\_in-vivo}$ and $M_{L1-2-Inc\_in-vivo}$ are the *in-vivo* increase in magnitudes of internal force and moment in the disc L1-2 due to change from upright to flexed posture, respectively. They were measured on vertebral body implants in patients with fractured vertebra (Dreischarf et al., 2015) (Table 4.2).
- $IDP_{L4-5\_FE}$ is the predicted IDP in the disc L4-5 in flexed posture.
- $IDP_{L4-5\_In-vivo}$ is the *in-vivo* IDP in the disc L4-5 in flexed posture reported by Sato et al., (1999) (Table 4.2).
- $IVR_{i\_FE}$ are the predicted IVRs along levels L1-S1 in flexed posture.
- $IVR_{i\_in-vivo}$ are the *in-vivo* IVRs along levels L1-S1 in flexed posture reported by Lin et al. (1994) (Table 4.2).
- $a = 0.5, b = 0.3$ and $c = 0.2$ are the weight factors.

Additional IDP *in-vivo* values measured in the disc L4-5 (Wilke et al. 2001) and IVRs along levels L1-S1 (Pearcy et al., 1984) were used for comparison only (Table 4.2).

**Table 4.2.** *In-vivo* values in flexion.

| ***In-vivo data*** | ***L1-2*** | ***L2-3*** | ***L3-4*** | ***L4-5*** | ***L5-S1*** | ***Reference*** |
|---|---|---|---|---|---|---|
| $F_{L1-2\_in-vivo}\ (N)$ | 450 (440-640)* | - | - | - | - | *Dreischarf et al., 2015* |
| $F_{L1-2-Inc\_in-vivo}\ (N)$ | 330 (210-350) * | - | - | - | - | |
| $M_{L1-2\_in-vivo}\ (Nm)$ | 2.6 | - | - | - | - | |
| $M_{L1-2-Inc\_in-vivo}\ (Nm)$ | 2 | - | - | - | - | |
| $IDP_{L4-5\_In-vivo}\ (MPa)$ | - | - | - | 1.32 (±0.22) | - | *Sato et al., 1999* |
| | - | - | - | 1.1 | - | *Wilke et al., 2001* |
| $IVR_{i\_in-vivo}\ (°)$ | 5.7 (±2.3) | 7.6 (±3.3) | 10.5(±2.8) | 12.6 (±3.5) | 8.4 (±3.6) | *Lin et al., 1994* |
| | 8 (±5) | 10 (±2) | 12 (±1) | 13 (±4) | 9 (±6) | *Pearcy et al., 1984* |

± Standard deviation, * Lower-upper limit

## 4.3. Results

### 4.3.1. Spine response

Applying various FL magnitudes combined with similar flexion moment produced almost equal IVRs but slightly different facet joint forces (FJF), ligaments force and discs moment. The IDP and discs force values varied substantially with FL magnitude at all spinal levels, though their patterns remained almost unchanged. Thus, as a typical result, only spinal response to a 500N FL combined with wide range of flexion moment is shown in Fig. 4.2.

- *FL alone*

The FL alone created small IVRs (less than 0.4°) but no force in the ligaments along the spine. However, it produced constant force (500N) and variable moment (ranged from 0.9Nm to 1.5Nm) and IDP (ranged between 0.44MPa and 0.55MPa) in all discs. The FJF occurred at levels L4-S1 only and the magnitude did not exceed 40N.

- *FL with flexion*

The IVRs, IDP, ligaments force, and disc force and moment increased with flexion at all spinal levels (Fig. 4.2). However, up to 1.2Nm flexion, the moment in the discs decreased and then increased afterwards (Fig. 4.2d). The IDP and disc force as well as ligaments force at levels L1-5 increased similarly; almost linearly with flexion (Figs. 4.2b,c,e), whereas, a jump in ligament

force and FJF occurred at level L5-S1 (Figs. 4.2e-f). Also, greater increase in IVRs and disc moment was noticed at levels L2-S1 (Fig. 4.2a) and L1-2 (Fig. 4.2d), respectively.

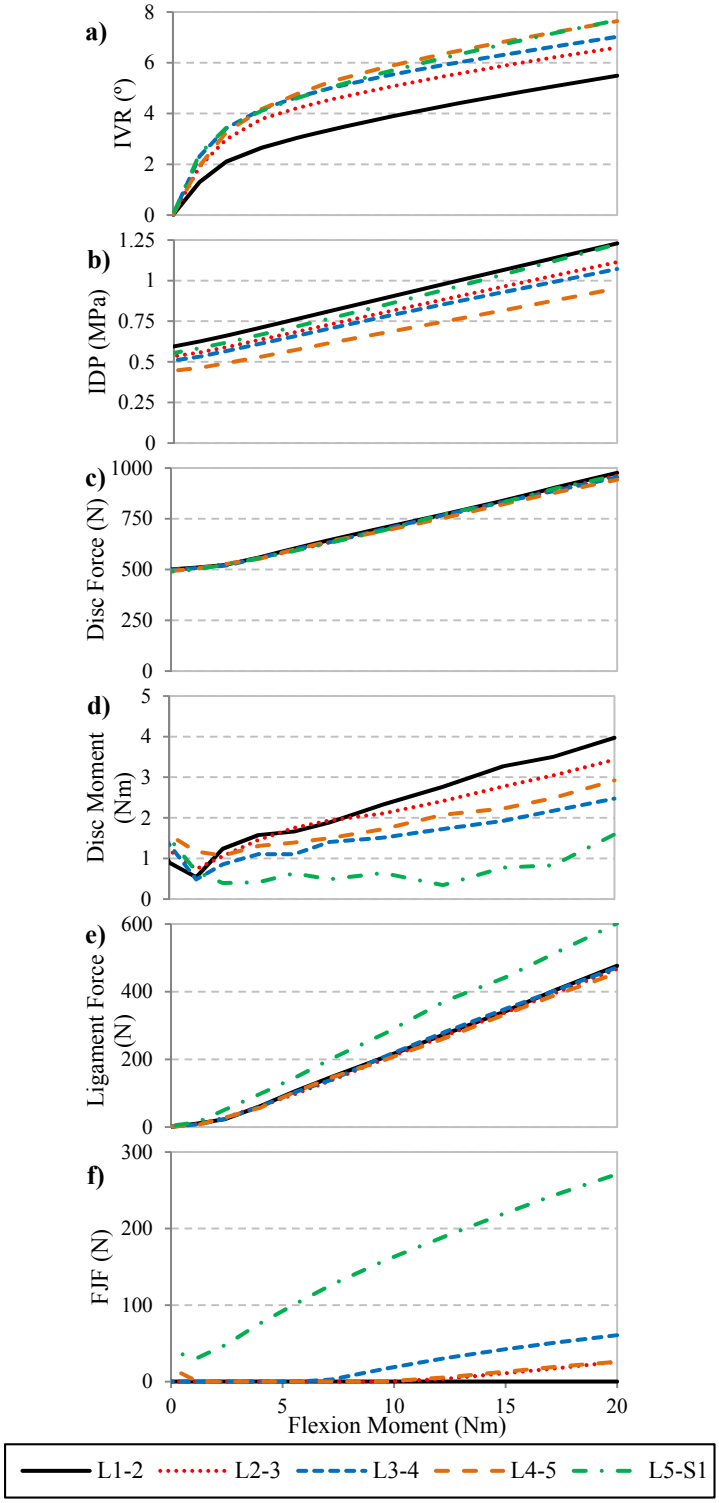


**Fig. 4.2.** Spinal response to a 500N FL combined with variable flexion moment.

### 4.3.2. Optimal magnitudes of FL and flexion moment

Deviations of the predicted values for each parameter from the corresponding *in-vivo* data are shown in Fig. 4.3. In all FL and moment combinations the predicted disc force was higher than *in-vivo* value. When combined with low moment magnitudes (<10Nm), all FL magnitudes underestimated the remaining parameters. Increasing the flexion moment magnitude up to 15Nm improved the model predictions except for the disc force and moment. Deviations of disc moment and IVRs were almost unaffected by the FL magnitude (<3% change). Also, the FL magnitude had negligible effects on the increase in disc moment and increase in disc force (<15% change). The most sensitive parameters to FL magnitude were disc force and IDP. Deviation of the predicted disc force from *in-vivo* value increased with FL and moment magnitudes. It reached 240% in case of 1100N FL combined with 20Nm flexion moment. Inversely, higher FL (1100N) and moment (20Nm) magnitudes produced IDP with a good agreement with *in-vivo* value (deviation <13%).

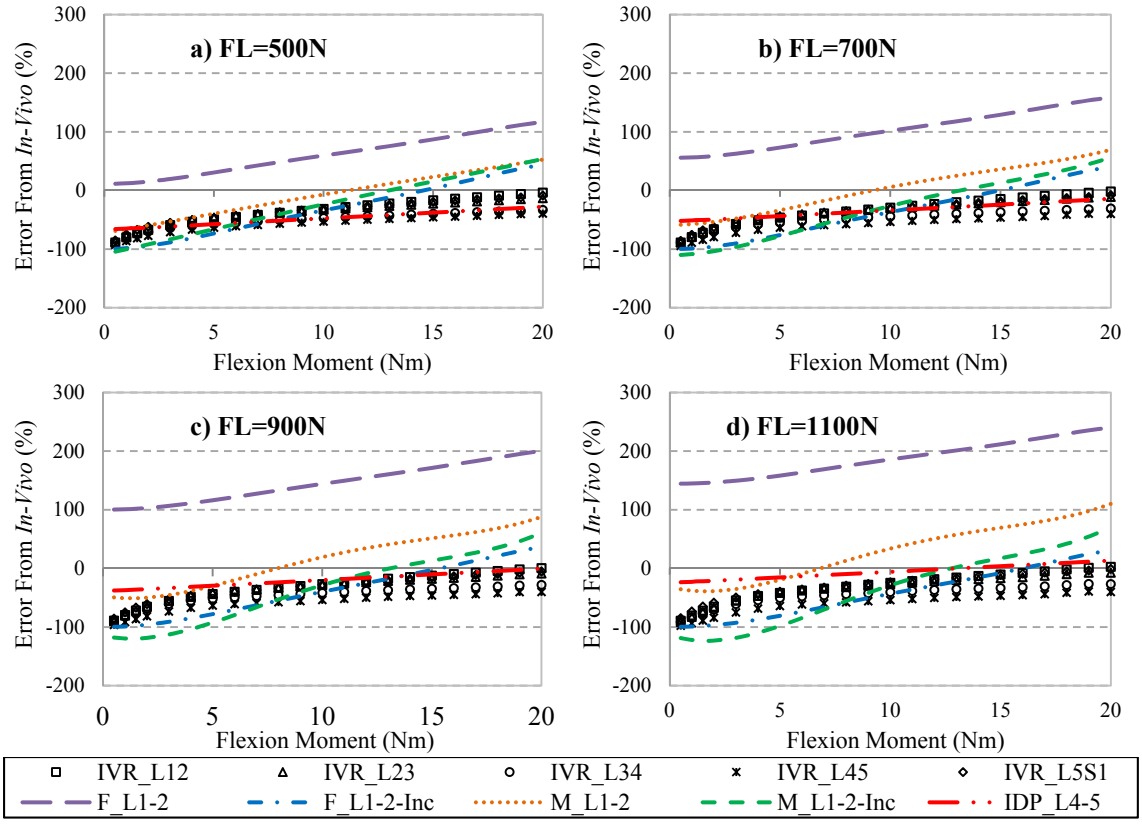


**Fig. 4.3.** Deviation of the FE predicted spinal parameters from *in-vivo* values: +ve and –ve errors indicate that predicted values were higher and lower than *in-vivo* values, respectively.

Variations of the objective function value with FL and moments magnitudes are shown in Fig. 4.4. For each FL magnitude the combined moment magnitude that minimized the deviation (objective function) is reported in Fig. 4.4. Optimal predictions (with smallest deviation) were found in case of 500N and 700N FL combined with 15.7Nm and 13.5Nm moment, respectively. High FL required small flexion moment to minimize the objective function and vice versa. Magnitude of 9.9Nm was necessary in case of 1100N FL while in case of 500N FL magnitude the required moment was 15.7Nm.

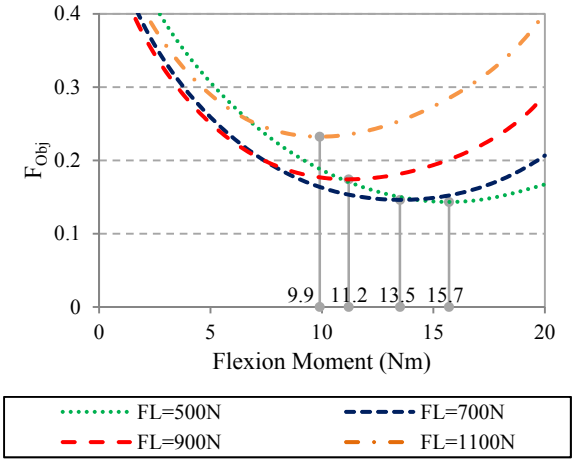


**Fig. 4.4.** Variations of the objective function with flexion moment magnitude for different FL cases.

The FE predicted values of the spinal parameters in case of optimal combination of FL and flexion moment were compared to their corresponding *in-vivo* values/ranges (Fig. 4.5). Results showed the disc force predicted was higher than the *in-vivo* value in all loading combination. The disc moment predicted was also higher than *in-vivo* value, though all load combinations produced almost similar disc moment. The increase in the disc force showed a good agreement with the *in-vivo* range in all loading cases while only the case of 900N FL with 11.2Nm flexion produced increase in the moment that matches the *in-vivo* value. The IDPs was well predicted with load combinations that considered 900N or 1100N FL but was underestimated with other FL magnitudes. The IVRs at levels L1-3 and L5-S1 fell inside the *in-vivo* ranges in all loading cases while values at levels L3-5 were underestimated.

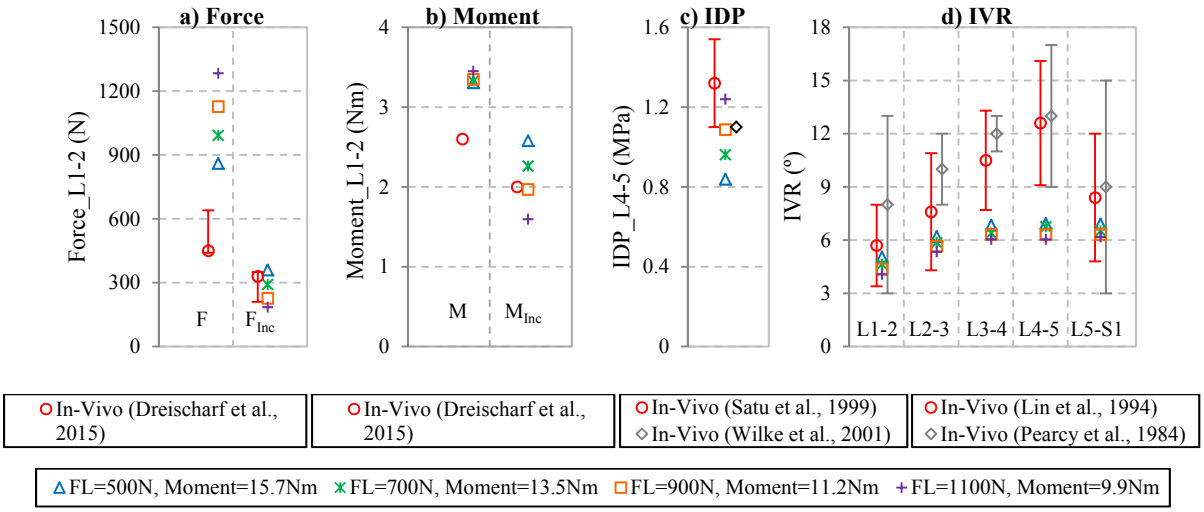


**Fig. 4.5.** Comparison of FE predicted spinal parameters with *in-vivo* values/ranges.

### 4.4. Discussions

There is a lack of consensus as to what magnitudes of FL and flexion moment simulate better the *in-vivo* flexed posture. This study investigated sensitivity of the spinal response to four FL magnitudes (500N, 700N, 900N and 1100N) combined with a wide range (0-20Nm) of flexion moment using a validated FE model of ligamentous lumbosacral spine (Naserkhaki et al., 2015). Optimal magnitudes of the FL and flexion moment that mimic *in-vivo* spinal response in flexed posture were determined. Particularly, these optimal magnitudes ensured the agreement with *in-vivo* data of not only the IDP and IVRs but also the internal loads developed in the disc. These optimal magnitudes minimized the deviation of all spinal parameters together from their corresponding *in-vivo* values.

There were some limitations associated with this study. Geometry and material properties of the employed FE model do not represent general population. The geometry was reconstructed from CT-Scan data of one individual and the material properties were taken from literature. The time-dependent properties of the spinal components as well as the fluid-flow phenomenon in the disc and porous bone were not considered as the current model studied only the immediate response of the spine to static loads.

Although the combination of FL and moment has been widely used in FE (Dreischarf et al., 2014; Chen et al., 2013; Park et al., 2013; Rohlmann et al., 2009b; Goto et al., 2003) and *in-vitro* (Fry et al., 2014; Rohlmann et al., 2001) studies of spinal response to mechanical load in the absence of muscles, it is a simplified loading scenario and does not simulate realistically the *in-*

*vivo* loading conditions. The FL concept (Patwardhan et al., 2001) while minimizing the intervertebral rotations only considers the compressive component of muscle force and neglects the shear one. Moreover, it imposes a constant compressive force along the spine, while the actual compressive force increases from cranial to caudal levels in both standing and flexed postures (Kim and Kim, 2008; Arjmand and Shirazi-Adl, 2005; El-Rich et al., 2004). In addition, previous studies have demonstrated that internal moments vary along the spine in upright (El-Rich et al., 2004) and flexed posture (Arjmand and Shirazi-Adl, 2005).

To account for uncertainties of *in-vivo* data (Table 4.2) particularly the disc loads and IVRs, smaller weights were assigned to these parameters compared to the IDP. Half of the total weight ($a$ =0.5) was assigned to the IDP since its measurement is more accurate and does not use skin-mounted device (Sato et al., 1999). Thirty percent ($b$ =0.3) of total weight were assigned to IVRs at levels L1-S1 and the remaining 20% ($c$ =0.2) of total weight were assigned disc loads (disc force, increase in disc force, disc moment, and increase in disc moment). Due to lack of *in-vivo* data of spinal loads in normal spine, the current study utilized data measured from implant used in vertebral body replacement (Dreischarf et al., 2015) which justified the low percentage of total weight assigned to spinal loads compared to those of IDP and IVRs. Other combinations of weight factors changed slightly the optimal magnitudes but did not affect the general conclusion. Findings were not sensitive to weight factors. The objective function used *in-vivo* data of IDP and IVRs taken from works done by Sato et al. (1999) and Lin et al. (1994), respectively as they covered large sample size compared to values reported by Wilke et al. (2001) and Pearcy et al. (1984) whose values were only used to compare results of the current study.

For a given FL magnitude, all spinal parameters increased more or less (with different slopes) with magnitude of flexion moment, while the IDP and disc loads were mainly affected by the FL magnitude.

Results showed that the disc force and IDP were very sensitive to FL magnitude than moment magnitude (resisting action of the ligaments against moment increased both disc force and IDP). The IVRs were mainly affected by the moment magnitude.

Our findings suggest that a FL of small magnitude (e.g. 500N) must be combined with large flexion moment (e.g. 15.7Nm) whereas a FL of large magnitude (e.g. 1100N) must be combined with smaller flexion moment (e.g. 9.9Nm). The first loading combination predicted disc force closer to the *in-vivo* value but highly underestimated the IDP. Contrariwise, the latter one

predicted IDP in acceptable agreement with *in-vivo* data but highly overestimated the disc force. This agrees with the magnitudes of 1175N for FL and 7.5Nm for flexion moment used by Rohlmann et al. (2009b). Nevertheless, applying small FL and relatively great moment e.g. 10 Nm (Chen et al., 2013; Park et al., 2013; Goto et al., 2003) may also produce spinal parameters in reasonable agreement with *in-vivo* data.

Results revealed that the two loading combinations of 900N FL and 11.2Nm moment as well as 1100N FL and 9.9Nm could deliver IDP in good agreement with *in-vivo* values (Wilke et al. 2001; Sato et al. 1999). Determination of optimal FL and moment magnitude should not only consider IVRs and IDP but also the disc load as this latter can hardly be found from the IDP (Dreischarf et al., 2013). The optimal combinations of 900N FL and 11.2Nm moment and 1100N FL and 9.9Nm moment produced compressive force of 1126N and 1285N at level L1-2 respectively which is in acceptable agreement with the value of 1171N predicted by a FE model that included muscle forces (Arjmand and Shirazi-Adl, 2005).

Although the magnitude of FL did not affect directly the IVRs, it was found that the smallest FL (500N) produced relatively higher IVRs as it necessitated large moment magnitude (15.7Nm) to mimic the *in-vivo* data. This confirms that small FL which implies small muscle stabilization force not only requests high resisting action of ligaments but also results in large IVRs (less stability). Flexion moment of magnitude smaller than 9.9Nm will not realistically simulate *in-vivo* condition. For instance, ours (Naserkhaki et al., 2015) and eight other published FE models (Dreischarf et al., 2014) have demonstrated that combining 7.5Nm flexion moment with 1175N FL underestimates the IVRs.

In conclusion, the current study demonstrated that IDP and disc force and moment predicted by FE model are more sensitive to magnitude of FL while the IVRs are mainly affected by intensity of the combined moment. It suggested that applying FL with magnitude greater than 900N will produce more realistic compression force in flexed posture. Since the disc force and IDP were measured at levels L1-2 and L4-5 respectively, we speculate that applying FL with magnitude that increases from level L1-2 to level L5-S1 to account for external load (e.g. gravity load) and muscles forces will improve the FE prediction. In addition, the intensity of flexion moment must be selected based on the FL magnitude; the lower the FL the higher the moment and vice versa. However, a minimum magnitude of 9.9Nm is recommended to better simulate the flexed posture.

Finally, it is important to mention that our study did not intend to support the combination of FL and moment as best loading mode to simulate *in-vivo* flexed posture; it rather provided insights on the sensitivity of spinal response to magnitudes of these combined loads which are largely used in spinal behavior studies.

**Conflict of interest statement**

The Authors have no conflict of interest to declare.

**Acknowledgements**

This study was supported by NSERC Discovery Grant, Canada.

**References**

Arjmand N., Shirazi-Adl, A., 2005. Biomechanics of changes in lumbar posture in static lifting. Spine 30, 2637-48.

Chen, S.H., Chiang, M.C., Lin, J.F., Lin, S.C., Hung, C.H., 2013. Biomechanical Comparison of Three Stand-Alone Lumbar Cages - a Three-Dimensional Finite Element Analysis. BMC Musculoskeletal Disorders 14, 281.

Dreischarf, M., Albiol, L., Zander, T., Arshad, R., Graichen, F., Bergmann, G., Schmidt, H., Rohlmann, A., 2015. In Vivo Implant Forces Acting on a Vertebral Body Replacement during Upper Body Flexion. Journal of Biomechanics 48, 560-565.

Dreischarf, M., Rohlmann, A., Bergmann, G., Zander, T., 2011. Optimised Loads for the Simulation of Axial Rotation in the Lumbar Spine. Journal of Biomechanics 44, 2323-2327.

Dreischarf, M., Rohlmann, A., Bergmann, G., Zander, T., 2012. Optimised in Vitro Applicable Loads for the Simulation of Lateral Bending in the Lumbar Spine. Medical Engineering & Physics 34, 777-780.

Dreischarf, M., Rohlmann, A., Zhu, R., Schmidt, H., Zander, T., 2013. Is it Possible to Estimate the Compressive Force in the Lumbar Spine from Intradiscal Pressure Measurements? A Finite Element Evaluation. Medical Engineering & Physics, 35, 1385-1390.

Dreischarf, M., Zander, T., Shirazi-Adl, A., Puttlitz, C.M., Adam, C.J., Chen, C.S., Goel, V.K., Kiapour, A., Kim, Y.H., Labus, K.M., Little, J.P., Park, W.M., Wang, Y.H., Wilke, H.J.,

Rohlmann, A., Schmidt, H., 2014. Comparison of Eight Published Static Finite Element Models of the Intact Lumbar Spine: Predictive Power of Models Improves when Combined Together. Journal of Biomechanics 47, 1757-1766.

El-Rich, M., Arnoux, P., Wagnac, E., Brunet, C., Aubin, C., 2009. Finite Element Investigation of the Loading Rate Effect on the Spinal Load-Sharing Changes Under Impact Conditions. Journal of Biomechanics 42, 1252-1262.

El-Rich, M., Shirazi-Adl., A, Arjmand, N., 2004. Muscle activity, internal loads, and stability of the human spine in standing postures: combined model and in vivo studies. Spine 29, 2633-42.

Fry, R.W., Alamin, T.F., Voronov, L.I., Fielding, L.C., Ghanayem, A.J., Parikh, A., Carandang, G., Mcintosh, B.W., Havey, R.M., Patwardhan, A.G., 2014. Compressive Preload Reduces Segmental Flexion Instability After Progressive Destabilization of the Lumbar Spine. Spine 39, E74-81.

Goel, V.K., Kong, W., Han, J.S., Weinstein, J.N., Gilbertson, L.G., 1993. A Combined Finite Element and Optimization Investigation of Lumbar Spine Mechanics with and without Muscles. Spine 18, 1531-1541.

Goto, K., Tajima, N., Chosa, E., Totoribe, K., Kubo, S., Kuroki, H., Arai, T., 2003. Effects of Lumbar Spinal Fusion on the Other Lumbar Intervertebral Levels (Three-Dimensional Finite Element Analysis). Journal of Orthopaedic Science: Official Journal of the Japanese Orthopaedic Association 8, 577-584.

Guan, Y., Yoganandan, N., Moore, J., Pintar, F.A., Zhang, J., Maiman, D.J., Laud, P., 2007. Moment-Rotation Responses of the Human Lumbosacral Spinal Column. Journal of Biomechanics 40, 1975-1980.

Kiapour, A., Anderson, D.G., Spenciner, D.B., Ferrara, L., Goel, V.K., 2012. Kinematic Effects of a Pedicle-Lengthening Osteotomy for the Treatment of Lumbar Spinal Stenosis. Journal of Neurosurgery Spine 17, 314-320.

Kim, K., Kim, Y.H., 2008. Role of Trunk Muscles in Generating Follower Load in the Lumbar Spine of Neutral Standing Posture. Journal of Biomechanical Engineering 130, 041005.

Lin, R.M., Yu, C.Y., Chang, Z.J., Lee, C.C., Su, F.C., 1994. Flexion-Extension Rhythm in the Lumbosacral Spine. Spine 19, 2204-2209.

Naserkhaki, S., Jaremko, J.L., Adeeb, S., El-Rich, M., 2015. On the Load-Sharing Along the Ligamentous Lumbosacral Spine: Finite Element Modeling and Static Equilibrium Approach. Journal of Biomechanics, DOI: http://dx.doi.org/10.1016/j.jbiomech.2015.09.050.

Naserkhaki, S., Jaremko, J.L., Kawchuk, G., Adeeb, S., El-Rich, M., 2014. Investigation of Lumbosacral Spine Anatomical Variation Effect on Load-Partitioning Under Follower Load Using Geometrically Personalized Finite Element Model. ASME International Mechanical Engineering Congress and Exposition, Proceedings (IMECE), Anonymous 3, DOI: 10.1115/IMECE201440231.

Niosi, C.A., Wilson, D.C., Zhu, Q., Keynan, O., Wilson, D.R., Oxland, T.R., 2008. The Effect of Dynamic Posterior Stabilization on Facet Joint Contact Forces: An in Vitro Investigation. Spine 33, 19-26.

Oxland, T.R., Lin, R.M., Panjabi, M.M., 1992. Three-Dimensional Mechanical Properties of the Thoracolumbar Junction. Journal of Orthopaedic Research: Official Publication of the Orthopaedic Research Society 10, 573-580.

Panjabi, M.M., 2007. Hybrid Multidirectional Test Method to Evaluate Spinal Adjacent-Level Effects. Clinical Biomechanics (Bristol, Avon) 22, 257-265.

Park, W.M., Kim, K., Kim, Y.H., 2013. Effects of Degenerated Intervertebral Discs on Intersegmental Rotations, Intradiscal Pressures, and Facet Joint Forces of the Whole Lumbar Spine. Computers in Biology and Medicine 43, 1234-1240.

Patwardhan, A.G., Havey, R.M., Meade, K.P., Lee, B., Dunlap, B., 1999. A Follower Load Increases the Load-Carrying Capacity of the Lumbar Spine in Compression. Spine 24, 1003-1009.

Patwardhan, A.G., Meade, K.P., Lee, B., 2001. A Frontal Plane Model of the Lumbar Spine Subjected to a Follower Load: Implications for the Role of Muscles. Journal of Biomechanical Engineering, 123, 212-217.

Pearcy, M., Portek, I., Shepherd, J., 1984. Three-Dimensional x-Ray Analysis of Normal Movement in the Lumbar Spine. Spine 9, 294-297.

Robin, S., Skalli, W., Lavaste, F., 1994. Influence of Geometrical Factors on the Behavior of Lumbar Spine Segments: A Finite Element Analysis. European Spine Journal: Official

Publication of the European Spine Society, the European Spinal Deformity Society, and the European Section of the Cervical Spine Research Society 3, 84-90.

Rohlmann, A., Bauer, L., Zander, T., Bergmann, G., Wilke, H.J., 2006. Determination of Trunk Muscle Forces for Flexion and Extension by using a Validated Finite Element Model of the Lumbar Spine and Measured in Vivo Data. Journal of Biomechanics 39, 981-989.

Rohlmann, A., Neller, S., Claes, L., Bergmann, G., Wilke, H.J., 2001. Influence of a Follower Load on Intradiscal Pressure and Intersegmental Rotation of the Lumbar Spine. Spine 26, E557-E561.

Rohlmann, A., Zander, T., Rao, M., Bergmann, G., 2009a. Applying a Follower Load Delivers Realistic Results for Simulating Standing. Journal of Biomechanics 42, 1520-1526.

Rohlmann, A., Zander, T., Rao, M., Bergmann, G., 2009b. Realistic Loading Conditions for Upper Body Bending. Journal of Biomechanics 42, 884-890.

Sato, K., Kikuchi, S., Yonezawa, T., 1999. In Vivo Intradiscal Pressure Measurement in Healthy Individuals and in Patients with Ongoing Back Problems. Spine 24, 2468-2474.

Sawa, A.G., Crawford, N.R., 2008. The use of Surface Strain Data and a Neural Networks Solution Method to Determine Lumbar Facet Joint Loads during in Vitro Spine Testing. Journal of Biomechanics 41, 2647-2653.

Schmidt, H., Heuer, F., Simon, U., Kettler, A., Rohlmann, A., Claes, L., Wilke, H.J., 2006. Application of a New Calibration Method for a Three-Dimensional Finite Element Model of a Human Lumbar Annulus Fibrosus. Clinical Biomechanics 21, 337-344.

Schmidt, H., Kettler, A., Heuer, F., Simon, U., Claes, L., Wilke, H.J., 2007. Intradiscal Pressure, Shear Strain, and Fiber Strain in the Intervertebral Disc Under Combined Loading. Spine 32, 748-755.

Schmidt, H., Shirazi-Adl, A., Galbusera, F., Wilke, H.J., 2010. Response Analysis of the Lumbar Spine during Regular Daily activities—A Finite Element Analysis. Journal of Biomechanics 43, 1849-1856.

Shirazi-Adl, A., 1994. Biomechanics of the Lumbar Spine in sagittal/lateral Moments. Spine 19, 2407-2414.

Shirazi-Adl, A., Ahmed, A.M., Shrivastava, S.C., 1986. Mechanical Response of a Lumbar Motion Segment in Axial Torque Alone and Combined with Compression. Spine 11, 914-927.

Wang, J.L., Parnianpour, M., Shirazi-Adl, A., Engin, A.E., 1999. Rate Effect on Sharing of Passive Lumbar Motion Segment Under Load-Controlled Sagittal Flexion: Viscoelastic Finite Element Analysis. Theoretical and Applied Fracture Mechanics 32, 119-128.

Wilke, H., Neef, P., Hinz, B., Seidel, H., Claes, L., 2001. Intradiscal Pressure Together with Anthropometric Data--a Data Set for the Validation of Models. Clinical Biomechanics (Bristol, Avon) 16, S111-26.

Woldtvedt, D.J., Womack, W., Gadomski, B.C., Schuldt, D., Puttlitz, C.M., 2011. Finite Element Lumbar Spine Facet Contact Parameter Predictions are Affected by the Cartilage Thickness Distribution and Initial Joint Gap Size. Journal of Biomechanical Engineering 133, 061009.

Yamamoto, I., Panjabi, M.M., Crisco, T., Oxland, T., 1989. Three-Dimensional Movements of the Whole Lumbar Spine and Lumbosacral Joint. Spine 14, 1256-1260.

# Chapter 5

## Effects of Inter-Individual Lumbar Spine Curvature Variation on Load-Sharing: Geometrically Personalized Finite Element Study

This chapter has been submitted as Naserkhaki, S., Jaremko, J.L., El-Rich, M., 2015, to Spine journal (Phila Pa.1976).

**Abstract**

There is a large, at times contradictory, body of research relating spinal curvature to Low Back Pain (LBP). Mechanical load is considered as one of the most important factors in LBP etiology. Computational modeling of the lumbar spine provides insights on kinematics and internal load development and distribution along the spine. Geometry (size and shape) of the spinal structures and sagittal curvature of the spine in particular govern its mechanical behavior and load-sharing. Thus, understanding how inter-individual sagittal curvature variation affects the spinal load-sharing becomes of high importance in LBP assessment. This study compared kinematics and load-sharing in three ligamentous lumbosacral spines: one hypo-lordotic (Hypo-L), i.e., flat spine, one normal-lordotic (Norm-L), and one hyper-lordotic (Hyper-L), i.e., with high lordosis spine, in flexed and extended postures using Finite Element (FE) modeling. These postures were simulated by applying Follower Load (FL) combined with flexion or extension moment. The Hypo-L spine demonstrated stiffer behavior in flexion but more flexible response to extension compared to the Norm- and Hyper-L spines. The excessive lordosis stiffened response of the Hyper-L spine to extension but did not affect its resistance to flexion compared to the Norm-L spine. In despite of different resisting action of the posterior ligaments to flexion moment, the increase of compression in the disc was similar in all the spines leading to similar load-sharing. However, resistance of the facet joints to extension was more significant in the Norm- and Hyper-L spines which reduced the disc compression. The internal forces produced by FL and flexion were mainly carried by the discs (75%) and posterior ligaments (25%) while contribution of ligaments in supporting internal moment was higher (~70%) compared to the discs (~20%). Role of the facet joints was negligible except at level L5-S1. In the case of FL and extension, the discs, ligaments and facet joints shared spinal force with proportion of 55%, 20%, 25% respectively in the Hypo-L spine while facet joints contribution did not exceed 10% at levels L1-4 and reached up to 30% at levels L5-S1 in the Norm- and Hyper-L spines. The facet joint carried up to 63% of the internal moment in the Hyper-L spine. The spinal curvature strongly influenced the magnitude and location of load on spinal components and also altered the load-sharing particularly in extension. Consideration of the sagittal curvature should be an integral part of mechanical analysis of the lumbar spine.

**Keywords:** lumbar spine; load-sharing; Lumbar Lordosis; Sacral Slope; Pelvic Incidence; Inter-Individual Variation; Finite Element Model; Spine Geometry; Spine Sagittal Curvature.

## 5.1. Introduction

The chance of experiencing Low Back Pain (LBP) in adults is higher than 50% in the lifetime with about 18% prevalence at any time (Panjabi, 2003; Trainor and Wiesel, 2002). There is a large, at times contradictory, body of research relating spinal curvature to LBP. For instance, higher risk of LBP has been reported for relatively flat spines (Chaleat-Valayer et al., 2011; Barrey et al., 2007; Rajnics et al., 2002; Tsuji et al., 2001; Adams et al., 1999; Korovessis et al., 1999; Harrison et al., 1998; Jackson and McManus 1994) compared to normal ones, though the reverse observation has been reported as well (Gautier et al., 1999; Tüzün et al., 1999; Christie et al., 1995). The sagittal curvatures of the spine which determine its balance are thought by some to be one of the main mechanical factors leading to degenerative change (Roussouly and Pinheiro-Franco, 2011). Since mechanical load is one of the most important factors in LBP etiology (Deyo and Weinstein, 2001; Pope and Novotny, 1993), determining the effects of inter-individual sagittal curvature variations on the spinal mechanical response in terms of kinematics and load-sharing becomes essential.

Previous investigations have been carried out to understand the kinematics and internal loads development in the spine and their relation to change of Lumbar Lordosis (LL) with posture (Putzer et al., 2015; Bruno et al., 2012; Arjmand and Shirazi-Adl, 2005; Keller et al., 2005; Shirazi-Adl and Parnianpour, 1996). For example, Bruno et al. (2012) reported that age-related increase in thoracic kyphosis was compensated by increase in pelvic tilt or LL to maintain stability which resulted in increase in vertebral compressive force. Another study by Arjmand and Shirazi-Adl (2005) demonstrated that alterations in the LL in lifting resulted in significant changes in the muscle forces and internal spinal loads. Furthermore, it has been demonstrated that variation of morphological spinal parameters such as Pelvic Incidence (PI) which is not affected by the posture or the pelvis position and is considered as invariable for a subject after the end of growth (Barrey et al., 2007), and the Sacral Slope (SS) affected the load transfer mechanism in the lumbar segment L5-S1 (El-Rich et al., 2006a,b). Nevertheless, effects of the inter-individual lumbar spine curvature (LL, SS and PI) variations on spinal response to mechanical load are not yet fully understood.

This study aimed at understanding how variation of the sagittal alignment parameters LL, SS, and PI in three lumbosacral spines with different geometry affects spinal response to flexion and extension by using Finite Element (FE) models with personalized geometry. Particularly,

kinematics, internal forces and moments, and load-sharing at all levels of these spines were predicted and compared.

## 5.2. Materials and methods

### 5.2.1. Measurement of the sagittal alignment parameters

In this study, the LL, SS, and PI were measured on CT-scans of 24 subjects (age median and range: 28 and 20-48 years, respectively). The images were obtained from the University of Alberta Hospital Database after receiving ethics approval for retrospective study. Measurements were taken at the median sagittal plane. The measured values showed that LL and PL increased with SS (Fig. 5.1). The normal ranges reported for these parameters (Vrtovec et al., 2012; Roussouly et al., 2005; Roussouly et al., 2003; De Smet,1985; Propst-Proctor and Bleck, 1983; Stagnara et al. 1982) are limited by the green rectangles. Spines of three subjects (35 years old female, 20 years old male, and 24 years female) with distinct sagittal alignment parameters were selected which are identified by different markers in Fig. 5.1. These spines were categorized as: Hypo-Lordotic (Hypo-L), Normal-Lordotic (Norm-L), and Hyper-Lordotic (Hyper-L) spines. The Hypo-L spine has lower while the Hyper-L spine has higher SS, PI and LL comparing to the Norm-L spine (Fig. 5.2).

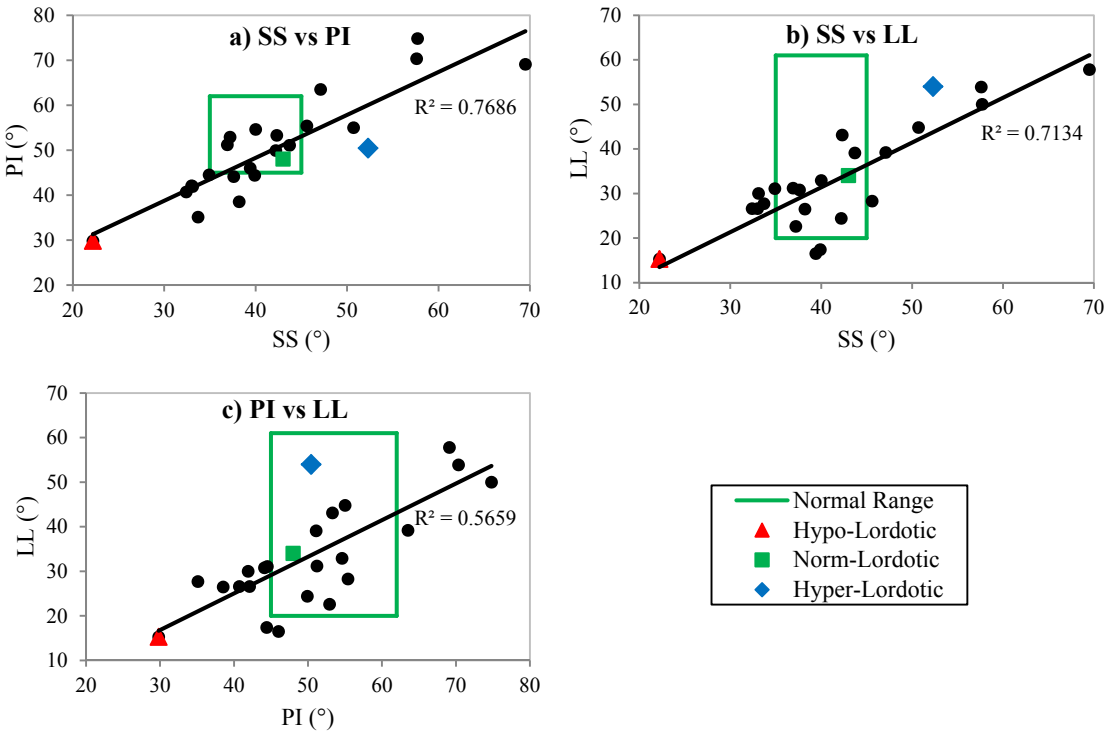


**Fig. 5.1.** Sagittal alignment parameters relationship.

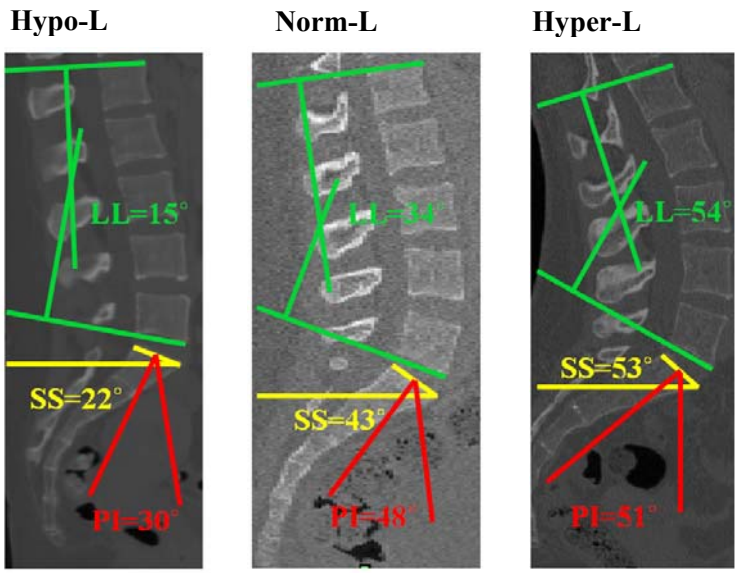


**Fig. 5.2.** Values of the sagittal alignment parameters in the three selected spines.

### 5.2.2. FE models

A geometrically personalized FE model was developed for each of the three selected spines (Fig. 5.3). Geometries of these models were reconstructed from the subjects CT-Scan data. The model of the Norm-L spine was created and validated in previous study (Naserkhaki et al., 2014; 2015). The kinematics, intervertebral rotations (IVRs), intradiscal pressure in the nucleus (IDP), and contact force in the facet joints (FJF) predicted by this model were compared to in-vivo and in-vitro measurements. In brief, the model consists of five lumbar vertebrae, five intervertebral discs, sacrum, and seven surrounding ligaments (Anterior Longitudinal Ligament, ALL, Posterior Longitudinal Ligament, PLL, Capsular Ligament, CL, Intertransverse Ligament, ITL, Ligamentum Flavum, LF, Supraspinous Ligament, SSL, and Interspinous Ligament, ISL).

The cortical shell was meshed by 3-node elements with a uniform thickness of 1 mm and the volume inside was filled with 4-node (tetrahedral) solid elements to represent the cancellous bone. The disc mesh was generated by seven layers of solid elements between two adjacent endplates. Each disc was divided into nucleus pulposus and annulus fibrosus with a proportion according to the histological findings (44%_nucleus and 56%_annulus) (El-Rich et al., 2009; Schmidt et al., 2006). The annular fibers were simulated using nonlinear unidirectional springs inserted in a crosswise pattern close to ±35° (El-Rich et al., 2009; Schmidt et al., 2007). The ligaments were also modeled by nonlinear unidirectional springs (Breau et al., 1991). Material

properties of the spinal components (Table 5.1) were taken from the literature (Park et al. 2013; Shih et al 2013; El-Rich et al. 2009; Schmidt et al. 2007; Schmidt et al. 2006; Rohlmann et al. 2006; Goto et al. 2003; Shirazi et al. 1986). The minimum gap distance between two adjacent articular facets was set at 2 mm and frictionless surface to surface contact was used to simulate the facet joint articulation.

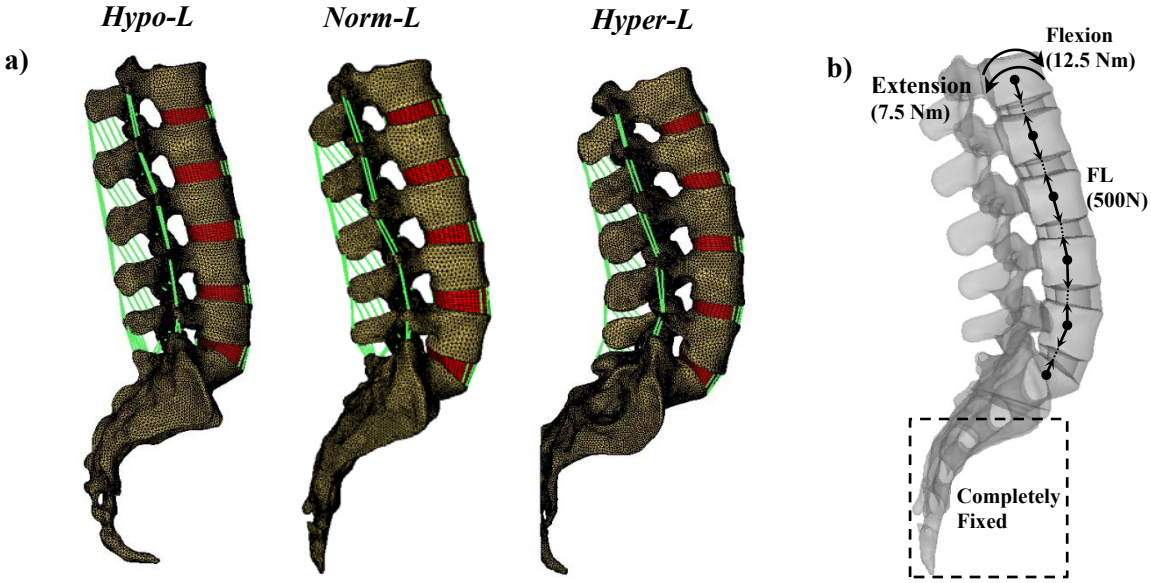


**Fig. 5.3.** FE models of the three selected spines: a) 3D mesh, b) Loading and boundary conditions.

**Table 5.1.** Material properties of the FE models.

| *Spinal Components* | | *Material Behaviour* | *Mechanical Properties* | |
|---|---|---|---|---|
| **Bone** | Cortical Bone | Linear Elastic | E=12000 (MPa) | $v$=0.30 |
| | Cartilaginous Endplate | | E=23.8 (MPa) | $v$=0.40 |
| | Cancellous Bone | | E=200 (MPa) | $v$=0.25 |
| **Disc** | Annulus Ground Substance | Hyper-Elastic (Mooney-Rivlin) | C10=0.18 | C01=0.045 |
| | Nucleus Pulposus | | C10=0.12 | C01=0.030 |
| **Collagen Fibers** | | Nonlinear force- displacement relationship (resisting tension only). | | |
| **Ligaments** | | | | |

In the current study, the models were subjected to 500N follower load (FL) combined with 12.5Nm flexion moment or 7.5Nm extension moment to simulate flexed and extended postures, respectively (Naserkhaki et al., 2015) while the lower sacrum region was completely fixed (Fig.

5.3). The FL whose line of action followed the lumbar spine curvature was applied by preloading (compressing) unidirectional nonlinear springs whose ends were connected to the vertebral bodies (Naserkhaki et al., 2014; 2015) (Fig. 5.3). The moments were applied to the centroid of the vertebral body of L1. Two cases were studied. In case 1 only the discs resisted load while the ligaments were removed from the model and the contact in the facet joints was deactivated. In case 2 the intact spine was studied. The analyses were performed using the FE solver Abaqus 6.13-4 (Abaqus 6.13-4, Dassault Systems Simulia Corp., USA).

The FE models predicted spinal response to applied load in terms of total rotation (L1-S1), IVRs, IDP, strains in the collagen fibers, FJF, and ligament forces. In addition, the disc force and moment developed at each spinal level were calculated at the disc center using the equilibrium equations of the Free Body Diagram (FBD) of that spinal level (Naserkhaki et al., 2015). Load-sharing was expressed as percentage (fraction) of total internal force/moment developed at each spinal level that each spinal component (i.e. disc, facet joints and ligaments) carried (Naserkhaki et al., 2015).

### 5.3. Results

*Case 1*

Results indicated that under both flexion and extension the Hypo-L spine was stiffer while the Hyper-L spine was more flexible than the Norm-L one (Fig. 5.4).

*Case 2*

Adding ligaments and facet joints stiffened responses of the three spines to both flexion and extension. The total rotation reduced by 37°, 67°, and 80° in the Hypo-, Norm- and Hyper-L spines respectively under flexion. In the extension case, it decreased by 12°, 22° and ?° (not converged) the Hypo-, Norm-, and Hyper-L spines respectively. Total rotations of the Hyper- and Norm-L spines were almost similar but greater than the Hypo-L one in the flexion case (Fig. 5.4a). However under extension, the Hypo-L spine had the largest rotation followed by the Norm-L then the Hyper-L spines. Under flexion, median of the IVRs (5.7°, 5.9° and 5.1° for the Hyper-, Norm- and Hypo-L spines, respectively) followed similar trend as the total rotation. In the extension case, the Hypo-L spine had the largest IVRs (median 4.1°) compared to the Norm-L (median 3.5°) and Hyper-L (median 2.7°) spines.

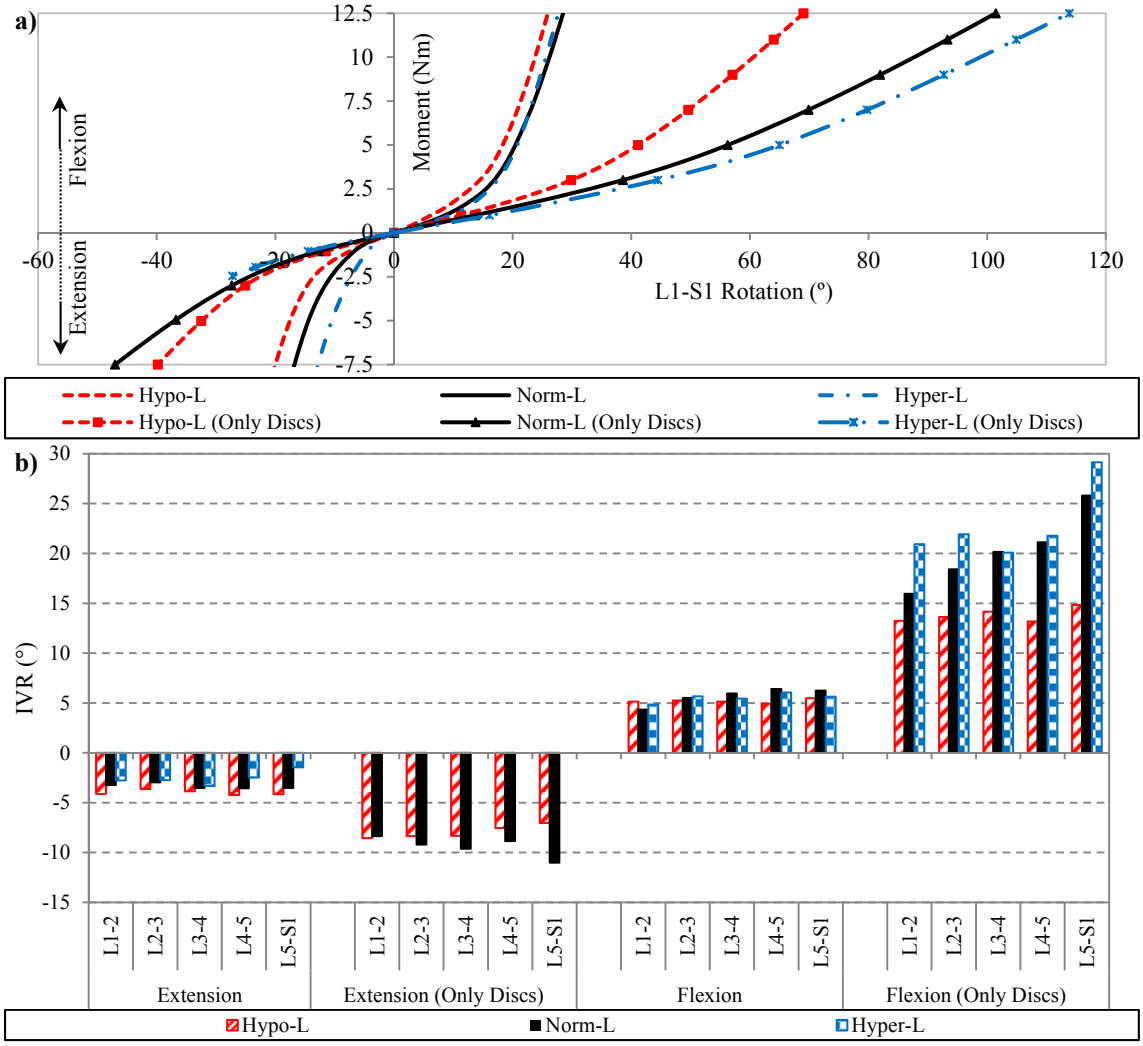


**Fig. 5.4.** Comparison of range of motion in the three spines: a) Total rotation-moment curves, b) IVRs.

Under the FL alone , the Hyper-L spine experienced the highest IDP at all levels except L5-S1 (Fig. 5.5). Results showed that IDP generally decreased from the cranial to caudal levels for all spines except for level L5-S1 of the Norm-L spine.

In flexed posture, IDP increased almost similarly for all spines at all levels (median increase was 0.35MPa). Extension decreased IDP remarkably at all levels of the Hyper- and Norm-L spines. It amplified IDP slightly at level L4-5, reduced it at level L2-4, and did not affect it at all at levels L-2 and L5-S1 for the Hypo-L spine.

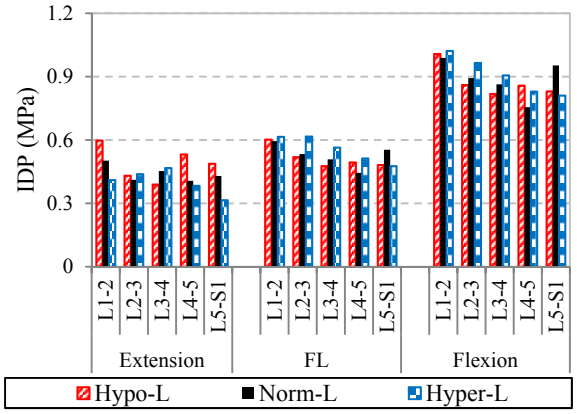


**Fig.5.5.** Comparison of IDP in the three spines.

For all spines, tensile strain in the annular fibers was higher in the flexion case (~3%) (Fig. 5.6b) compared to extension (~1.7%) (Fig. 5.6). In the flexion case, maximum magnitude was located in the posterolateral area of the inner lamellae and expanded toward the outer lamellae at all levels of the Hypo- and Norm-L spines but only at levels L1-5 of the Hyper-L spine (Fig. 5.6b). Maximum magnitudes (~3%) occurred at levels L1-2 and L1-4 of the Hypo- and Norm-L spines respectively, whereas, a small strain value was predicted in the annular fibers of the Hyper-L spine.

In the extension case, lamellae located in the anterior region of the annulus at all levels of the three spines experienced high tensile strain except at level L5-S1 of the Hyper-L one. Great strain magnitude was also predicted in the outer layers of the annular fibers at all levels of the three spines (Fig. 5.6a).

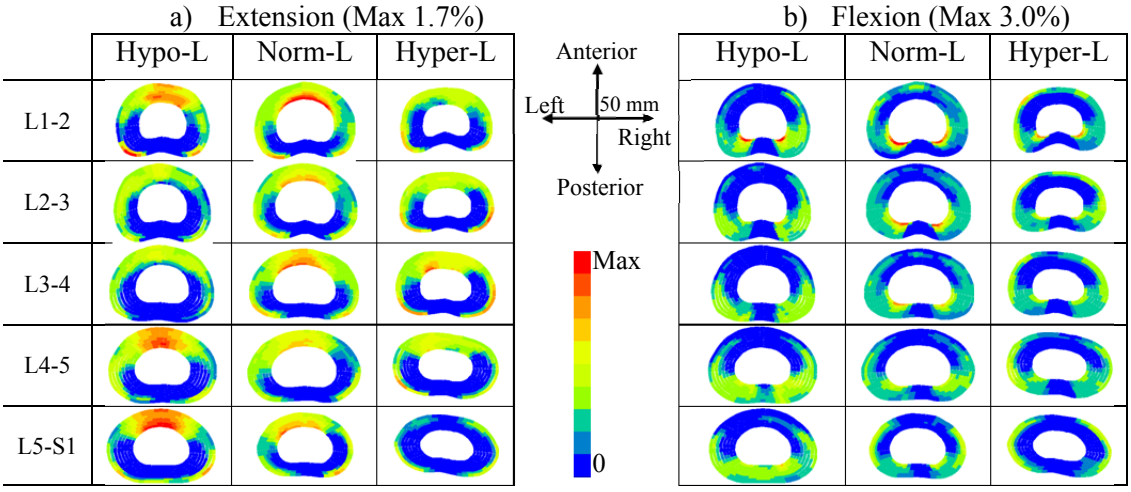


**Fig. 5.6.** Comparison of annular fibers strain in the three spines.

Adding flexion to the FL increased compression in the disc by ~52% at all levels of the three spines (Fig. 5.7). The Hyper-L spine experienced a slightly smaller increase compared to the other spines. Small (up to 65N) sagittal shear occurred at level L4-5 and no noticeable difference was found between the spines. Conversely, adding extension to the FL reduced compression in the discs particularly for the Norm- and Hyper-L (up to 36% at level L5-S1) spines. Compression also dropped by ~25% at levels L2-4 of the Hypo-L spine while it remained almost unchanged at levels L1-2 and L4-5 (Fig. 5.8). A high sagittal shear in the disc was produced at all levels of the Hypo-L spine (up to 135N at level L4-5) compared to the other spines. The Norm-L one also experienced high shear (up to 108N) at levels L4-S1 whereas the maximum value in the Hyper-L spine did not exceed 48N. Lateral shear was negligible in all discs of three spines in both, flexion and extension cases.

In the flexion case, sagittal moment was more significant in the Hyper-L spine at all levels (it reached up to 4Nm at level L1-2) compared to the other spines. The Norm-L spine experienced the lowest moment magnitude at almost all levels. The maximum value did not exceed 2.5Nm and 2.7Nm in the Hypo- and Norm-L spines, respectively. Almost no moment was produced at level L5-S1 of the Hyper- and Norm-L spines (Fig. 5.7).

In the extension case, discs of the Hyper-L spine experienced the lowest sagittal moment (less than 2.3Nm) while the largest magnitude (~3.6Nm) occurred at levels L4-S1 of the Hypo-L one (Fig. 5.8). All discs of the three spines resisted relatively small lateral bending moment and axial torque.

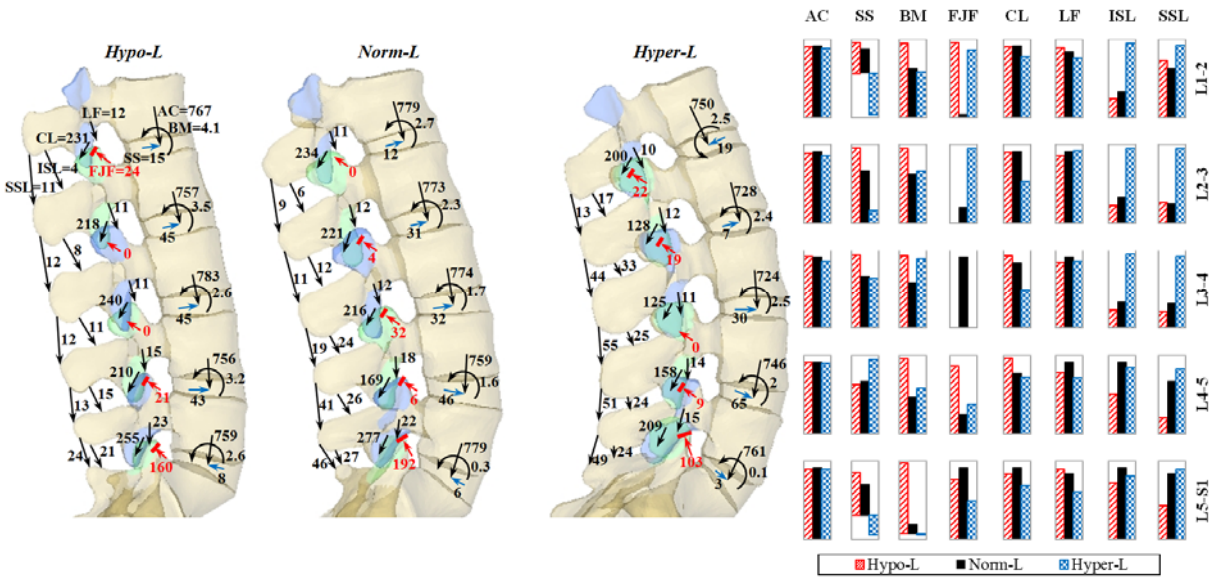


**Fig. 5.7.** Spinal force (N) and moment (Nm) in the three spines under flexion. The arrows and solid rectangles represent the actual direction and location of forces and contact respectively. The column charts indicate the discs force and moment as well as ligaments and contact forces of three spines normalized to one (Norm-L spine). AC, SS and BM are axial compression, sagittal shear and bending moment in the disc, respectively. Contribution of the ligaments PLL and ITL in load-sharing was very small.

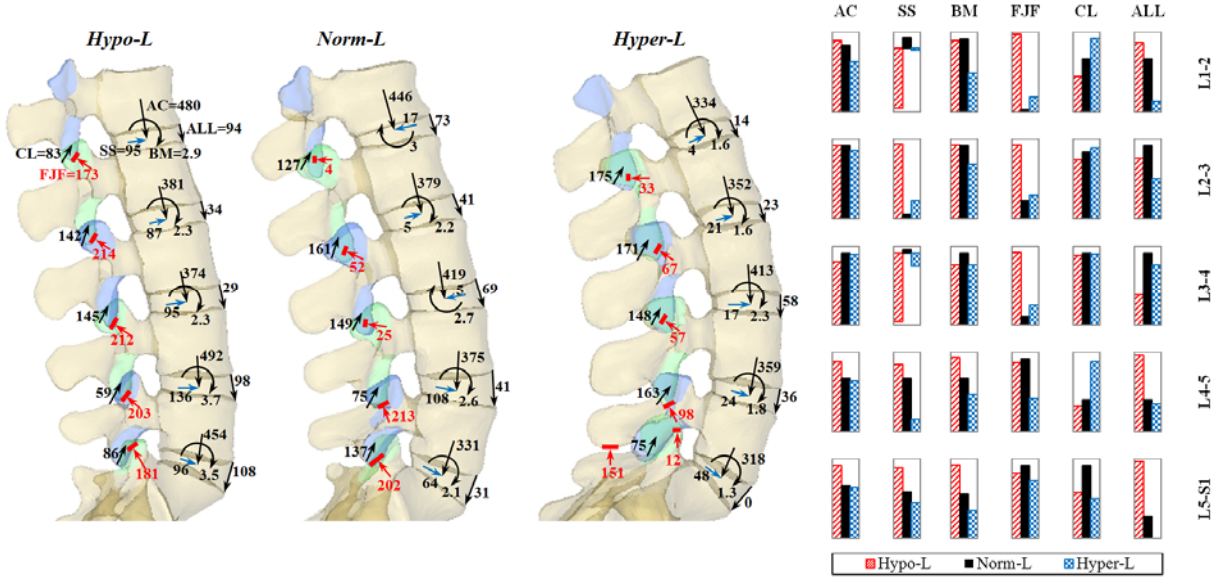


**Fig. 5.8.** Spinal force (N) and moment (Nm) in the three spines under extension. The arrows and solid rectangles represent the actual direction and location of forces and contact respectively. The column charts indicate the discs force and moment as well as ligaments and contact forces of three spines normalized to one (Norm-L spine). AC, SS and BM are axial compression, sagittal shear and bending moment in the disc, respectively.

Contribution of the discs (75%) and ligaments (25%) in resisting the total spinal force was almost similar at levels L1-5 of the three spines in case of flexion (Fig. 5.9a). The facet joints had no contribution at those levels but carried up to 12% of the spinal force at level L5-S1 which reduced the disc contribution. Contribution of the discs and ligaments in resisting spinal moment was reversed (Fig. 5.9b). The ligament resisted 73%, 88%, and 90% of the moment at level L5-S1 of the Hypo-, Norm-, and Hyper-L spines, respectively. Similar trend with lower percentage was found at all discs of the three spines. Resistance of the facet joints to spinal moment was negligible at all levels except L5-S1 of all spines.

A more noticeable variation in force- and moment-sharing was found when comparing the spines in the extension case (Fig. 5.9). Force-sharing was almost similar at all levels of the Hypo-L spine. The discs carried up to 58% of the spinal force while the remaining portion was carried almost equally by the ligaments and facet joints.

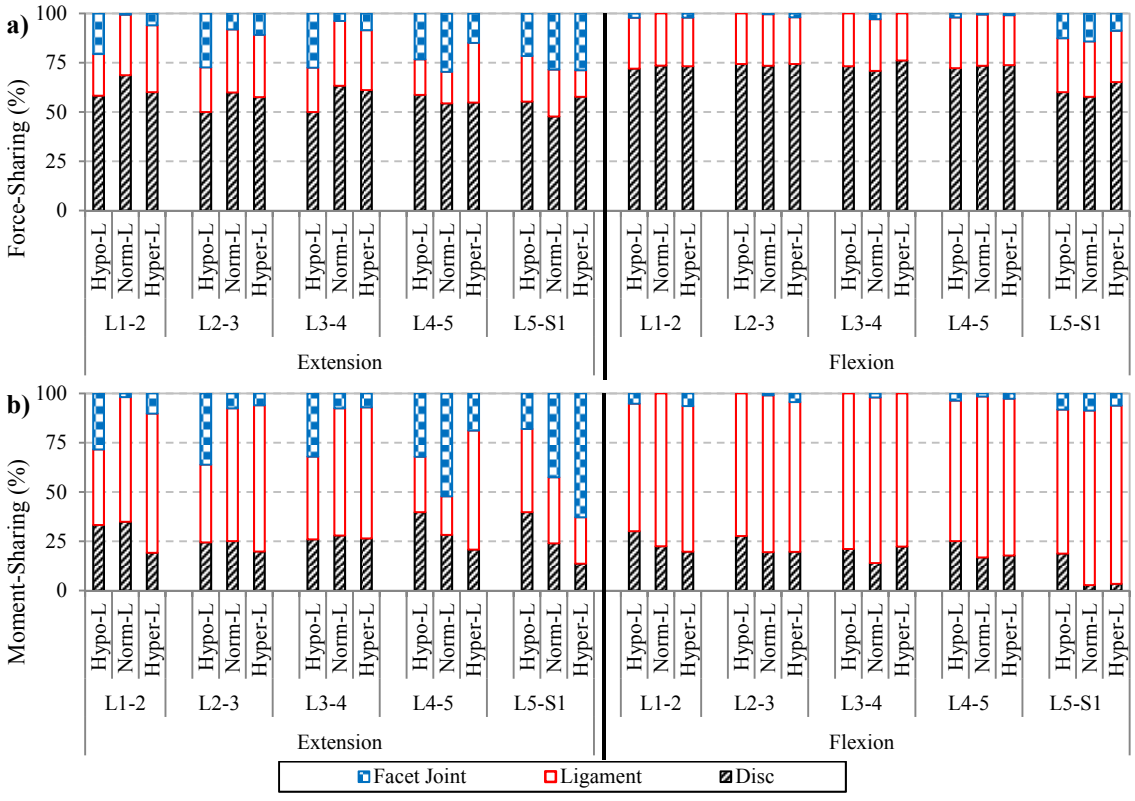


**Fig. 5.9.** Comparison of a) force-sharing and b) moment-sharing at different levels of the three spines.

Contribution of the disc in resisting spinal force was also remarkable and reached up to 68% compared to the discs and facet joints in the Norm- and Hyper-L spines. The remaining percentage was shared between the ligaments and facet joints with higher contribution of the facet joints at levels L4-S1.

Moment-sharing varied along the Norm- and Hyper-L spines while almost similar contribution was found in the discs, ligaments and facet joints of the Hypo-L spine. Ligaments resisted major portion of spinal moment at levels L1-4 while contribution of the facet joints was more important at lower levels particularly at level L5-S1 of the Hyper-L spine and levels L4-S1 of the Norm-L one.

### 5.4. Discussions

Prediction of a personalized spinal response to mechanical load is very challenging due to inter-individual variability of geometry, material properties, and loading conditions. It is almost impossible to develop a model that uses geometry and material properties of the same individual. Therefore, if studying the effects of only inter-individual geometry variation on spinal response is of interest for example, then it will be more feasible although not very realistic to use similar material properties and loading conditions. In the current study, we measured the sagittal alignment parameters LL, SS and PI from CT-scan data of 24 subjects lying in supine position with slight gravity effects which were ignorable (Meakin et al., 2013). There were association between these parameters where all of them were smaller for flat but larger for more curved spine as compared to the normal range (Vaz et al., 2002). Three spines with distinct sagittal alignment parameters were selected and modeled for load-sharing analyses. One with normal LL (Norm-L), one flat with smaller LL (Hypo-L), and one very curved with greater LL (Hyper-L). Realistic geometry with no simplification or modification was created for the three spines. Particular attention was paid to morphological details such as facet joints and endplates orientation, and distance between two adjacent spinous processes to detect any anomaly that might result from low or excessive LL (Aylott et al., 2012; Jentzsch et al., 2013). FL which minimizes intervertebral rotations and improves capacity of the ligamentous spine to resist compression (Fry et al., 2014; Kim et al., 2011, Renner et al., 2007; Shirazi-Adl, 2006) was used. Flexion and extension moments were added to the FL to simulate flexed and extended posture respectively.

Kinematics of the three spines was affected by the geometry variation. In case 1, the flexible behaviour of the Hyper-L spine might be due to the small area and height (thickness) as well as the high wedge angle of its discs compared to the other spines which affected the resistance of the annular fibers to bending. In the extension, the sharp wedge angle caused high element distortion under large extension which caused some numerical issues in Hyper-L spine. Geometry of the discs of the Hypo-L spine had reverse effects and produced smaller rotations. Overall, the geometry (size and shape) and orientation (horizontal vs. inclined) of the disc affected the spine kinematics in flexion and extension movement (Niemeyer et al., 2012; Meijer et al., 2011; Dupont et al., 2002; Natarajan and Andersson, 1999; Lu et al., 1996; Robin et al., 1994).

Geometry of the ligaments (i.e. location, orientation and length), discs (size and shape) and facet joints (location and orientation) was dissimilar in the three spines which affected their kinematics in flexed and extended posture. The greatest IVRs occurred at the caudal and proximal levels of the Hypo-L spine while the mid-levels of the Hyper-L spine experienced higher IVR which agrees with clinical findings (Keorochana et al., 2011). The stiffer behaviour of the Hyper-L spine and more flexible response of the Hypo-L spine to extension compared to the Norm-L one corroborate previous clinical findings (Keorochana et al., 2011). In the flexion, the behaviour was reversed and Hypo-L spine became the stiffest spine which can be related to the posterior ligament properties. The ligaments SSL, ISL, LF and ITL were longer in the Hypo-L spine compared to the Hyper- and Norm-L spines which affected the ligament resistance to flexion. Forces in the ligaments SSL and ISL were higher in the Hyper-L spine which reduced the total rotation found in case 1 by 80° whereas in the Hypo-L and Norm-L spines the total rotation decreased by 67° and 37° respectively. These two ligaments affected significantly the spine stiffness due to their large moment arms. The ligament CL, despite its shorter moment arm, also played a significant role in reducing the rotations due to its high stiffness and short length. Forces produced in this ligament were relatively high in all three spines. Interaction of these posterior ligaments was noticeable. Higher resistance of ligaments SSL and ISL to flexion was combined with lower contribution of ligament CL in the Hyper-L spine compared to the Norm-L spine while reversed trend was found in the Hypo-L spine.

In extended posture, the force in the facet joints was almost similar along the Hypo-L spine while high magnitudes were found in the caudal levels of the Norm- and Hyper-L spines which

may lead to facet joint arthritis and more sagittal orientation of the facet joint (Fig. 5.8,9) (Jentzsch et al., 2013). Due to their locations with respect to the disc, the forces in the ligaments ALL and CL counterbalanced those developed in the facet joints which reduced the disc compression. In the extension case, results demonstrated that IVRs increased in the Hypo-L spine and decreased in the Hyper-L one comparing to the Norm-L spine. Thus, the excessive lordosis in the Hyper-L spine stiffened response to extension compared to the Hypo-L spine which is confirmed by the moment-total rotation curves. Moreover, it is worth mentioning that the high LL in the Hyper-L spine reduced the gap between the spinous process of the vertebra L5 and the dorsal wall of the sacrum and limited rotation of L5 in extended posture. The inferior articular and spinous processes of the vertebra L5 touched the dorsal wall of the sacrum creating contact force (Fig. 5.8). This phenomenon is known as Basstrup or kissing spine syndrome (Filippiadis et al., 2015).

The FL concept did not demonstrate significant difference in response to compressive load between the spines as the FL followed the spine curvature. The discs of all spines experienced similar compressive but slightly different shear forces at all levels when subjected to flexion. Variation of shear was mainly due to the ligaments and facet joints forces components that aligned with shear direction. These components depended on the ligaments orientation and length which varied between the three spines as well as the contact location in the articular joints (Fig. 5.7,8).

Effects of the sagittal alignment parameters variation on the discs forces were more evident in extended posture. In particular, orientation of the contact forces in the facet joints of the Hypo-L spine produced higher sagittal shear compared to other spines (Fig. 5.8).

Noticeable difference in force- and moment-sharing was found between the three spines in the case of extension compared to flexion. Resistance of the facet joints to extension was similar along the Hypo-L spine while their force-sharing was more significant at the lower levels of the Norm- and Hyper-L spines particularly at level L4-5. This might be caused by the change in the facet joints orientation (more horizontal) with increased LL (Jentzsch et al., 2013).

The moment-sharing was almost similar at all levels of the Hypo-L spine while a more significant contribution of the facet joints was found at levels L4-S1 and level L5-S1 of the Norm- and Hyper-L spines respectively due the great moment arms of the contact forces measured from their lines of action to the discs centers. These moment arms were small in the

Hypo-L spine comparing to the other two. Variation of ligaments length and location with respect to discs centers in the three spines also affected the ligament load-sharing. For instance, the force in the ligament ALL was significantly higher in the Hypo-L spine compared to the others spines in case of extension while the CL experienced in general greater force in the Hyper-L spine under the same load.

In conclusion, this study demonstrated that internal forces produced by FL and flexion moment were mainly carried by the discs (~75%) and posterior ligaments (~25%) including the CL while contribution of ligaments was significantly greater (~70%) in resisting internal moments comparing to the discs (~20%). Role of the facet joints was negligible except at level L5-S1. This force-sharing was almost similar in all the three spines while the effects of inter-individual sagittal curvature variation were observed in the interaction between the posterior ligaments in particular CL, ISL and SSL.

In the case of FL combined with extension, results revealed that spinal load-sharing varies with the sagittal alignment parameters considered in this study. The discs, ligaments and facet joints shared spinal force with proportion of 50%, 25%, 25% respectively in the Hypo-L spine while facet joints contribution did not exceed 10% at levels L1-4 and reached up to 30% at levels L5-S1 in the Norm- and Hyper-L spines. The facet joint carried up to 63% of the internal moment in the Hyper-L spine.

Analyzing response of additional spines in each category under different loading conditions such as gravity load in future studies may reveal more significant effects of inter-individual curvature variations on the load-sharing.

**Conflict of interest statement**

The Authors have no conflict of interest to declare.

**Acknowledgements**

This study was supported by NSERC Discovery Grant, Canada.

**References**

Adams, M.A., Mannion, A.F., Dolan, P., 1999. Personal risk factors for first-time low back pain. Spine 24, 2497-2505.

Arjmand, N., Shirazi-Adl, A., 2005. Biomechanics of Changes in Lumbar Posture in Static Lifting. Spine 30, 2637-2648.

Aylott, C.E., Puna, R., Robertson, P.A., Walker, C., 2012. Spinous process morphology: The effect of ageing through adulthood on spinous process size and relationship to sagittal alignment. European Spine Journal: Official Publication of the European Spine Society, the European Spinal Deformity Society, and the European Section of the Cervical Spine Research Society 21, 1007-1012.

Barrey, C., Jund, J., Noseda, O., Roussouly, P., 2007. Sagittal balance of the pelvis-spine complex and lumbar degenerative diseases. A comparative study about 85 cases. European Spine Journal: Official Publication of the European Spine Society, the European Spinal Deformity Society, and the European Section of the Cervical Spine Research Society 16, 1459-1467.

Breau, C., Shirazi-Adl, A., de Guise, J., 1991. Reconstruction of a Human Ligamentous Lumbar Spine using CT Images--a Three-Dimensional Finite Element Mesh Generation. Annals of Biomedical Engineering 19, 291-302.

Bruno, A.G., Anderson, D.E., D'Agostino, J., Bouxsein, M.L., 2012. The Effect of Thoracic Kyphosis and Sagittal Plane Alignment on Vertebral Compressive Loading. Journal of Bone and Mineral Research 27, 2144-2151.

Chaleat-Valayer, E., Mac-Thiong, J.M., Paquet, J., Berthonnaud, E., Siani, F., Roussouly, P., 2011. Sagittal spino-pelvic alignment in chronic low back pain. European Spine Journal: Official Publication of the European Spine Society, the European Spinal Deformity Society, and the European Section of the Cervical Spine Research Society 20, 634-640.

Christie, H.J., Kumar, S., Warren, S.A., 1995. Postural aberrations in low back pain. Archives of Physical Medicine and Rehabilitation 76, 218-224.

De Smet, A.A., 1985. Radiographic Evaluation, Chapter 2. Radiology of Spinal Curvature, Edited by A. A. De Smet. St. Louis, CV Mosby Company, 23-58.

Deyo, R.A., Weinstein, J.N., 2001. Low back pain. The New England Journal of Medicine 344, 363-370.

Dupont, P., Lavaste, F., Skalli, W., 2002. The Role of Disc, Facets and Fibres in Degenerative Process: A Sensitivity Study. Studies in Health Technology and Informatics 88, 356-359.

El-Rich, M, Aubin C.E., Villemure, I, Labelle, H., 2006a. A biomechanical study of low-grade isthmic spondylolisthesis using a personalized finite element model. Journal of Biomechanics 39, S419.

El-Rich, M., Aubin, C.E., Villemure, I., Labelle, H. 2006b. A biomechanical study of L5-S1 low-grade isthmic spondylolisthesis using a personalized finite element model. Studies in Health Technology and Informatics 123, 431-434.

El-Rich, M., Arnoux, P., Wagnac, E., Brunet, C., Aubin, C.E., 2009. Finite Element Investigation of the Loading Rate Effect on the Spinal Load-Sharing Changes Under Impact Conditions. Journal of Biomechanics 42, 1252-1262.

Filippiadis, D.K., Mazioti, A., Argentos, S., Anselmetti, G., Papakonstantinou, O., Kelekis, N., Kelekis, A., 2015. Baastrup's disease (kissing spines syndrome): A pictorial review. Insights into Imaging 6, 123-128.

Fry, R.W., Alamin, T.F., Voronov, L.I., Fielding, L.C., Ghanayem, A.J., Parikh, A., Carandang, G., Mcintosh, B.W., Havey, R.M., Patwardhan, A.G., 2014. Compressive Preload Reduces Segmental Flexion Instability After Progressive Destabilization of the Lumbar Spine. Spine 39, E74-81.

Gautier, J., Morillon, P., Marcelli, C., 1999. Does spinal morphology influence the occurrence of low back pain? A retrospective clinical, anthropometric, and radiological study. Revue Du Rhumatisme (English Ed.) 66, 29-34.

Goto, K., Tajima, N., Chosa, E., Totoribe, K., Kubo, S., Kuroki, H., Arai, T., 2003. Effects of Lumbar Spinal Fusion on the Other Lumbar Intervertebral Levels (Three-Dimensional Finite Element Analysis). Journal of Orthopaedic Science : Official Journal of the Japanese Orthopaedic Association 8, 577-584.

Harrison, D.D., Cailliet, R., Janik, T.J., Troyanovich, S.J., Harrison, D.E., Holland, B., 1998. Elliptical modeling of the sagittal lumbar lordosis and segmental rotation angles as a method to discriminate between normal and low back pain subjects. Journal of Spinal Disorders 11, 430-439.

Jackson, R.P., McManus, A.C., 1994. Radiographic analysis of sagittal plane alignment and balance in standing volunteers and patients with low back pain matched for age, sex, and size. A prospective controlled clinical study. Spine 19, 1611-1618.

Jentzsch, T., Geiger, J., Bouaicha, S., Slankamenac, K., Nguyen-Kim, T.D., Werner, C.M., 2013. Increased Pelvic Incidence may Lead to Arthritis and Sagittal Orientation of the Facet Joints at the Lower Lumbar Spine. BMC Medical Imaging 13, 34-2342-13-34.

Keller, T.S., Colloca, C.J., Harrison, D.E., Harrison, D.D., Janik, T.J., 2005. Influence of Spine Morphology on Intervertebral Disc Loads and Stresses in Asymptomatic Adults: Implications for the Ideal Spine. The Spine Journal 5, 297-309.

Keorochana, G., Taghavi, C.E., Lee, K.B., Yoo, J.H., Liao, J.C., Fei, Z., Wang, J.C., 2011. Effect of sagittal alignment on kinematic changes and degree of disc degeneration in the lumbar spine: An analysis using positional MRI. Spine 36, 893-898.

Kim, K., Kim, Y.H., Lee, S., 2011. Investigation of Optimal Follower Load Path Generated by Trunk Muscle Coordination. Journal of Biomechanics 44, 1614-1617.

Korovessis, P., Stamatakis, M., Baikousis, A., 1999. Segmental roentgenographic analysis of vertebral inclination on sagittal plane in asymptomatic versus chronic low back pain patients. Journal of Spinal Disorders 12, 131-137.

Lu, Y.M., Hutton, W.C., Gharpuray, V.M., 1996. Can Variations in Intervertebral Disc Height Affect the Mechanical Function of the Disc? Spine 21, 2208-16.

Meakin, J.R., Fulford, J., Seymour, R., Welsman, J.R., Knapp, K.M., 2013. The relationship between sagittal curvature and extensor muscle volume in the lumbar spine. Journal of Anatomy 222, 608-614.

Meijer, G.J., Homminga, J., Veldhuizen, A.G., Verkerke, G.j., 2011. Influence of Interpersonal Geometrical Variation on Spinal Motion Segment Stiffness: Implications for Patient-Specific Modeling. Spine 36, E929-935.

Naserkhaki, S., El-Rich, M., 2015. Sensitivity of Lumbar Spine Response to Follower Load and Flexion Moment: Finite Element Study. Journal of Biomechanical Engineering, submitted.

Naserkhaki, S., Jaremko, J.L., Adeeb, S., El-Rich, M., 2015. On the Load-Sharing Along the Ligamentous Lumbosacral Spine: Finite Element Modeling and Static Equilibrium Approach. Journal of Biomechanics, DOI: http://dx.doi.org/10.1016/j.jbiomech.2015.09.050.

Naserkhaki, S., Jaremko, J.L., Kawchuk, G., Adeeb, S., El-Rich, M., 2014. Investigation of lumbosacral spine anatomical variation effect on load-partitioning under follower load

using geometrically personalized finite element model. ASME International Mechanical Engineering Congress and Exposition, Proceedings (IMECE), Anonymous 3, DOI: 10.1115/IMECE201440231.

Natarajan, R.N., Andersson, G.B., 1999. The Influence of Lumbar Disc Height and Cross-Sectional Area on the Mechanical Response of the Disc to Physiologic Loading. Spine 24, 1873-1881.

Niemeyer, F., Wilke, H.J., Schmidt, H., 2012. Geometry Strongly Influences the Response of Numerical Models of the Lumbar Spine--a Probabilistic Finite Element Analysis. Journal of Biomechanics 45, 1414-1423.

Noailly, J., Wilke, H., Planell, J.A., Lacroix, D., 2007. How does the Geometry Affect the Internal Biomechanics of a Lumbar Spine Bi-Segment Finite Element Model? Consequences on the Validation Process. Journal of Biomechanics 40, 2414-2425.

Panjabi, M.M., 2003. Clinical spinal instability and low back pain. Journal of Electromyography and Kinesiology 13, 371-379.

Park, W.M., Kim, K., Kim, Y.H., 2013. Effects of Degenerated Intervertebral Discs on Intersegmental Rotations, Intradiscal Pressures, and Facet Joint Forces of the Whole Lumbar Spine. Computers in Biology and Medicine 43, 1234-1240.

Pope, M.H., Novotny, J.E., 1993. Spinal biomechanics. Journal of Biomechanical Engineering 115, 569-574.

Propst-Proctor, S.L., Bleck, E.E., 1983. Radiographic determination of lordosis and kyphosis in normal and scoliotic children. Journal of Pediatric Orthopedics 3, 344-346.

Putzer, M., Ehrlich, I., Rasmussen, J., Gebbeken, N., Dendorfer, S., 2015. Sensitivity of lumbar spine loading to anatomical parameters. Journal of Biomechanics http://dx.doi.org/10.1016/j.jbiomech.2015.11.003.

Rajnics, P., Templier, A., Skalli, W., Lavaste, F., Illes, T., 2002. The importance of spinopelvic parameters in patients with lumbar disc lesions. International Orthopaedics 26, 104-108.

Renner, S.M., Natarajan, R.N., Patwardhan, A.G., Havey, R.M., Voronov, L.I., Guo, B.Y., Andersson, G.B., An, H.S., 2007. Novel Model to Analyze the Effect of a Large Compressive Follower Pre-Load on Range of Motions in a Lumbar Spine. Journal of Biomechanics 40, 1326-1332.

Robin, S., Skalli, W., Lavaste, F., 1994. Influence of Geometrical Factors on the Behavior of Lumbar Spine Segments: A Finite Element Analysis. European Spine Journal: Official Publication of the European Spine Society, the European Spinal Deformity Society, and the European Section of the Cervical Spine Research Society 3, 84-90.

Rohlmann, A., Bauer, L., Zander, T., Bergmann, G., Wilke, H.J., 2006. Determination of Trunk Muscle Forces for Flexion and Extension by using a Validated Finite Element Model of the Lumbar Spine and Measured in Vivo Data. Journal of Biomechanics 39, 981-989.

Roussouly, P., Pinheiro-Franco, J.L., 2011. Biobmechanical Analysis of the Spino-Pelvic Organization and Adaptation in Pathology. European Spine Journal: Official Publication of the European Spine Society, the European Spinal Deformity Society, and the European Section of the Cervical Spine Research Society 20, S609-618.

Roussouly, P., Berthonnaud, E., Dimnet, J., 2003. Geometrical and Mechanical Analysis of Lumbar Lordosis in an Asymptomatic Population: Proposed Classification. Revue Du Chirurgie Orthopedique Et Traumatologique 89, 632-639.

Roussouly, P., Gollogly, S., Berthonnaud, E., Dimnet, J., 2005. Classification of the Normal Variation in the Sagittal Alignment of the Human Lumbar Spine and Pelvis in the Standing Position. Spine 30, 346-353.

Schmidt, H., Heuer, F., Simon, U., Kettler, A., Rohlmann, A., Claes, L., Wilke, H.J., 2006. Application of a New Calibration Method for a Three-Dimensional Finite Element Model of a Human Lumbar Annulus Fibrosus. Clinical Biomechanics 21, 337-344.

Schmidt, H., Kettler, A., Heuer, F., Simon, U., Claes, L., Wilke, H.J., 2007. Intradiscal Pressure, Shear Strain, and Fiber Strain in the Intervertebral Disc under Combined Loading. Spine 32, 748-755.

Shih, S.L., Liu, C.L., Huang, L.Y., Huang, C.H., Chen, C.S., 2013. Effects of Cord Pretension and Stiffness of the Dynesys System Spacer on the Biomechanics of Spinal Decompression- a Finite Element Study. BMC Musculoskeletal Disorders, 14, 191-2474-14-191.

Shirazi-Adl, A., Parnianpour, M., 1996. Role of posture in mechanics of the lumbar spine in compression. Journal of Spine Disorders 9, 277-286.

Shirazi-Adl, A., 2006. Analysis of Large Compression Loads on Lumbar Spine in Flexion and in Torsion using a Novel Wrapping Element. Journal of Biomechanics 39, 267-275.

Shirazi-Adl, A., Ahmed, A.M., Shrivastava, S.C., 1986. Mechanical Response of a Lumbar Motion Segment in Axial Torque Alone and Combined with Compression. Spine 11, 914-927.

Stagnara, P., De Mauroy, J. C., Dran, G., Gonon, G. P., Costanzo, G., Dimnet, J., Pasquet, A. 1982. Reciprocal angulation of vertebral bodies in a sagittal plane: Approach to references for the evaluation of kyphosis and lordosis. Spine 7, 335-342.

Trainor, T. J., Wiesel, S.W., 2002. Epidemiology of back pain in the athlete. Clinics in Sports Medicine 21, 93-103.

Tsuji, T., Matsuyama, Y., Sato, K., Hasegawa, Y., Yimin, Y., Iwata, H., 2001. Epidemiology of low back pain in the elderly: Correlation with lumbar lordosis. Journal of Orthopaedic Science 6, 307-311.

Tüzün, Ç., Yorulmaz, İ., Cindaş, A., Vatan, S., 1999. Low back pain and posture. Clinical Rheumatology 18, 308-312.

Vaz, G., Roussouly, P., Berthonnaud, E., Dimnet, J., 2002. Sagittal morphology and equilibrium of pelvis and spine. European Spine Journal: Official Publication of the European Spine Society, the European Spinal Deformity Society, and the European Section of the Cervical Spine Research Society 11, 80-87.

Vrtovec, T., Janssen, M.M.A., Likar, B., Castelein, R.M., Viergever, M.A., Pernuš, F., 2012. A review of methods for evaluating the quantitative parameters of sagittal pelvic alignment. The Spine Journal 12, 433-446.

# Chapter 6
# Summary and Conclusions

## 6.1. Summary

This research aimed at understanding: 1. How spinal load-sharing varies along the lumbosacral spine and 2. How inter-individual sagittal curvature variation affects spinal load-sharing in flexed and extended postures.

Three lumbosacral spines with different curvatures were created: one hypo-lordotic (Hypo-L), one normal-lordotic (Norm-L) and one hyper-lordotic (Hyper-L) spines with low, normal and high lumbar lordosis (LL), respectively.

A 3D nonlinear FE model of the Norm-L spine was created and validated against experimental studies. The model predictions in various loading scenarios were compared with *in-vivo*, *in-vitro* and other numerical data. The spine kinematics was in a satisfactory agreement with reported data. The overall rotation (L1-S1) and IVRs both fell inside the *in-vitro* and numerical ranges. Nonetheless, like the majority of previous FE models, the current model demonstrated relatively stiffer response to flexion with smaller rotations compared to *in-vivo* data which might be due to the applied load. The IDP and FJF were in a very good agreement with published values.

The model was subjected to FL combined with moment to investigate load-sharing along the spine in flexed and extended posture. Spinal load-sharing was defined as the percentage of total internal force/moment that each spinal component carried at each level.

FE models were developed for the Hypo-L and Hyper-L spines to investigate effects of inter-individual sagittal curvature variation on load-sharing. Their responses in flexed and extended postures were compared.

## 6.2. Conclusions

### 6.2.1. Load-sharing along the spine in flexed and extended posture (Objective1, Chapter 3)

The contribution of the facet joints and ligaments in resisting bending moment produced additional forces and moments in the discs. The discs carried up to 81% and 68% of the total internal force in flexed and extended postures, respectively. The ligaments withstood up to 67% and 81% of the total internal moment in extended and flexed postures, respectively. Contribution of the facet joints in resisting internal force and moment was noticeable at levels L4-S1 only particularly in case of extension and reached up 29% and 52% of the internal moment and force, respectively. Results demonstrated that spinal load-sharing depend on the applied load and varied along the spine.

### 6.2.2. Sensitivity of spinal response to FL and moment magnitudes (Objective 1, Chapter 4)

The optimal magnitudes of FL and moment were defined as the magnitudes for which deviation of the model predictions from *in-vivo* data was minimized.

The IVRs, disc moment, and the increase in disc force and moment from neutral to flexed posture were more sensitive to the moment magnitude than FL magnitude in case of flexion. The disc force and IDP were more sensitive to the FL magnitude than moment magnitude. The FL magnitude had reverse effect on the IDP and disc force. To obtain reasonable compromise between the IDP and disc force, our findings recommend that FL of low magnitude must be combined with flexion moment of high intensity and vice versa.

### 6.2.3. Effects of inter-individual sagittal curvature variation on spinal load-sharing (Objective 2, Chapter 5)

Kinematics of the three spines was affected by the curvature variation. In the flexion case, the Hypo-L spine demonstrated stiffer behavior whereas no significant difference was found between the Norm-L and Hyper-L spines. In the extension case, the excessive lordosis stiffened the spine against extension while the Hypo-L produced reverse effect comparing to Norm-L spine.

The three spines studied demonstrated that inter-individual curvature variation affects spinal load-sharing only in extended posture while no noticeable difference between the spines was found in flexed posture. Analyzing response of additional spines in each category under different loading conditions such as gravity load in future studies may reveal more significant effects of inter-individual curvature variations.

## 6.3. Recommendations for the future research

- The current FE model as well as other models of the ligamentous spine showed stiffer response to flexion compared to *in-vivo* data which might due to the loading condition and/or material properties, in particular ligament properties. Sensitivity of the predictions to properties of the ligaments should be investigated.
- The simplified loading mode which consists of FL combined with moment needs to be improved to mimic better the physiological conditions. For instance, increasing magnitude of

the FL from the cranial to caudal levels instead of using constant magnitude to simulate flexed posture will yield more realistic results.

- Considering muscle forces can be a great improvement to the model especially if the muscle forces are personalized. It is expected that effects of lumbar curvature variation on load-sharing become more significant if personalized muscle forces are considered.
- Comparison of additional spines responses to more realistic loading mode such as gravity load may reveal more significant difference which will help find correlation between spinal curvature and mechanical response. Furthermore, personalized spinal stress profile can be correlated with the individual clinical history (for example effect of disc degeneration can be considered).

**Bibliography**

Abouhossein, A., Weisse, B., Ferguson, S.J., 2011. A Multibody Modelling Approach to Determine Load Sharing between Passive Elements of the Lumbar Spine. Computer Methods in Biomechanics and Biomedical Engineering 14, 527-537.

Adams, M.A., 2004. Biomechanics of Back Pain. Acupuncture in Medicine 22, 178-188.

Adams, M.A., Dolan, P., Hutton, W.C., 1988. The Lumbar Spine in Backward Bending. Spine 13, 1019-1026.

Adams, M.A., Hutton, W.C., Stott, J.R., 1980. The Resistance to Flexion of the Lumbar Intervertebral Joint. Spine 5, 245-253.

Adams, M.A., Mannion, A.F., Dolan, P., 1999. Personal risk factors for first-time low back pain. Spine 24, 2497-2505.

Alapan, Y., Sezer, S., Demir, C., Kaner,T., Inceoglu, S., 2014. Load Sharing in Lumbar Spinal Segment as a Function of Location of Center of Rotation. Journal of Neurosurgery Spine 20, 542-549.

Arjmand N., Shirazi-Adl, A., 2005. Biomechanics of changes in lumbar posture in static lifting. Spine 30, 2637-48.

Arjmand, N., Shirazi-Adl, A., 2006. Model and in Vivo Studies on Human Trunk Load Partitioning and Stability in Isometric Forward Flexions. Journal of Biomechanics 39, 510-521.

Aylott, C.E., Puna, R., Robertson, P.A., Walker, C., 2012. Spinous process morphology: The effect of ageing through adulthood on spinous process size and relationship to sagittal alignment. European Spine Journal: Official Publication of the European Spine Society, the European Spinal Deformity Society, and the European Section of the Cervical Spine Research Society 21, 1007-1012.

Ayturk, U.M., Puttlitz, C.M., 2011. Parametric Convergence Sensitivity and Validation of a Finite Element Model of the Human Lumbar Spine. Computer Methods in Biomechanics and Biomedical Engineering 14, 695-705.

Barrey, C., Jund, J., Noseda, O., Roussouly, P., 2007. Sagittal balance of the pelvis-spine complex and lumbar degenerative diseases. A comparative study about 85 cases. European Spine Journal: Official Publication of the European Spine Society, the European Spinal

Deformity Society, and the European Section of the Cervical Spine Research Society 16, 1459-1467.

Bazrgari, B., Shirazi-Adl, A., 2007. Spinal stability and role of passive stiffness in dynamic squat and stoop lifts. Computer Methods in Biomechanics and Biomedical Engineering 10, 351-360.

Breau, C., Shirazi-Adl, A., de Guise, J., 1991. Reconstruction of a Human Ligamentous Lumbar Spine using CT Images--a Three-Dimensional Finite Element Mesh Generation. Annals of Biomedical Engineering 19, 291-302.

Brinckmann, P., Grootenboer, H., 1991. Change of disc height, radial disc bulge, and intradiscal pressure from discectomy. An *in vitro* investigation on human lumbar discs. Spine 16, 641-646.

Bruno, A.G., Anderson, D.E., D'Agostino, J., Bouxsein, M.L., 2012. The Effect of Thoracic Kyphosis and Sagittal Plane Alignment on Vertebral Compressive Loading. Journal of Bone and Mineral Research 27, 2144-2151.

Chaleat-Valayer, E., Mac-Thiong, J.M., Paquet, J., Berthonnaud, E., Siani, F., Roussouly, P., 2011. Sagittal spino-pelvic alignment in chronic low back pain. European Spine Journal : Official Publication of the European Spine Society, the European Spinal Deformity Society, and the European Section of the Cervical Spine Research Society 20, 634-640.

Chen, C.S., Cheng, C.K., Liu, C.L., Lo, W.H., 2001. Stress Analysis of the Disc Adjacent to Interbody Fusion in Lumbar Spine. Medical Engineering & Physics 23, 483-491.

Chen, S.H., Chiang, M.C., Lin, J.F., Lin, S.C., Hung, C.H., 2013. Biomechanical Comparison of Three Stand-Alone Lumbar Cages - a Three-Dimensional Finite Element Analysis. BMC Musculoskeletal Disorders 14, 281.

Christie, H.J., Kumar, S., Warren, S.A., 1995. Postural aberrations in low back pain. Archives of Physical Medicine and Rehabilitation 76, 218-224.

De Smet, A.A., 1985. Radiographic Evaluation, Chapter 2. Radiology of Spinal Curvature, Edited by A. A. De Smet. St. Louis, CV Mosby Company, 23-58.

Deyo, R.A., Weinstein, J.N., 2001. Low back pain. The New England Journal of Medicine 344, 363-370.

Dolan, P., Adams, M.A., 2001. Recent Advances in Lumbar Spinal Mechanics and their Significance for Modelling. Clinical Biomechanics (Bristol, Avon) 16, S8-S16.

Dreischarf, M., Albiol, L., Zander, T., Arshad, R., Graichen, F., Bergmann, G., Schmidt, H., Rohlmann, A., 2015. In Vivo Implant Forces Acting on a Vertebral Body Replacement during Upper Body Flexion. Journal of Biomechanics 48, 560-565.

Dreischarf, M., Rohlmann, A., Bergmann, G., Zander, T., 2011. Optimised Loads for the Simulation of Axial Rotation in the Lumbar Spine. Journal of Biomechanics 44, 2323-2327.

Dreischarf, M., Rohlmann, A., Bergmann, G., Zander, T., 2012. Optimised in Vitro Applicable Loads for the Simulation of Lateral Bending in the Lumbar Spine. Medical Engineering & Physics 34, 777-780.

Dreischarf, M., Rohlmann, A., Zhu, R., Schmidt, H., Zander,T., 2013. Is it Possible to Estimate the Compressive Force in the Lumbar Spine from Intradiscal Pressure Measurements? A Finite Element Evaluation. Medical Engineering & Physics, 35, 1385-1390.

Dreischarf, M., Zander, T., Shirazi-Adl, A., Puttlitz, C.M., Adam, C.J., Chen, C.S., Goel, V.K., Kiapour, A., Kim, Y.H., Labus, K.M., Little, J.P., Park, W.M., Wang, Y.H., Wilke, H.J., Rohlmann, A., Schmidt, H., 2014. Comparison of Eight Published Static Finite Element Models of the Intact Lumbar Spine: Predictive Power of Models Improves when Combined Together. Journal of Biomechanics 47, 1757-1766.

Dupont, P., Lavaste, F., Skalli, W., 2002. The Role of Disc, Facets and Fibres in Degenerative Process: A Sensitivity Study. Studies in Health Technology and Informatics 88, 356-359.

El-Rich, M, Aubin C.E., Villemure, I, Labelle, H., 2006. A biomechanical study of low-grade isthmic spondylolisthesis using a personalized finite element model. Journal of Biomechanics 39, S419.

El-Rich, M., Arnoux, P., Wagnac, E., Brunet, C., Aubin, C.E., 2009. Finite Element Investigation of the Loading Rate Effect on the Spinal Load-Sharing Changes Under Impact Conditions. Journal of Biomechanics 42, 1252-1262.

El-Rich, M., Aubin, C.E., Villemure, I., Labelle, H., 2006. A Biomechanical Study of L5-S1 Low-Grade Isthmic Spondylolisthesis using a Personalized Finite Element Model. Studies in Health Technology and Informatics 123, 431-434.

El-Rich, M., Shirazi-Adl, A., Arjmand, N., 2004. Muscle Activity, Internal Loads, and Stability of the Human Spine in Standing Postures: Combined Model and in Vivo Studies. Spine 29, 2633-2642.

Filippiadis, D.K., Mazioti, A., Argentos, S., Anselmetti, G., Papakonstantinou, O., Kelekis, N., Kelekis, A., 2015. Baastrup's disease (kissing spines syndrome): A pictorial review. Insights into Imaging 6, 123-128.

Fry, R.W., Alamin, T.F., Voronov, L.I., Fielding, L.C., Ghanayem, A.J., Parikh, A., Carandang, G., Mcintosh, B.W., Havey, R.M., Patwardhan, A.G., 2014. Compressive Preload Reduces Segmental Flexion Instability After Progressive Destabilization of the Lumbar Spine. Spine 39, E74-E81.

Gautier, J., Morillon, P., Marcelli, C., 1999. Does spinal morphology influence the occurrence of low back pain? A retrospective clinical, anthropometric, and radiological study. Revue Du Rhumatisme (English Ed.) 66, 29-34.

Goel, V.K., Clausen, J.D., 1998. Prediction of Load Sharing among Spinal Components of a C5-C6 Motion Segment using the Finite Element Approach. Spine 23, 684-691.

Goel, V.K., Kong, W., Han, J.S., Weinstein, J.N., Gilbertson, L.G., 1993. A Combined Finite Element and Optimization Investigation of Lumbar Spine Mechanics with and without Muscles. Spine 18, 1531-1541.

Goel, V.K., Winterbottom, J.M., Weinstein, J.N., Kim, Y.E., 1987. Load Sharing among Spinal Elements of a Motion Segment in Extension and Lateral Bending. Journal of Biomechanical Engineering 109, 291-297.

Goto, K., Tajima, N., Chosa, E., Totoribe, K., Kubo, S., Kuroki, H., Arai, T., 2003. Effects of Lumbar Spinal Fusion on the Other Lumbar Intervertebral Levels (Three-Dimensional Finite Element Analysis). Journal of Orthopaedic Science : Official Journal of the Japanese Orthopaedic Association 8, 577-584.

Guan, Y., Yoganandan, N., Moore, J., Pintar, F.A., Zhang, J., Maiman, D.J., Laud, P., 2007. Moment-Rotation Responses of the Human Lumbosacral Spinal Column. Journal of Biomechanics 40, 1975-1980.

Harrison, D.D., Cailliet, R., Janik, T.J., Troyanovich, S.J., Harrison, D.E., Holland, B., 1998. Elliptical modeling of the sagittal lumbar lordosis and segmental rotation angles as a method to discriminate between normal and low back pain subjects. Journal of Spinal Disorders 11, 430-439.

Harrison, D.E., Harrison, D.D., Troyanovich, S.J., Harmon, S., 2000. A normal spinal position: It's time to accept the evidence. Journal of Manipulative and Physiological Therapeutics 23, 623-644.

Heuer, F., Schmidt, H., Klezl, Z., Claes, L., Wilke, H.J., 2007. Stepwise Reduction of Functional Spinal Structures Increase Range of Motion and Change Lordosis Angle. Journal of Biomechanics 40, 271-280.

Ibarz, E., Herrera, A., Mas, Y., Rodriguez-Vela, J., Cegonino, J., Puertolas, S., Gracia, L., 2013. Development and Kinematic Verification of a Finite Element Model for the Lumbar Spine: Application to Disc Degeneration. BioMed Research International 2013, 705185.

Ivicsics, M.F., Bishop, N.E., Püschel, K., Morlock, M.M., Huber, G., 2014. Increase in Facet Joint Loading after Nucleotomy in the Human Lumbar Spine. Journal of Biomechanics 47, 1712-1717.

Jackson, R.P., McManus, A.C., 1994. Radiographic analysis of sagittal plane alignment and balance in standing volunteers and patients with low back pain matched for age, sex, and size. A prospective controlled clinical study. Spine 19, 1611-1618.

Jentzsch, T., Geiger, J., Bouaicha, S., Slankamenac, K., Nguyen-Kim, T.D., Werner, C.M., 2013. Increased Pelvic Incidence may Lead to Arthritis and Sagittal Orientation of the Facet Joints at the Lower Lumbar Spine. BMC Medical Imaging 13, 34-2342-13-34.

Keller, T.S., Colloca, C.J., Harrison, D.E., Harrison, D.D., Janik, T.J., 2005. Influence of Spine Morphology on Intervertebral Disc Loads and Stresses in Asymptomatic Adults: Implications for the Ideal Spine. The Spine Journal 5, 297-309.

Keorochana, G., Taghavi, C.E., Lee, K.B., Yoo, J.H., Liao, J.C., Fei, Z., Wang, J.C., 2011. Effect of sagittal alignment on kinematic changes and degree of disc degeneration in the lumbar spine: An analysis using positional MRI. Spine 36, 893-898.

Kiapour, A., Anderson, D.G., Spenciner, D.B., Ferrara, L., Goel, V.K., 2012. Kinematic Effects of a Pedicle-Lengthening Osteotomy for the Treatment of Lumbar Spinal Stenosis. Journal of Neurosurgery Spine 17, 314-320.

Kiefer, A., Shirazi-Adl, A., Parnianpour, M., 1997. Stability of the Human Spine in Neutral Postures. European Spine Journal : Official Publication of the European Spine Society, the European Spinal Deformity Society, and the European Section of the Cervical Spine Research Society 6, 45-53.

Kim, K., Kim, Y.H., 2008. Role of Trunk Muscles in Generating Follower Load in the Lumbar Spine of Neutral Standing Posture. Journal of Biomechanical Engineering 130, 041005.

Kim, K., Kim, Y.H., Lee, S., 2011. Investigation of Optimal Follower Load Path Generated by Trunk Muscle Coordination. Journal of Biomechanics 44, 1614-1617.

Korovessis, P., Stamatakis, M., Baikousis, A., 1999. Segmental roentgenographic analysis of vertebral inclination on sagittal plane in asymptomatic versus chronic low back pain patients. Journal of Spinal Disorders 12, 131-137.

Lin, R.M., Yu, C.Y., Chang, Z.J., Lee, C.C., Su, F.C., 1994. Flexion-Extension Rhythm in the Lumbosacral Spine. Spine 19, 2204-2209.

Little, J.P., de Visser, H., Pearcy, M.J., Adam, C.J., 2008. Are Coupled Rotations in the Lumbar Spine Largely due to the Osseo-Ligamentous Anatomy?-a Modeling Study. Computer Methods in Biomechanics and Biomedical Engineering 11, 95-103.

Manchikanti, L., Singh, V., Datta, S., Cohen, S.P., Hirsch, J.A., 2009. Comprehensive Review of Epidemiology, Scope, and Impact of Spinal Pain. Pain Physician, 12, E35-70.

Meakin, J.R., Fulford, J., Seymour, R., Welsman, J.R., Knapp, K.M., 2013. The relationship between sagittal curvature and extensor muscle volume in the lumbar spine. Journal of Anatomy 222, 608-614.

Meijer, G. J., Homminga, J., Veldhuizen, A.G., Verkerke, G.J., 2011. Influence of Interpersonal Geometrical Variation on Spinal Motion Segment Stiffness: Implications for Patient-Specific Modeling. Spine 36, E929-E935.

Mustafy, T., El-Rich, M., Mesfar, W., Moglo, K., 2014. Investigation of Impact Loading Rate Effects on the Ligamentous Cervical Spinal Load-Partitioning using Finite Element Model of Functional Spinal Unit C2-C3. Journal of Biomechanics 47, 2891-2903.

Najarian, S., Dargahi, J., Heidari, B., 2005. Biomechanical Effect of Posterior Elements and Ligamentous Tissues of Lumbar Spine on Load Sharing. Bio-Medical Materials and Engineering 15, 145-158.

Naserkhaki, S., El-Rich, M., 2015. Sensitivity of Lumbar Spine Response to Follower Load and Flexion Moment: Finite Element Study. Journal of Biomechanical Engineering, submitted.

Naserkhaki, S., Jaremko, J.L., Adeeb, S., El-Rich, M., 2015. On the Load-Sharing Along the Ligamentous Lumbosacral Spine: Finite Element Modeling and Static Equilibrium

Approach. Journal of Biomechanics, DOI: http://dx.doi.org/10.1016/j.jbiomech.2015.09.050.

Naserkhaki, S., Jaremko, J.L., Kawchuk, G., Adeeb, S., El-Rich, M., 2014. Investigation of Lumbosacral Spine Anatomical Variation Effect on Load-Partitioning Under Follower Load Using Geometrically Personalized Finite Element Model. ASME International Mechanical Engineering Congress and Exposition, Proceedings (IMECE), IMECE2014-40231, 3-V003T03A050.

Niosi, C.A., Wilson, D.C., Zhu, Q., Keynan, O., Wilson, D.R., Oxland, T.R., 2008. The Effect of Dynamic Posterior Stabilization on Facet Joint Contact Forces: An in Vitro Investigation. Spine 33, 19-26.

Noailly, J., Wilke, H., Planell, J.A., Lacroix, D., 2007. How does the Geometry Affect the Internal Biomechanics of a Lumbar Spine Bi-Segment Finite Element Model? Consequences on the Validation Process. Journal of Biomechanics 40, 2414-2425.

Oxland, T.R., Lin, R.M., Panjabi, M.M., 1992. Three-Dimensional Mechanical Properties of the Thoracolumbar Junction. Journal of Orthopaedic Research: Official Publication of the Orthopaedic Research Society 10, 573-580.

Panjabi, M.M., 1992. The Stabilizing System of the Spine. Part I. Function, Dysfunction, Adaptation, and Enhancement. Journal of Spinal Disorders 5, 383-389, discussion 397.

Panjabi, M.M., 2003. Clinical spinal instability and low back pain. Journal of Electromyography and Kinesiology 13, 371-379.

Panjabi, M.M., 2007. Hybrid Multidirectional Test Method to Evaluate Spinal Adjacent-Level Effects. Clinical Biomechanics (Bristol, Avon) 22, 257-265.

Panjabi, M.M., Goel, V.K., Takata, K., 1982. Physiologic Strains in the Lumbar Spinal Ligaments. an in Vitro Biomechanical Study 1981 Volvo Award in Biomechanics. Spine 7, 192-203.

Panjabi, M.M., Oxland, T.R., Yamamoto, I., Crisco, J.J., 1994. Mechanical Behavior of the Human Lumbar and Lumbosacral Spine as shown by Three-Dimensional Load-Displacement Curves. The Journal of Bone and Joint Surgery. American Volume 76, 413-424.

Panzer, M.B., Cronin, D.S., 2009. C4-C5 Segment Finite Element Model Development, Validation, and Load-Sharing Investigation. Journal of Biomechanics 42, 480-490.

Park, W. M., Kim, K., Kim, Y. H., 2013. Effects of Degenerated Intervertebral Discs on Intersegmental Rotations, Intradiscal Pressures, and Facet Joint Forces of the Whole Lumbar Spine. Computers in Biology and Medicine 43, 1234-1240.

Park, W.M., Kim, K., Kim, Y.H., 2013. Effects of Degenerated Intervertebral Discs on Intersegmental Rotations, Intradiscal Pressures, and Facet Joint Forces of the Whole Lumbar Spine. Computers in Biology and Medicine 43, 1234-1240.

Patwardhan, A.G., Havey, R.M., Meade, K.P., Lee, B., Dunlap, B., 1999. A Follower Load Increases the Load-Carrying Capacity of the Lumbar Spine in Compression. Spine 24, 1003-1009.

Patwardhan, A.G., Meade, K.P., Lee, B., 2001. A Frontal Plane Model of the Lumbar Spine Subjected to a Follower Load: Implications for the Role of Muscles. Journal of Biomechanical Engineering, 123, 212-217.

Pearcy, M., Portek, I., Shepherd, J., 1984. Three-Dimensional x-Ray Analysis of Normal Movement in the Lumbar Spine. Spine 9, 294-297.

Pearcy, M.J., 1985. Stereo radiography of lumbar spine motion. Acta orthopaedica Scandinavica, S212, 1-45.

Pearcy, M.J., Tibrewal, S.B., 1984. Axial rotation and lateral bending in the normal lumbar spine measured by three-dimensional radiography. Spine 9, 582-587.

Pollintine, P., Dolan, P., Tobias, J.H., Adams, M.A., 2004. Intervertebral Disc Degeneration can Lead to "Stress-Shielding" of the Anterior Vertebral Body: A Cause of Osteoporotic Vertebral Fracture? Spine 29, 774-782.

Pope, M.H., Novotny, J.E., 1993. Spinal biomechanics. Journal of Biomechanical Engineering 115, 569-574.

Propst-Proctor, S.L., Bleck, E.E., 1983. Radiographic determination of lordosis and kyphosis in normal and scoliotic children. Journal of Pediatric Orthopedics 3, 344-346.

Putzer, M., Ehrlich, I., Rasmussen, J., Gebbeken, N., Dendorfer, S., 2015. Sensitivity of lumbar spine loading to anatomical parameters. Journal of Biomechanics http://dx.doi.org/10.1016/j.jbiomech.2015.11.003.

Rajnics, P., Templier, A., Skalli, W., Lavaste, F., Illes, T., 2002. The importance of spinopelvic parameters in patients with lumbar disc lesions. International Orthopaedics 26, 104-108.

Renner, S.M., Natarajan, R.N., Patwardhan, A.G., Havey, R.M., Voronov, L.I., Guo, B.Y., Andersson, G.B., An, H.S., 2007. Novel Model to Analyze the Effect of a Large Compressive Follower Pre-Load on Range of Motions in a Lumbar Spine. Journal of Biomechanics 40, 1326-1332.

Robin, S., Skalli, W., Lavaste, F., 1994. Influence of Geometrical Factors on the Behavior of Lumbar Spine Segments: A Finite Element Analysis. European Spine Journal: Official Publication of the European Spine Society, the European Spinal Deformity Society, and the European Section of the Cervical Spine Research Society 3, 84-90.

Rohlmann, A., Bauer, L., Zander, T., Bergmann, G., Wilke, H.J., 2006. Determination of Trunk Muscle Forces for Flexion and Extension by using a Validated Finite Element Model of the Lumbar Spine and Measured in Vivo Data. Journal of Biomechanics 39, 981-989.

Rohlmann, A., Neller, S., Claes, L., Bergmann, G., Wilke, H.J., 2001. Influence of a follower load on intradiscal pressure and intersegmental rotation of the lumbar spine. Spine 26, E557-E561.

Rohlmann, A., Zander, T., Rao, M., Bergmann, G., 2009. Realistic Loading Conditions for Upper Body Bending. Journal of Biomechanics 42, 884-890.

Rohlmann, A., Zander, T., Rao, M., Bergmann, G., 2009a. Applying a Follower Load Delivers Realistic Results for Simulating Standing. Journal of Biomechanics 42, 1520-1526.

Rohlmann, A., Zander, T., Rao, M., Bergmann, G., 2009b. Realistic Loading Conditions for Upper Body Bending. Journal of Biomechanics 42, 884-890.

Roussouly, P., Berthonnaud, E., Dimnet, J., 2003. Geometrical and Mechanical Analysis of Lumbar Lordosis in an Asymptomatic Population: Proposed Classification," Revue Du Chirurgie Orthopedique Et Traumatologique 89, 632-639.

Roussouly, P., Gollogly, S., Berthonnaud, E., Dimnet,J., 2005. Classification of the Normal Variation in the Sagittal Alignment of the Human Lumbar Spine and Pelvis in the Standing Position. Spine 30, 346-353.

Roussouly, P., Pinheiro-Franco, J.L., 2011. Biobmechanical Analysis of the Spino-Pelvic Organization and Adaptation in Pathology. European Spine Journal: Official Publication of the European Spine Society, the European Spinal Deformity Society, and the European Section of the Cervical Spine Research Society 20, S609-S618.

Rubin, D.I., 2007. Epidemiology and Risk Factors for Spine Pain. Neurologic Clinics, 25, 353-371.

Sato, K., Kikuchi, S., Yonezawa, T., 1999. In Vivo Intradiscal Pressure Measurement in Healthy Individuals and in Patients with Ongoing Back Problems. Spine 24, 2468-2474.

Sawa, A.G., Crawford, N.R., 2008. The use of Surface Strain Data and a Neural Networks Solution Method to Determine Lumbar Facet Joint Loads during in Vitro Spine Testing. Journal of Biomechanics 41, 2647-2653.

Schmidt, H., Galbusera, F., Rohlmann, A., Shirazi-Adl,A., 2013. What have we Learned from Finite Element Model Studies of Lumbar Intervertebral Discs in the Past Four Decades? Journal of Biomechanics 46, 2342-2355.

Schmidt, H., Heuer, F., Simon, U., Kettler, A., Rohlmann, A., Claes, L., Wilke, H.J., 2006. Application of a New Calibration Method for a Three-Dimensional Finite Element Model of a Human Lumbar Annulus Fibrosus. Clinical Biomechanics 21, 337-344.

Schmidt, H., Kettler, A., Heuer, F., Simon, U., Claes, L., Wilke, H.J., 2007. Intradiscal Pressure, Shear Strain, and Fiber Strain in the Intervertebral Disc Under Combined Loading. Spine 32, 748-755.

Schmidt, H., Shirazi-Adl, A., Galbusera, F., Wilke, H.J., 2010. Response Analysis of the Lumbar Spine during Regular Daily activities—A Finite Element Analysis. Journal of Biomechanics 43, 1849-1856.

Sharma, M., Langrana, N.A., Rodriguez, J., 1995. Role of Ligaments and Facets in Lumbar Spinal Stability. Spine 20, 887-900.

Shih, S.L., Liu, C.L., Huang, L.Y., Huang, C.H., Chen, C.S., 2013. Effects of Cord Pretension and Stiffness of the Dynesys System Spacer on the Biomechanics of Spinal Decompression- a Finite Element Study. BMC Musculoskeletal Disorders, 14, 191-2474-14-191.

Shirazi-Adl, A., 1994. Biomechanics of the Lumbar Spine in sagittal/lateral Moments. Spine 19, 2407-2414.

Shirazi-Adl, A., 2006. Analysis of Large Compression Loads on Lumbar Spine in Flexion and in Torsion using a Novel Wrapping Element. Journal of Biomechanics 39, 267-275.

Shirazi-Adl, A., Ahmed, A.M., Shrivastava, S.C., 1986. Mechanical Response of a Lumbar Motion Segment in Axial Torque Alone and Combined with Compression. Spine 11, 914-927.

Shirazi-Adl, A., Parnianpour, M., 2000. Load-bearing and stress analysis of the human spine under a novel wrapping compression loading. Clinical Biomechanics 15, 718–725

Shirazi-Adl, A., Parnianpour, M., 1996. Role of posture in mechanics of the lumbar spine in compression. Journal of Spine Disorders 9, 277-286.

Stagnara, P., De Mauroy, J. C., Dran, G., Gonon, G. P., Costanzo, G., Dimnet, J., & Pasquet, A. (1982). Reciprocal angulation of vertebral bodies in a sagittal plane: Approach to references for the evaluation of kyphosis and lordosis. Spine, 7(4), 335-342.

Terai, T., Sairyo, K., Goel, V.K., Ebraheim, N., Biyani, A., Faizan, A., Sakai, T., Yasui, N., 2010. Spondylolysis Originates in the Ventral Aspect of the Pars Interarticularis: A Clinical and Biomechanical Study. Journal of Bone and Joint Surger (Br) 98, 1123-1127.

Trainor, T. J., Wiesel, S.W., 2002. Epidemiology of back pain in the athlete. Clinics in Sports Medicine 21, 93-103.

Tsuji, T., Matsuyama, Y., Sato, K., Hasegawa, Y., Yimin, Y., Iwata, H., 2001. Epidemiology of low back pain in the elderly: Correlation with lumbar lordosis. Journal of Orthopaedic Science 6, 307-311.

Tüzün, Ç., Yorulmaz, İ., Cindaş, A., Vatan, S., 1999. Low back pain and posture. Clinical Rheumatology 18, 308-312.

Vaz, G., Roussouly, P., Berthonnaud, E., Dimnet, J., 2002. Sagittal morphology and equilibrium of pelvis and spine. European Spine Journal: Official Publication of the European Spine Society, the European Spinal Deformity Society, and the European Section of the Cervical Spine Research Society 11, 80-87.

Vrtovec, T., Janssen, M.M.A., Likar, B., Castelein, R.M., Viergever, M.A., Pernuš, F., 2012. A review of methods for evaluating the quantitative parameters of sagittal pelvic alignment. The Spine Journal 12, 433-446.

Wang, J.L., Parnianpour, M., Shirazi-Adl, A., Engin, A.E., 1999. Rate Effect on Sharing of Passive Lumbar Motion Segment Under Load-Controlled Sagittal Flexion: Viscoelastic Finite Element Analysis. Theoretical and Applied Fracture Mechanics 32, 119-128.

Wilke, H., Neef, P., Hinz, B., Seidel, H., Claes, L., 2001. Intradiscal pressure together with anthropometric data - a data set for the validation of models. Clinical Biomechanics (Bristol, Avon) 16, S111-S126.

Wilson, D.C., Niosi, C.A., Zhu, Q.A., Oxland, T.R., Wilson, D.R., 2006. Accuracy and repeatability of a new method for measuring facet loads in the lumbar spine. Journal of Biomechanics 39, 348-353.

Woldtvedt, D.J., Womack, W., Gadomski, B.C., Schuldt, D., Puttlitz, C.M., 2011. Finite Element Lumbar Spine Facet Contact Parameter Predictions are Affected by the Cartilage Thickness Distribution and Initial Joint Gap Size. Journal of Biomechanical Engineering 133, 061009.

Yamamoto, I., Panjabi, M.M., Crisco, T., Oxland, T., 1989. Three-Dimensional Movements of the Whole Lumbar Spine and Lumbosacral Joint. Spine 14, 1256-1260.